

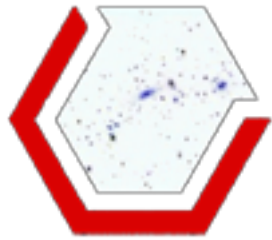
News from The Dark Energy Survey

Aurélien Benoit-Lévy

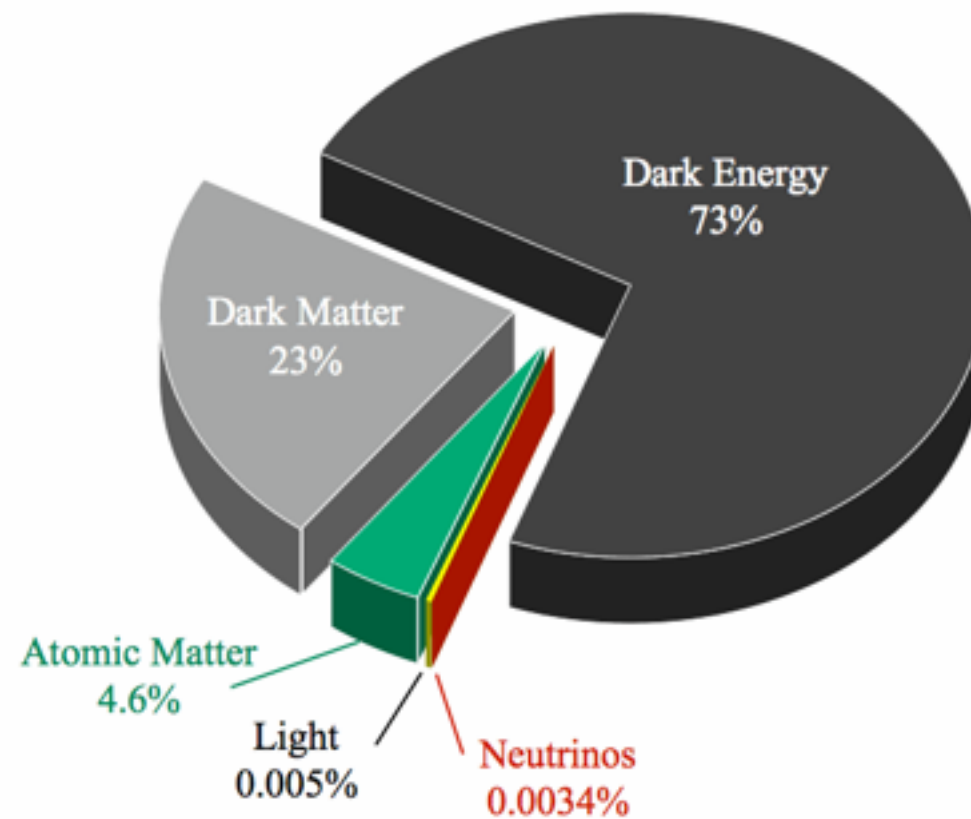
Institut d'Astrophysique de Paris



Journées LSST France - 20-22 Mars 2017



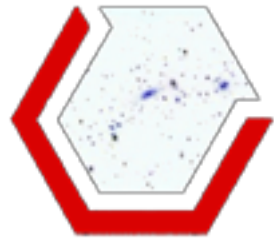
What is the physical cause of cosmic acceleration?



Dark Energy or modification of General Relativity?

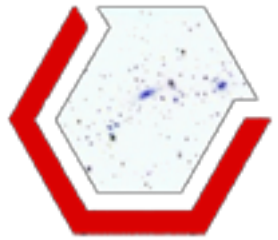
If Dark Energy, is it Λ (the vacuum) or something else?

What is the DE equation of state parameter w and (how) does it evolve?



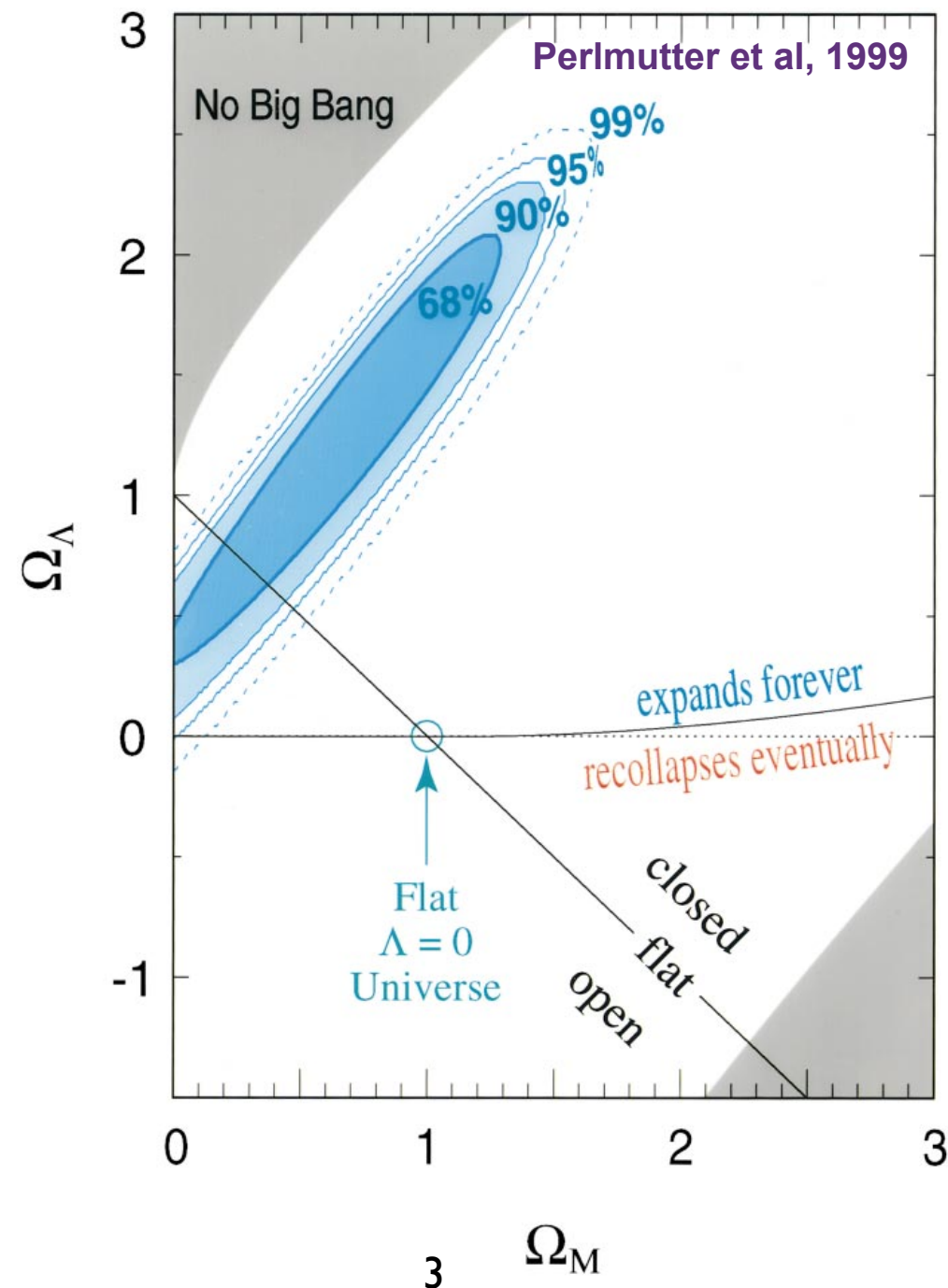
Dark Energy!

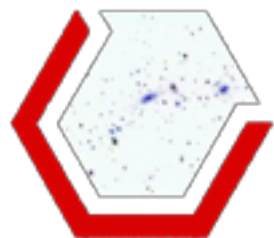
Type Ia Supernovae are the main indication for the acceleration of the expansion



Dark Energy!

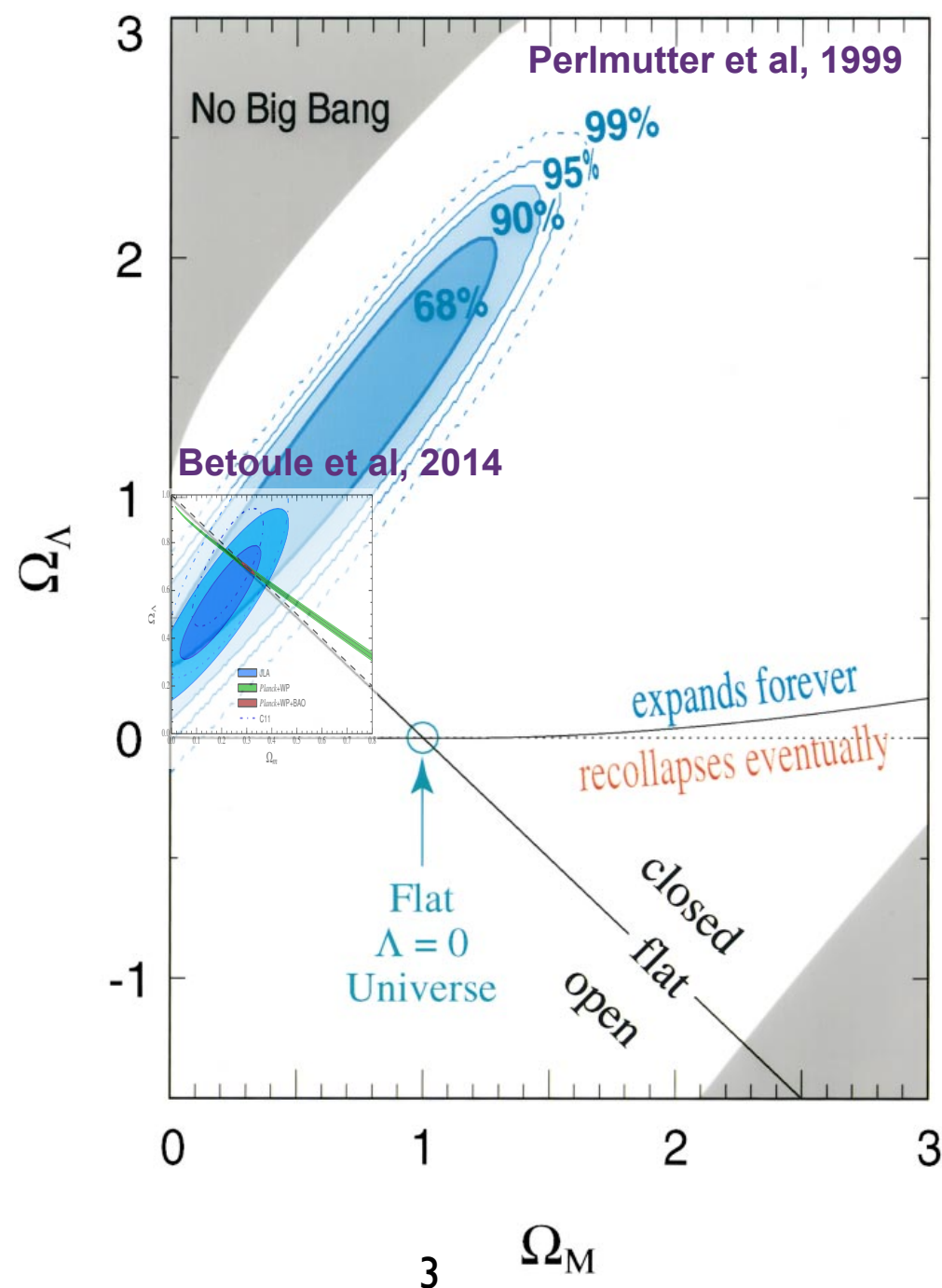
Type Ia Supernovae are the main indication for the acceleration of the expansion

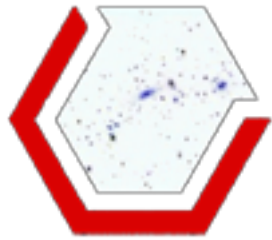




Dark Energy!

Type Ia Supernovae are the main indication for the acceleration of the expansion



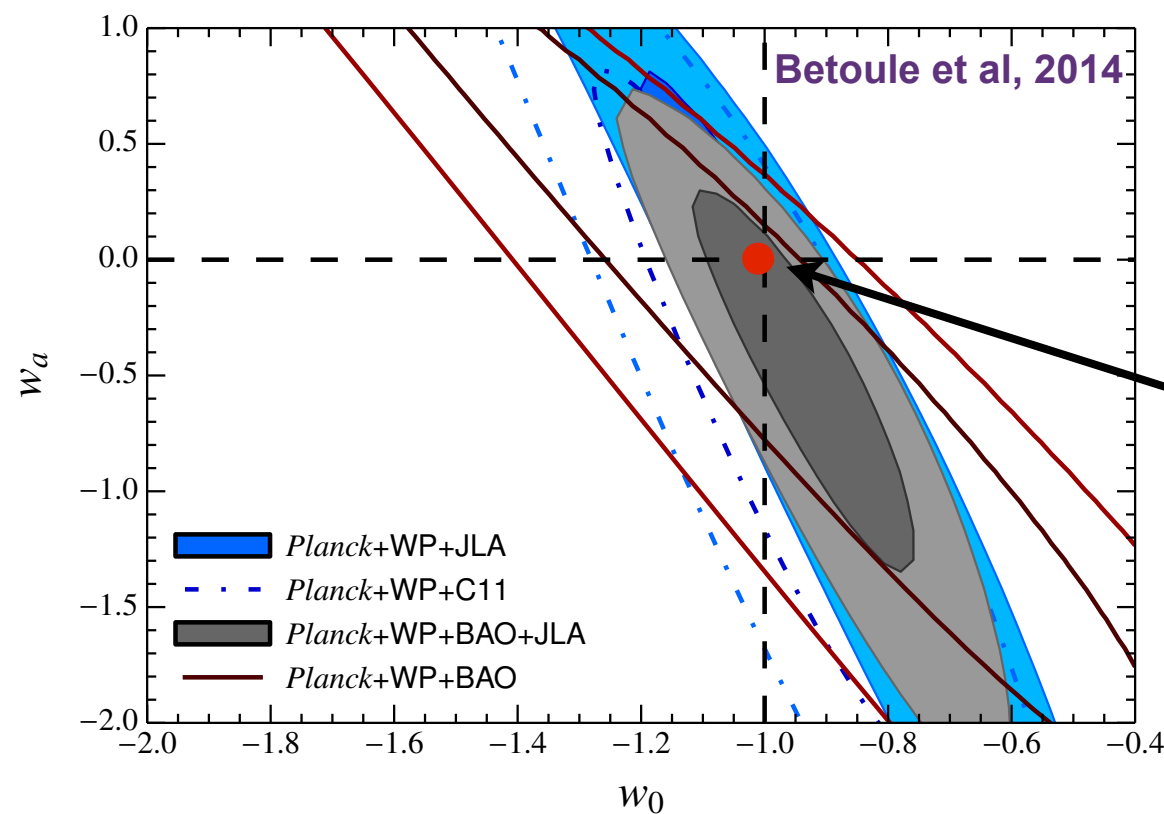


What could be Dark Energy?

Pure cosmological constant?, vacuum energy?, quintessence?,
Modification of gravity?, ...

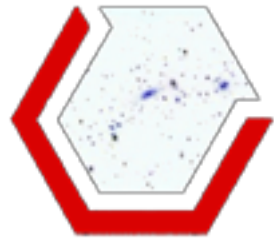
$$p = w\rho$$

$$w(a) = w_0 + w_a(1 - a)$$



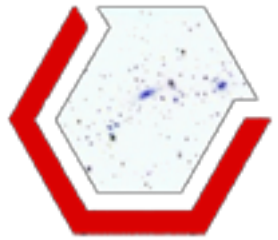
Pure cosmological constant

Best constraint on DE currently brought by SNIa.



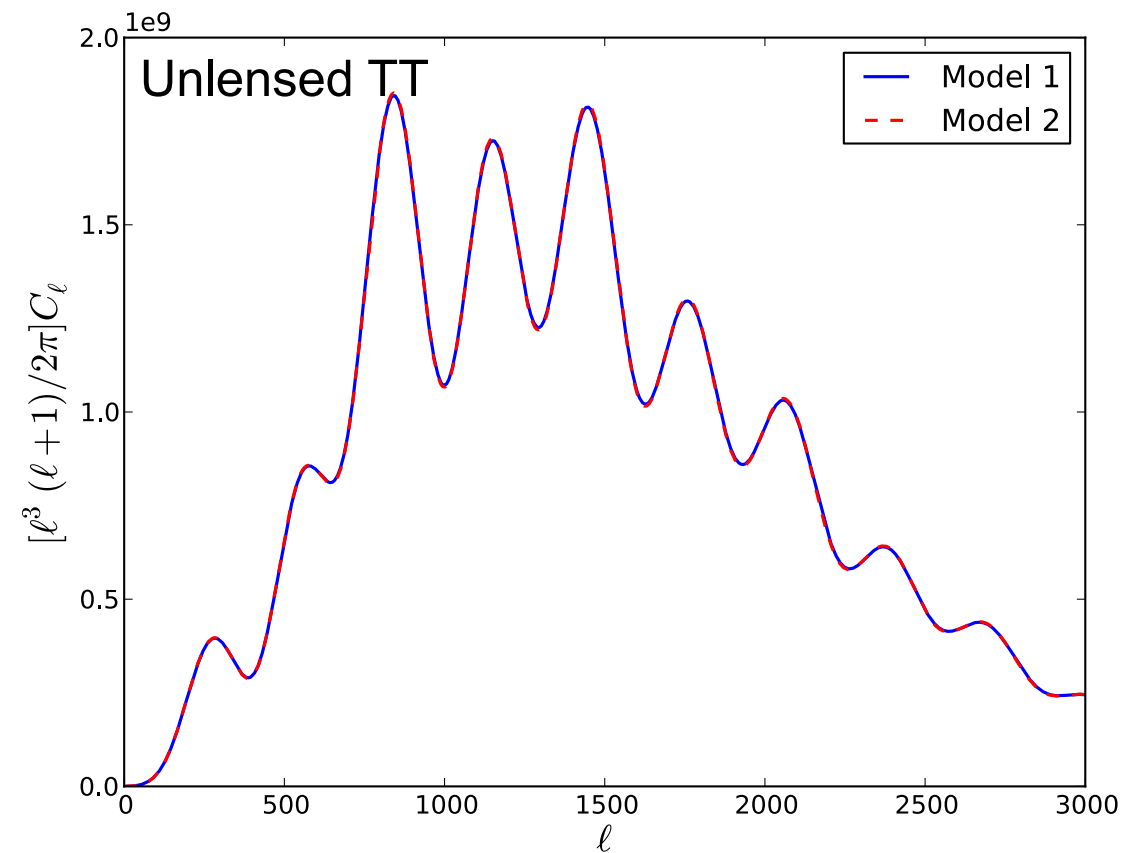
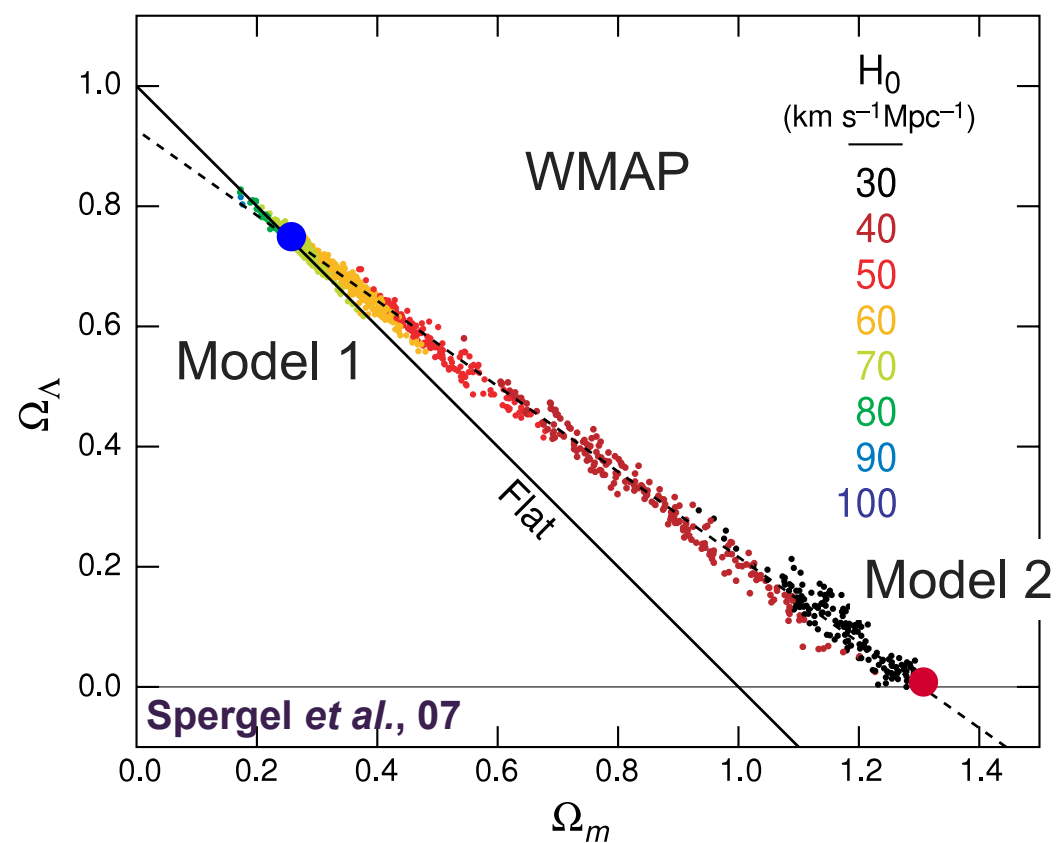
Parameter degeneracies

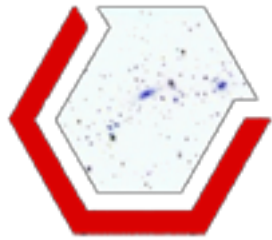
Dark Energy has no direct effect on the CMB anisotropies at recombination. Its effect are mainly geometrical but are degenerated with other parameters



Parameter degeneracies

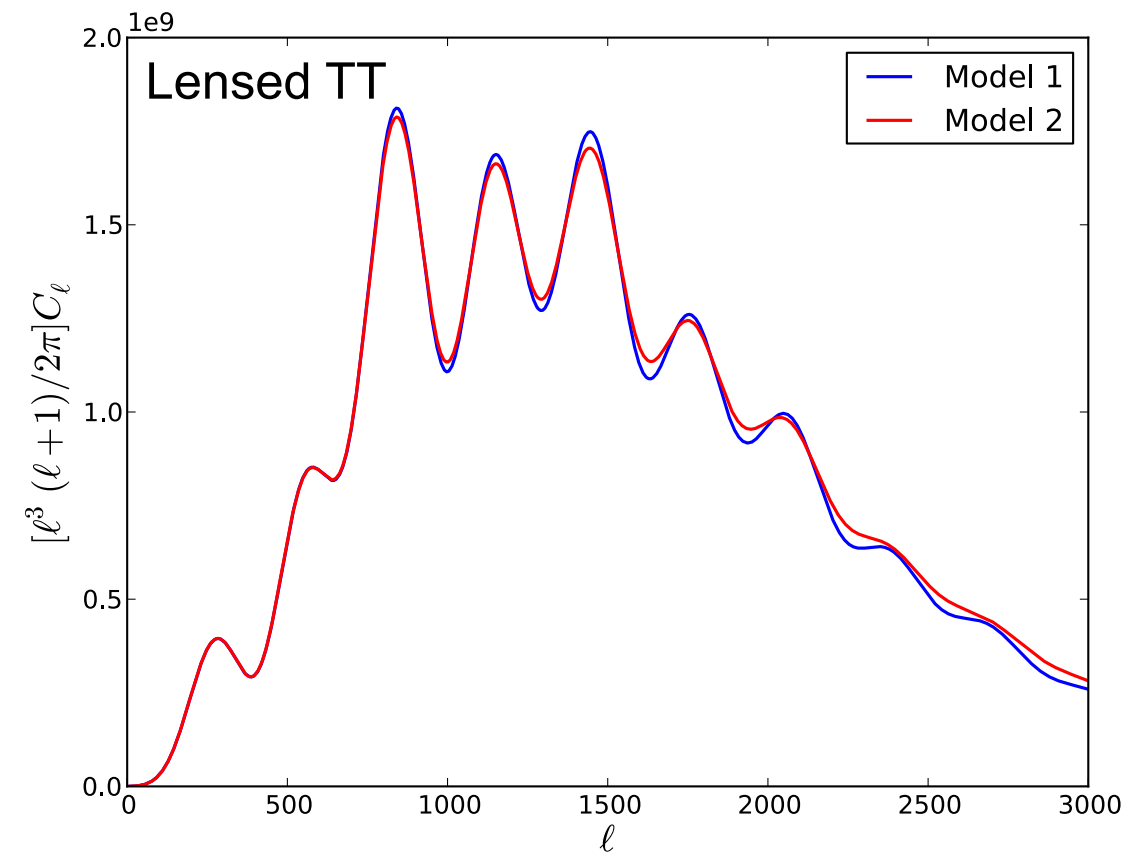
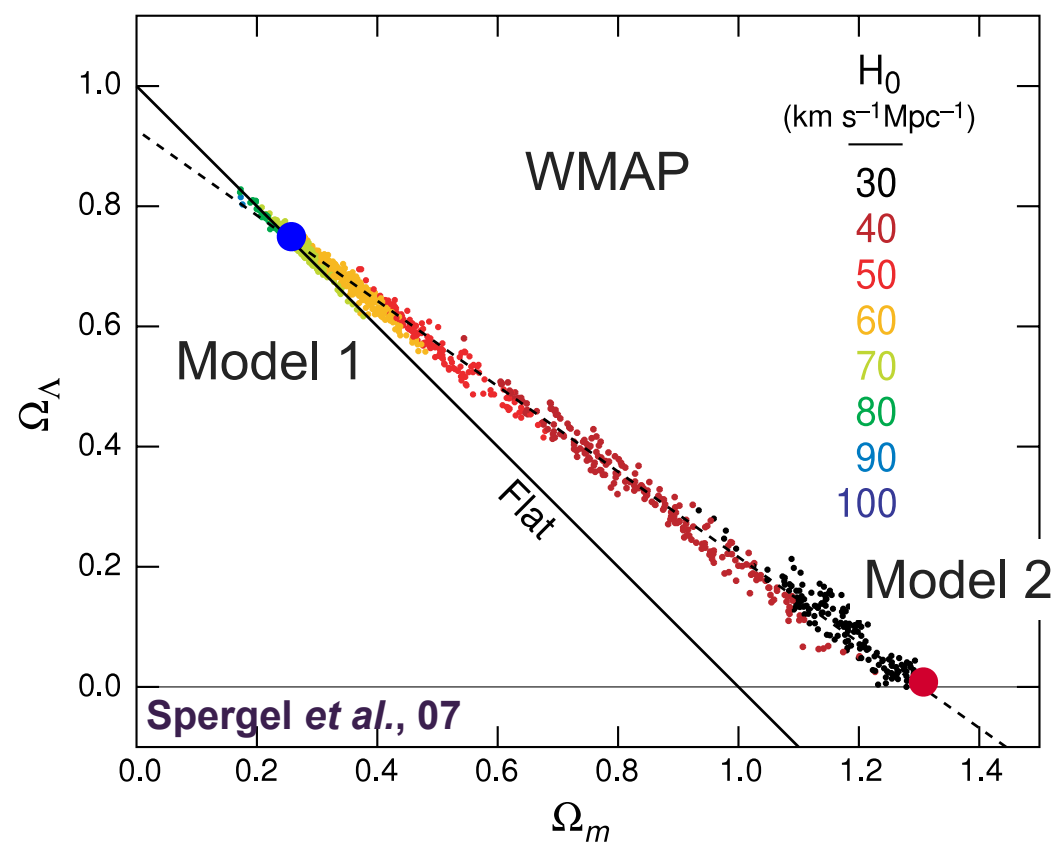
Dark Energy has no direct effect on the CMB anisotropies at recombination. Its effects are mainly geometrical but are degenerated with other parameters

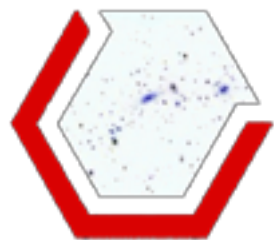




Parameter degeneracies

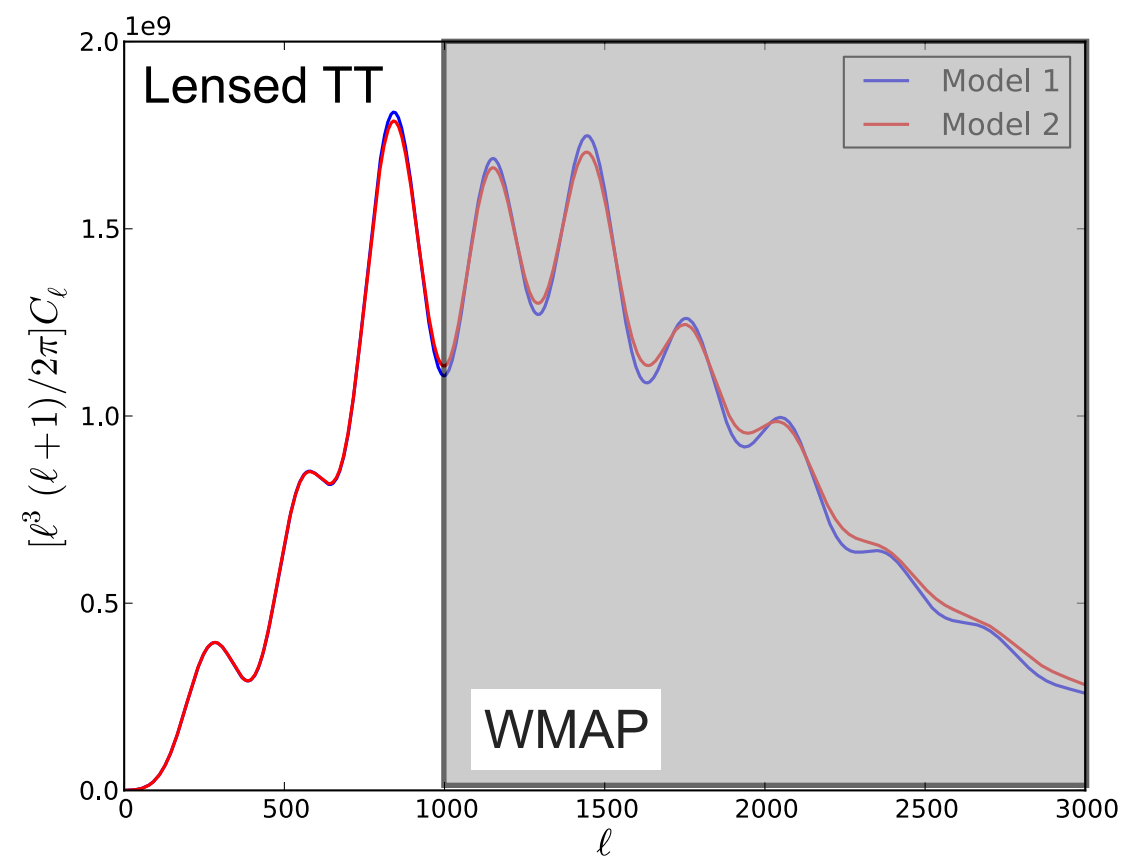
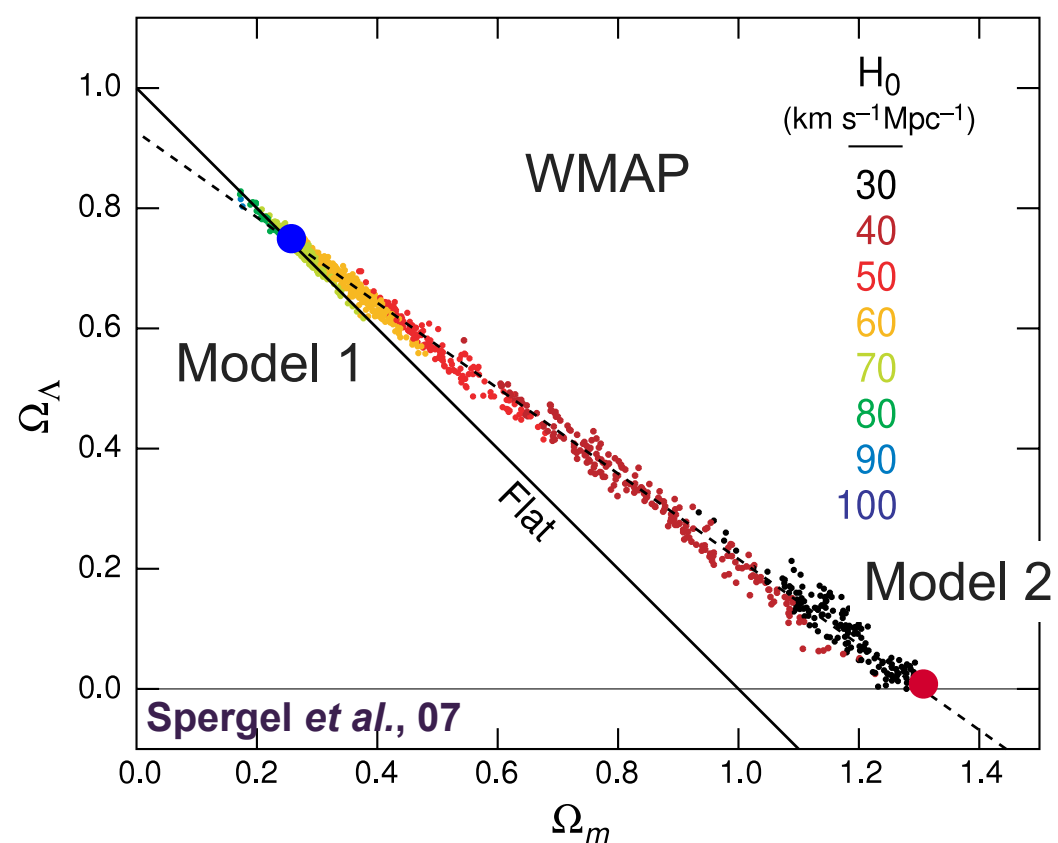
Dark Energy has no direct effect on the CMB anisotropies at recombination. Its effect are mainly geometrical but are degenerated with other parameters

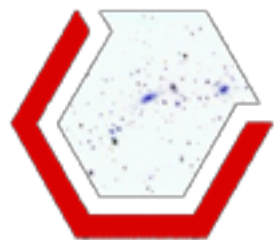




Parameter degeneracies

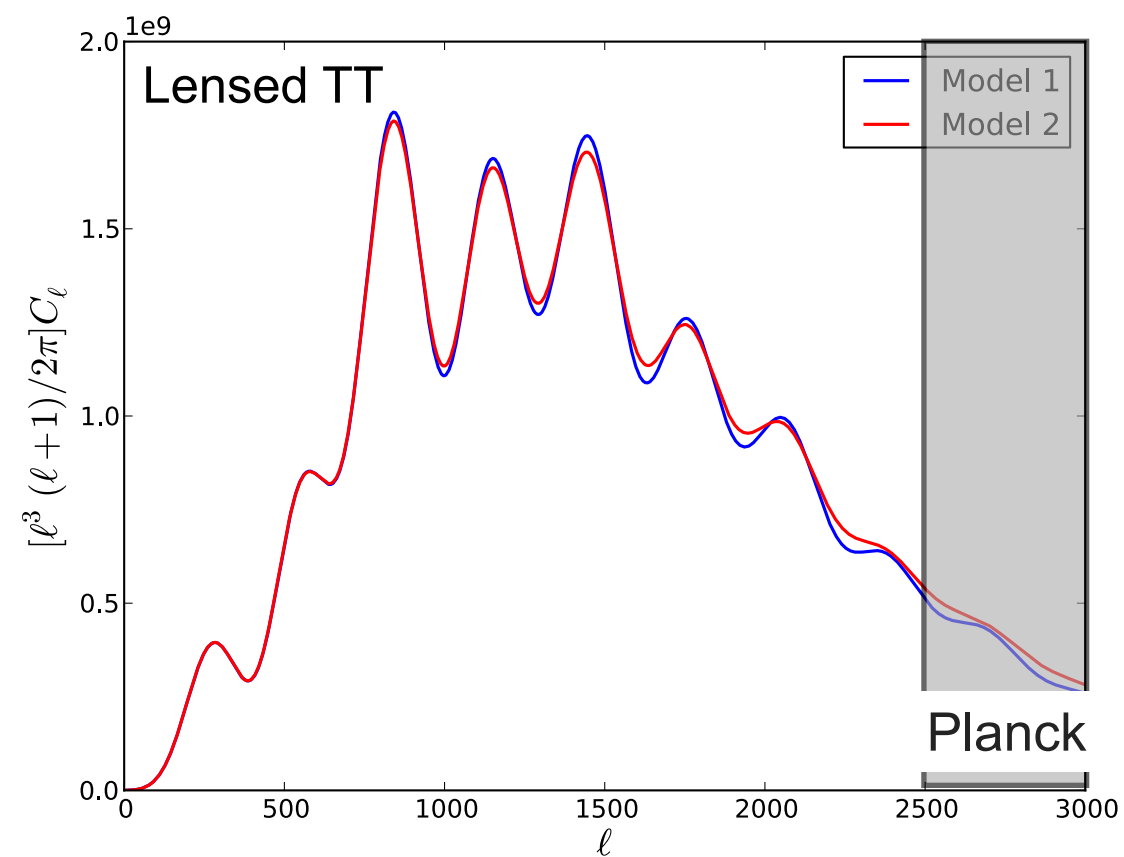
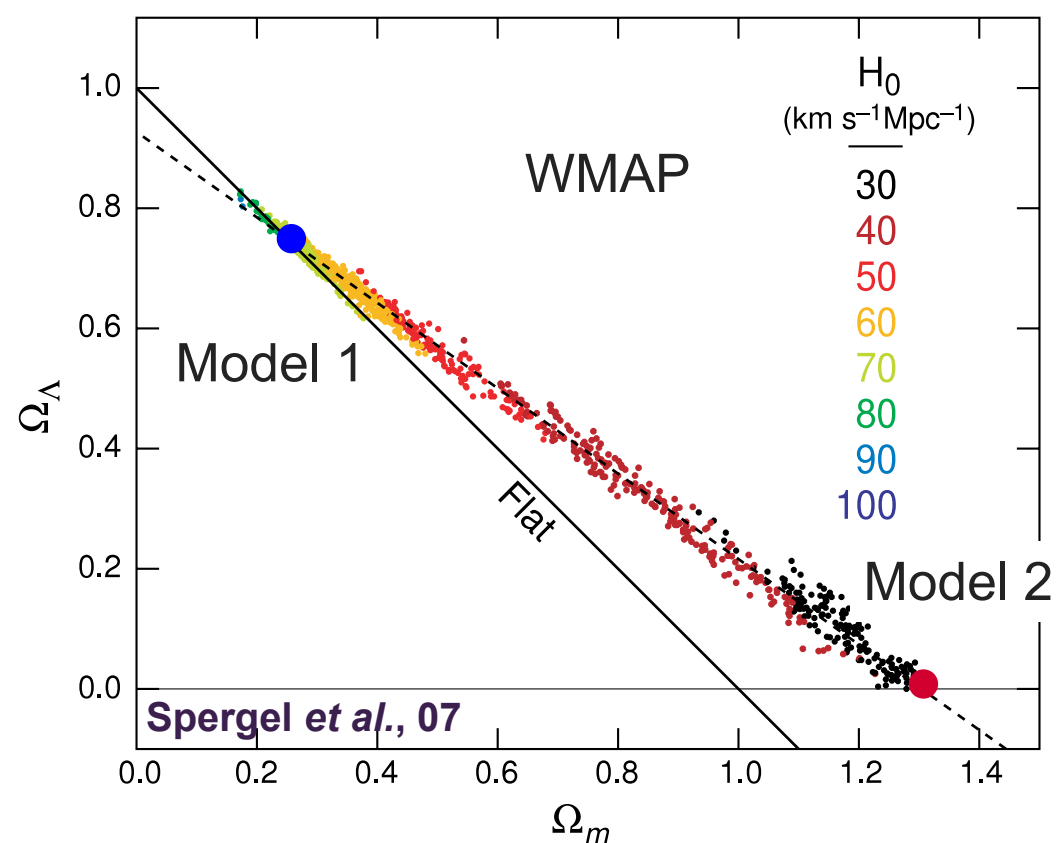
Dark Energy has no direct effect on the CMB anisotropies at recombination. Its effect are mainly geometrical but are degenerated with other parameters

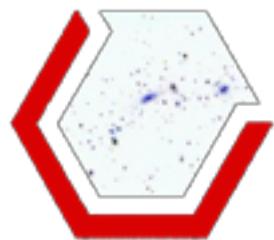




Parameter degeneracies

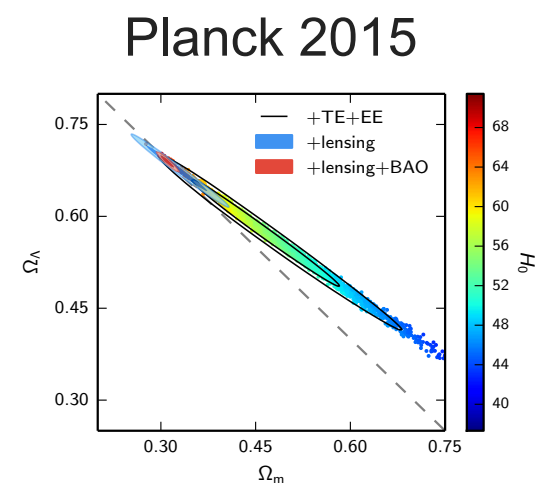
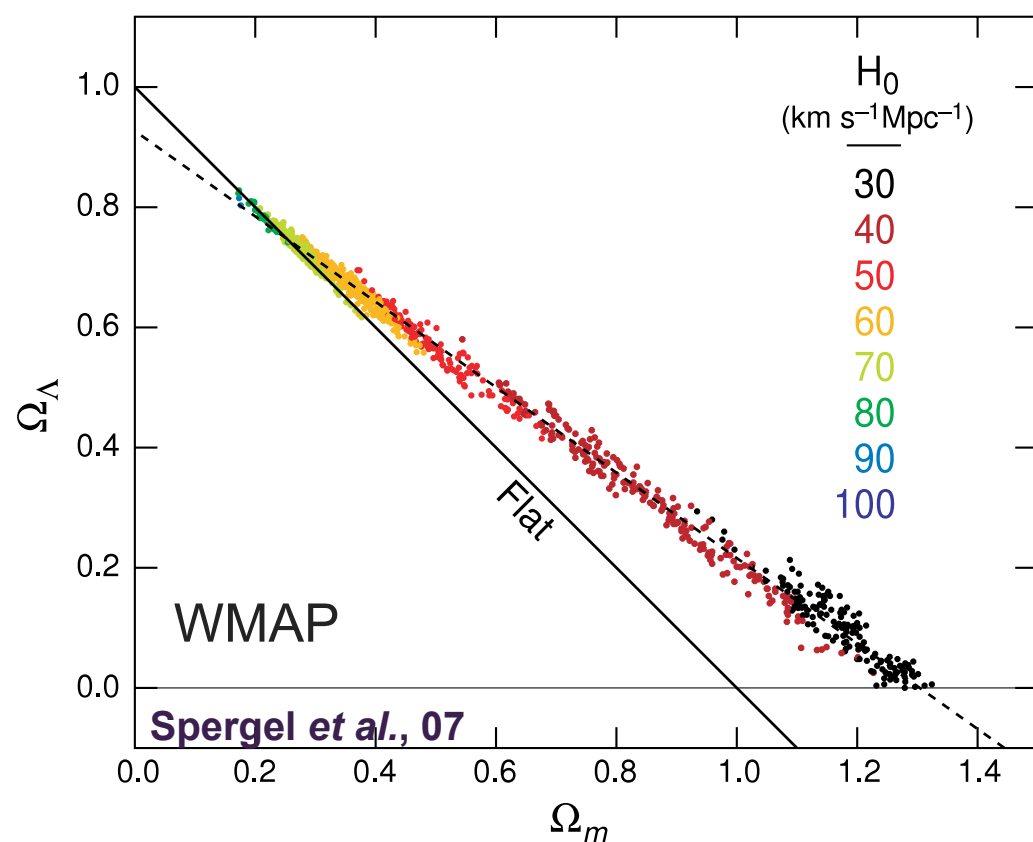
Dark Energy has no direct effect on the CMB anisotropies at recombination. Its effects are mainly geometrical but are degenerated with other parameters

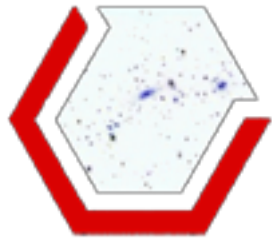




Parameters degeneracies

Information from the large-scale structure can break those degeneracies!

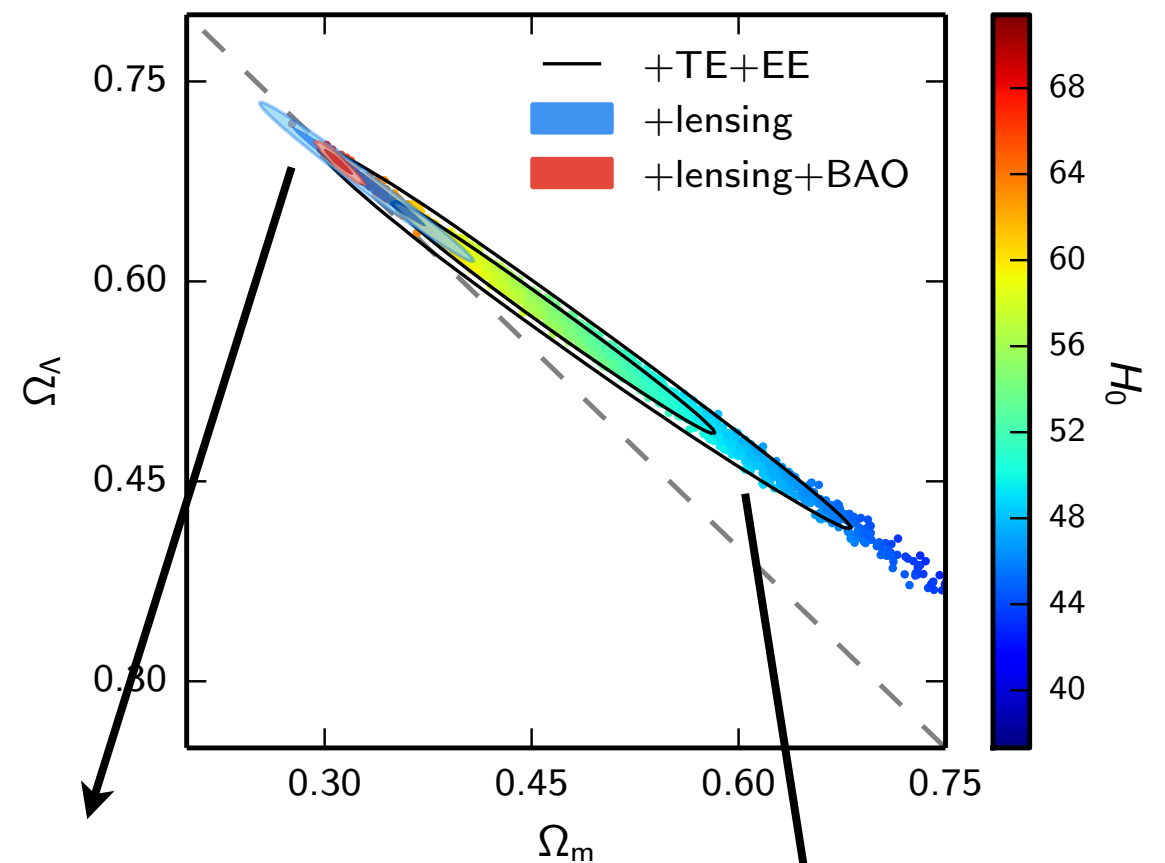
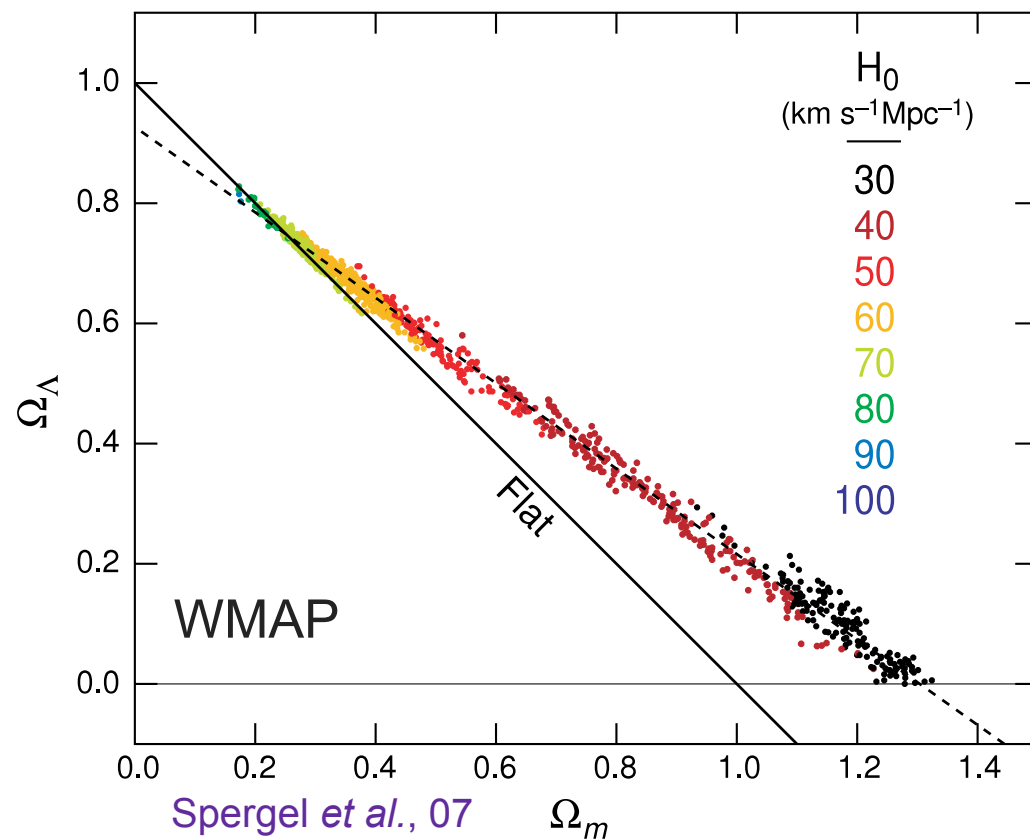




Parameters degeneracies

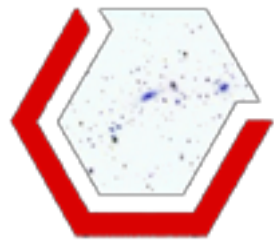
Information from the large-scale structure can break those degeneracies!

Planck 2015



Adding CMB lensing
reconstruction

Using only T+P power
spectra



Parameters degeneracies

Large-scale structure will provide constraints on cosmology from

Geometry

- The scale of the sound horizon at recombination is imprinted in the matter distribution: Baryonic Acoustic Oscillations
- Distances

Structure growth

- Dark Energy, hence acceleration of the expansion will impede structure formation

So... Let's observe those galaxies!

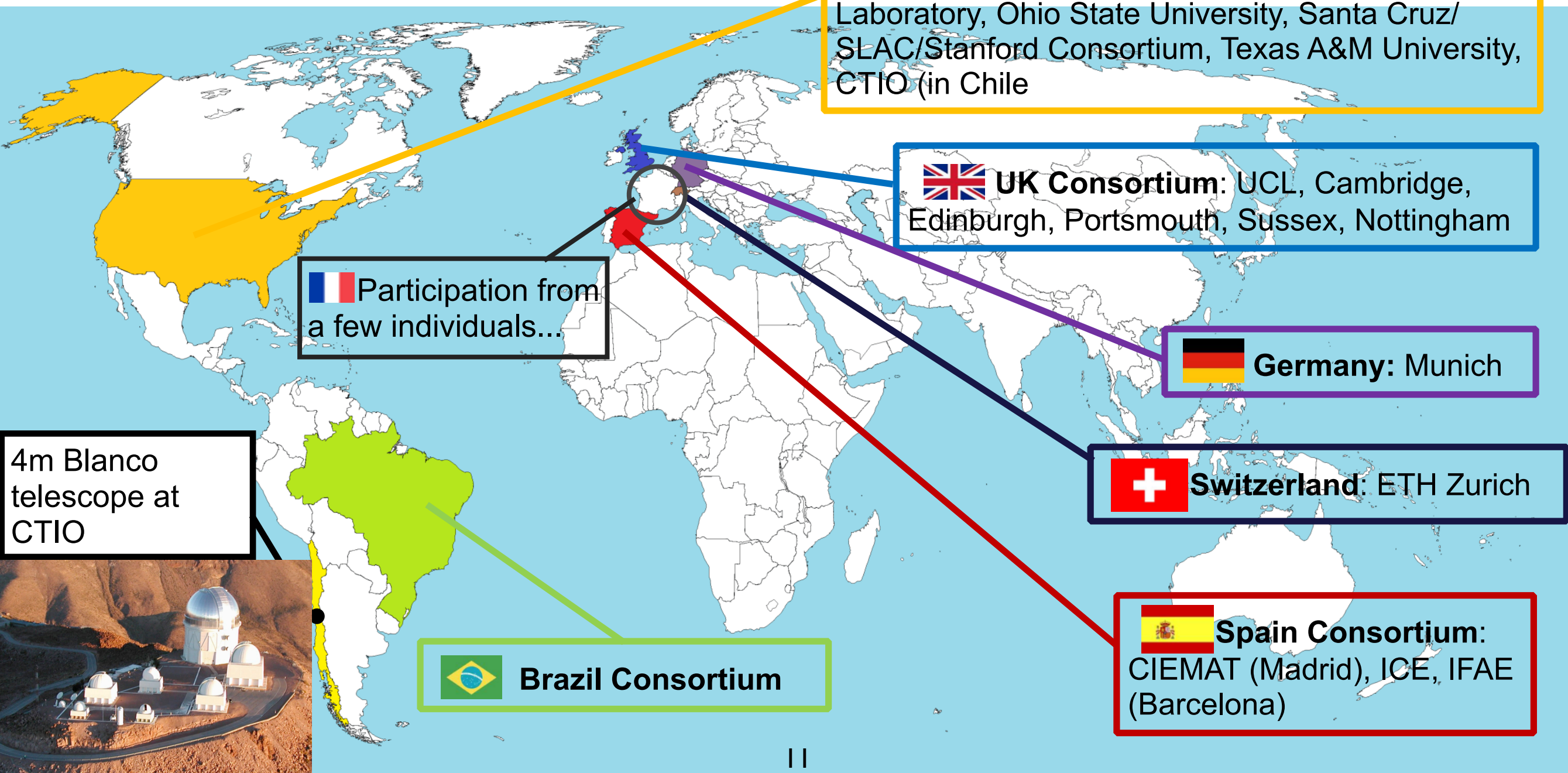


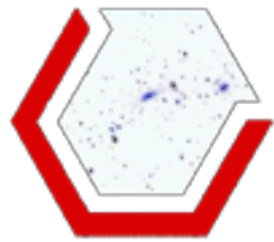
The DES Collaboration

~300 scientists from 28 institutions from around the world

DARK ENERGY
SURVEY

facebook.com/darkenergysurvey
<http://darkenergysurvey.org>

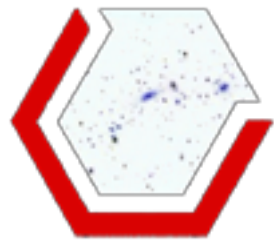




The Dark Energy Survey



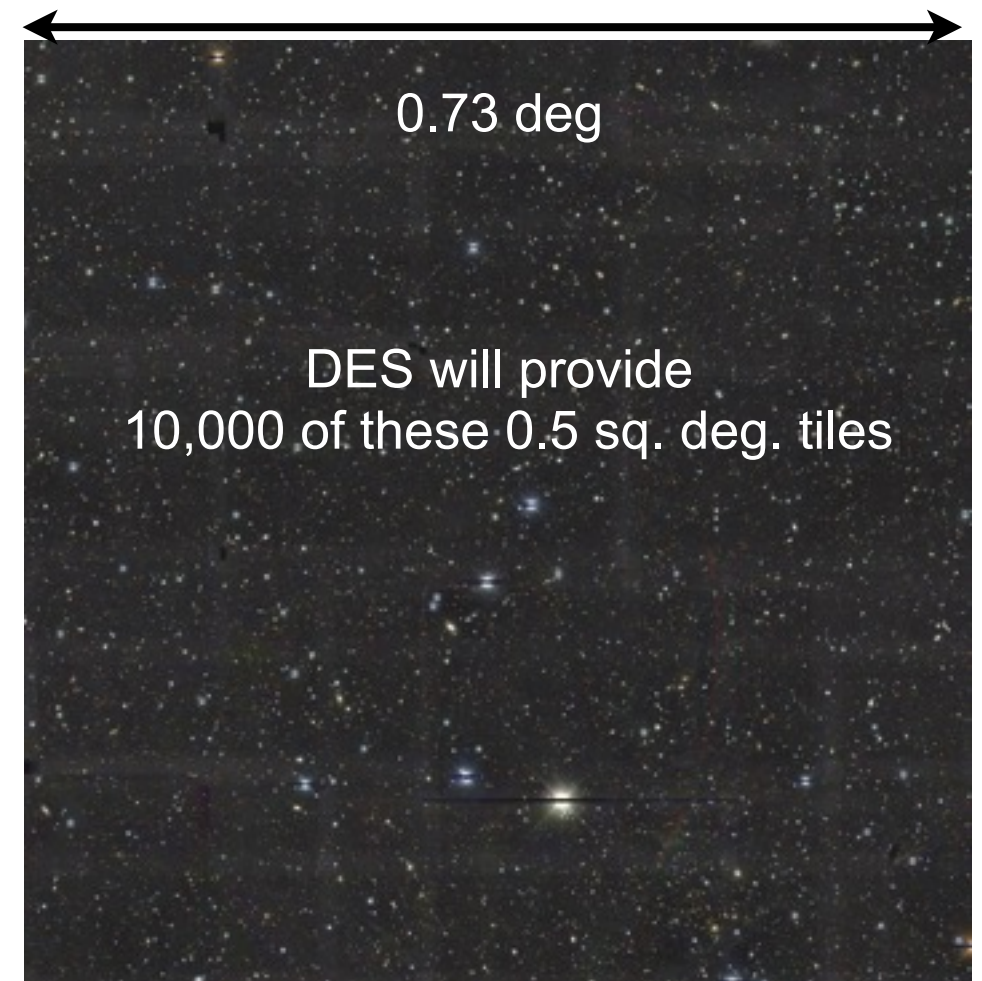
New camera mounted on the 4m Blanco telescope at Cerro-Tololo Inter-American Observatory in Chile

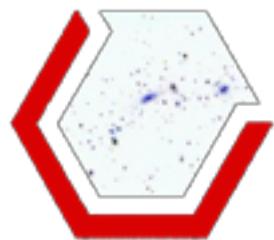


What is DES ?

DES is:

- 1" resolution picture of the sky (pixel size 0.26")
- 5000 sq. deg. (1/8th of the sky)
- Five photometric bands (grizY)
- 24th magnitude (galaxies, 10σ)





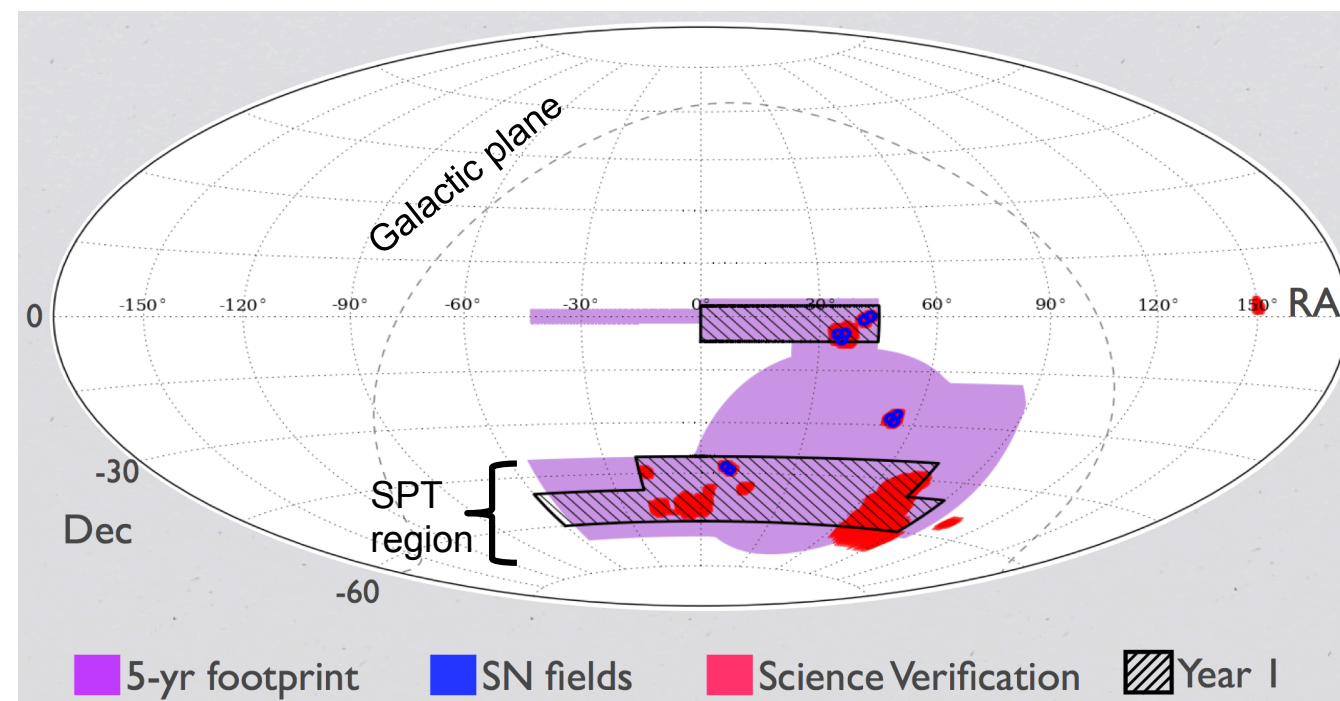
What is DES ?

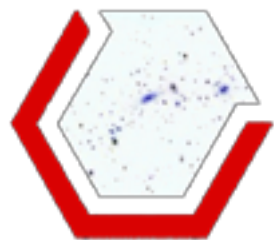
DES is:

- 1'' resolution picture of the sky (pixel size 0.26'')
- 5000 sq. deg. (1/8th of the sky)
- Five photometric bands (grizY)
- 24th magnitude (galaxies, 10σ)

Supplemented by:

- 2500 sq. deg. South Pole Telescope
- Vista Hemisphere Survey (JHK)





What is DES ?

DES is:

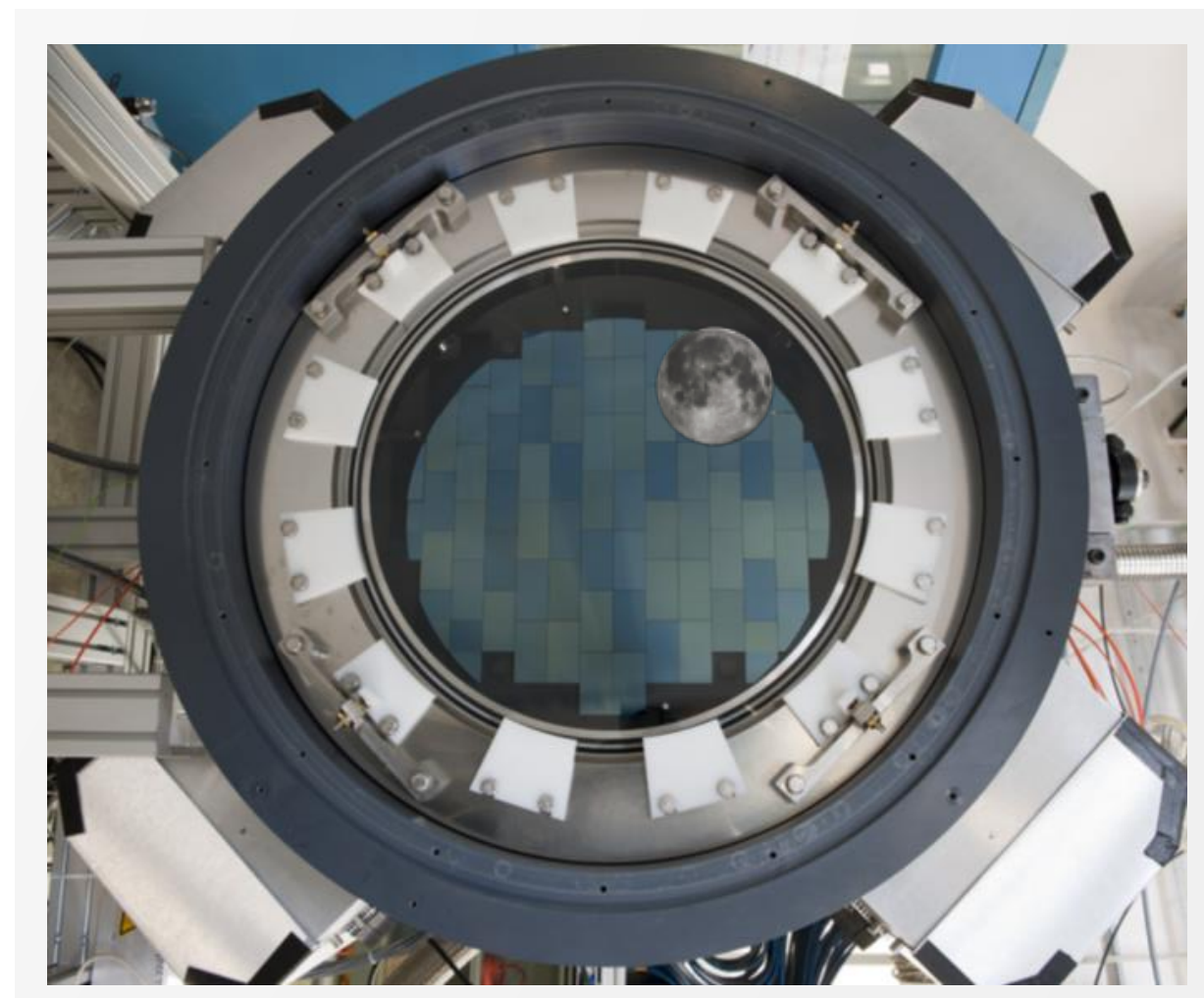
- 1" resolution picture of the sky (pixel size 0.26")
- 5000 sq. deg. (1/8th of the sky)
- Five photometric bands (grizY)
- 24th magnitude (galaxies, 10σ)

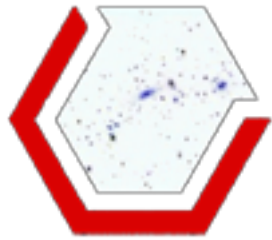
Supplemented by:

- 2500 sq. deg. South Pole Telescope
- Vista Hemisphere Survey (JHK)

DECam:

- 570 Mpixels, 62 CCD
- 3 sq. deg. field of view





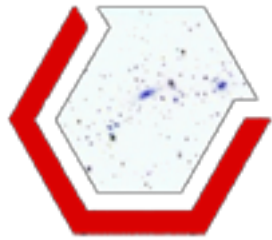
4 probes of Dark Energy

Galaxy Clusters (distance, structure growth)

ten of thousands of clusters up to $z \sim 1$

synergies with SPT, VHS

$$\frac{d^2 N(z)}{dz d\Omega} = \frac{c}{H(z)} D_A^2 (1+z)^2 \int_0^\infty f(M, z) \frac{dn(z)}{dM} dM ,$$



4 probes of Dark Energy

Galaxy Clusters (distance, structure growth)

ten of thousands of clusters up to $z \sim 1$

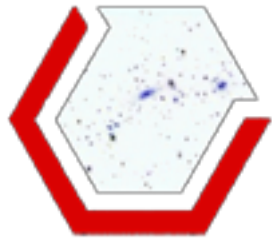
synergies with SPT, VHS

Weak lensing (distance, structure growth)

shape and measurements of 200

millions galaxies

$$C_l^{x_a x_b} = \int dz \frac{H(z)}{D_A^2} W_a(z) W_b(z) P^{s_a s_b}(k = l/D_A; z),$$



4 probes of Dark Energy

Galaxy Clusters (distance, structure growth)

ten of thousands of clusters up to $z \sim 1$

synergies with SPT, VHS

Weak lensing (distance, structure growth)

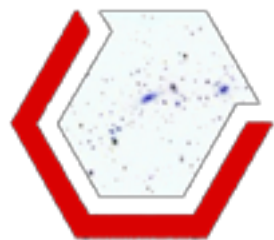
shape and measurements of 200

millions galaxies

Baryonic acoustic Oscillations (distance)

300 millions galaxies to $z=1$ and beyond

$$C_{\text{gal}}^i(l) = \int_0^\infty k^2 dk \frac{2}{\pi} f_i^2(l, k) P_{\text{gal}}(k),$$



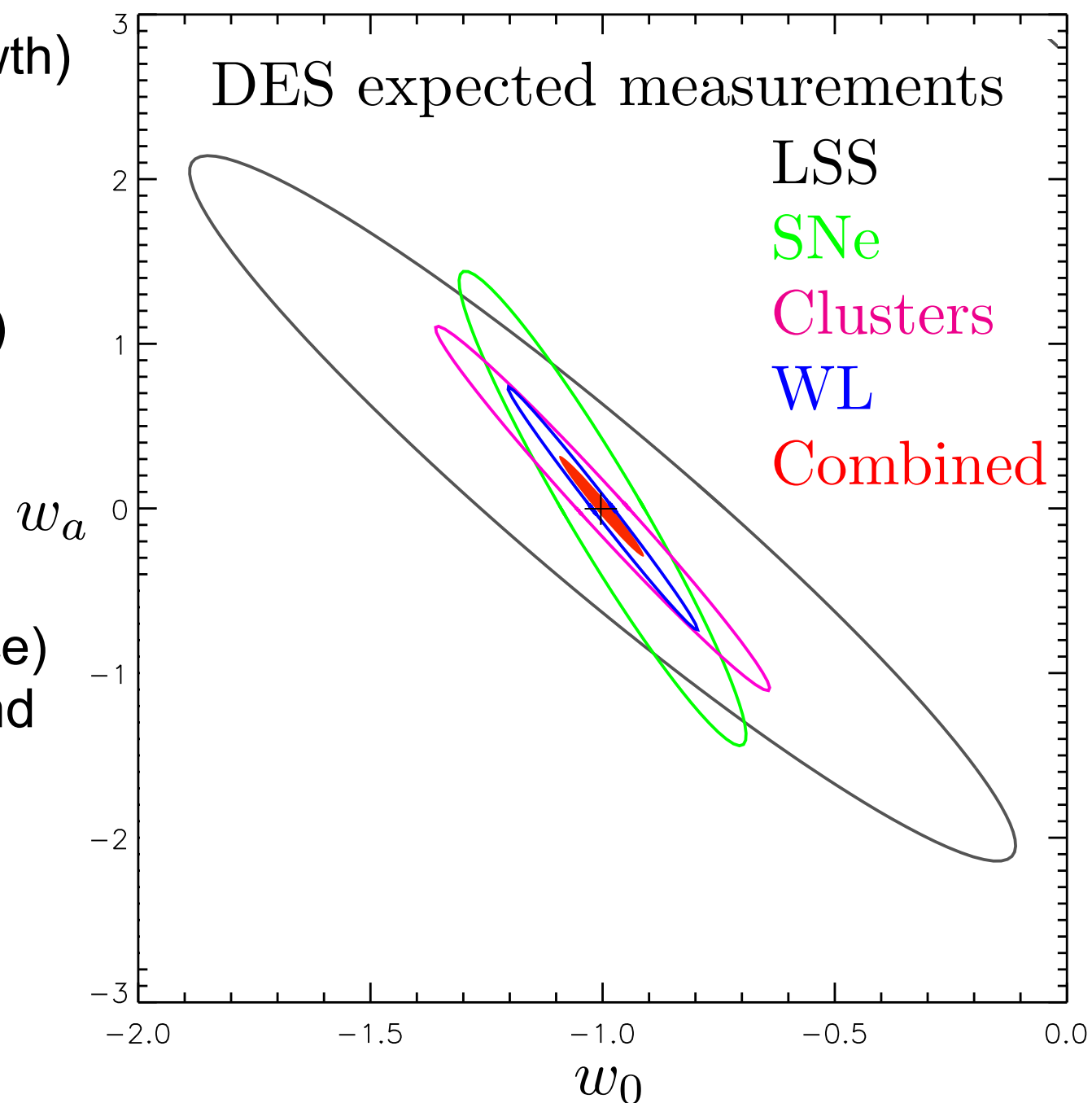
4 probes of Dark Energy

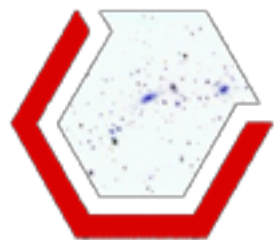
Galaxy Clusters (distance, structure growth)
ten of thousands of clusters up to $z \sim 1$
synergies with SPT, VHS

Weak lensing (distance, structure growth)
shape and measurements of 200
millions galaxies

Baryonic acoustic Oscillations (distance)
300 millions galaxies to $z=1$ and beyond

Type Ia supernovae (distance)
30 sq. deg. SN fields
3500 SNIa to $z \sim 1$





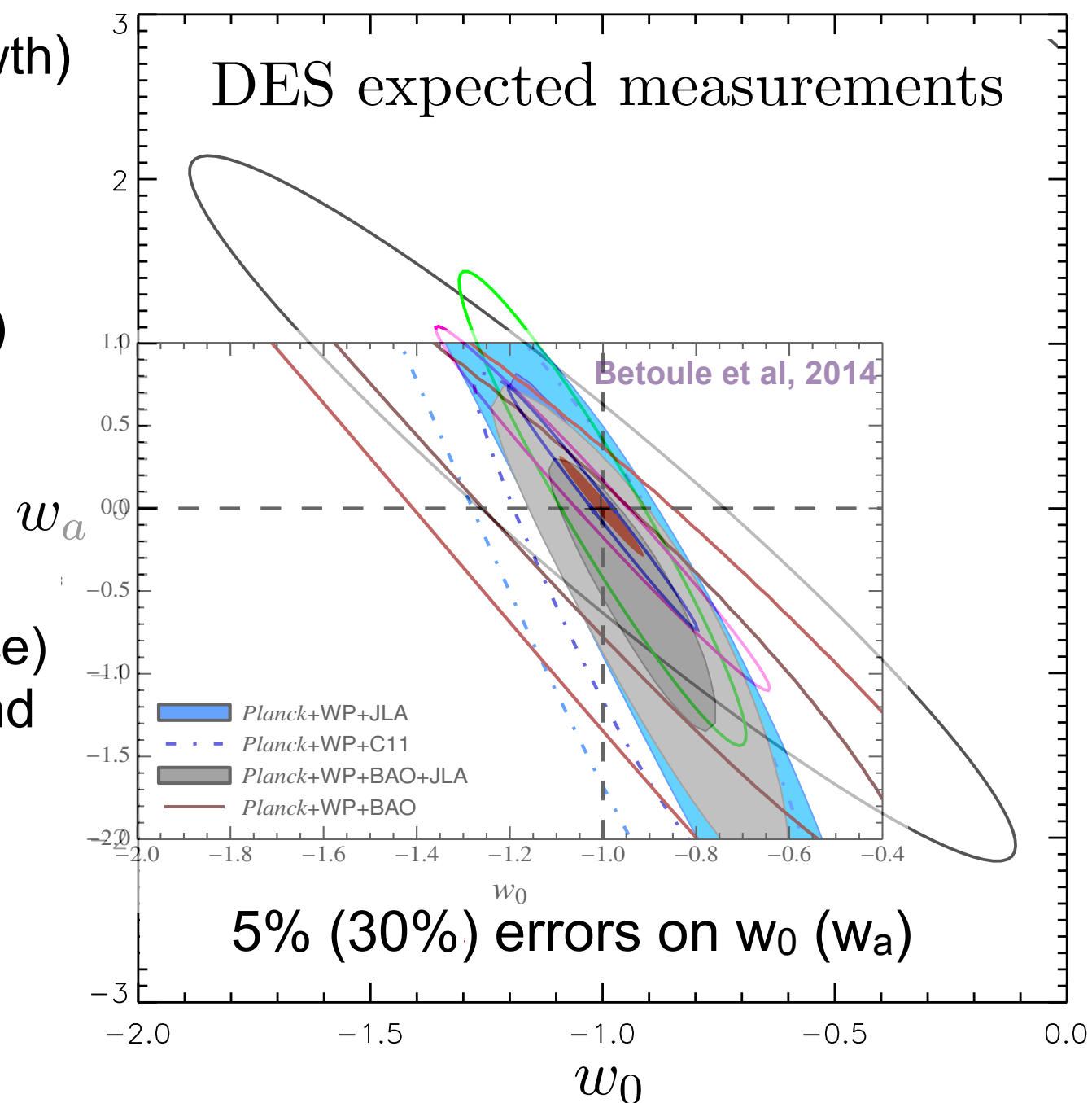
4 probes of Dark Energy

Galaxy Clusters (distance, structure growth)
ten of thousands of clusters up to $z \sim 1$
synergies with SPT, VHS

Weak lensing (distance, structure growth)
shape and measurements of 200
millions galaxies

Baryonic acoustic Oscillations (distance)
300 millions galaxies to $z=1$ and beyond

Type Ia supernovae (distance)
30 sq. deg. SN fields
3500 SNIa to $z \sim 1$





DES Timeline

DARK ENERGY
SURVEY

2003

Project start

2004-8

R&D

2008-11

DECam construction

2012 [Sept]

Installation and first light

2012 [Sept-Oct]

Commissioning

Nov 2012 - Feb 2013

Science Verification

Aug 31 2013 - 9 Feb 2014

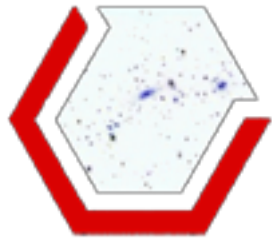
First Season (Y1)

Aug 15 2014 - Feb 2015

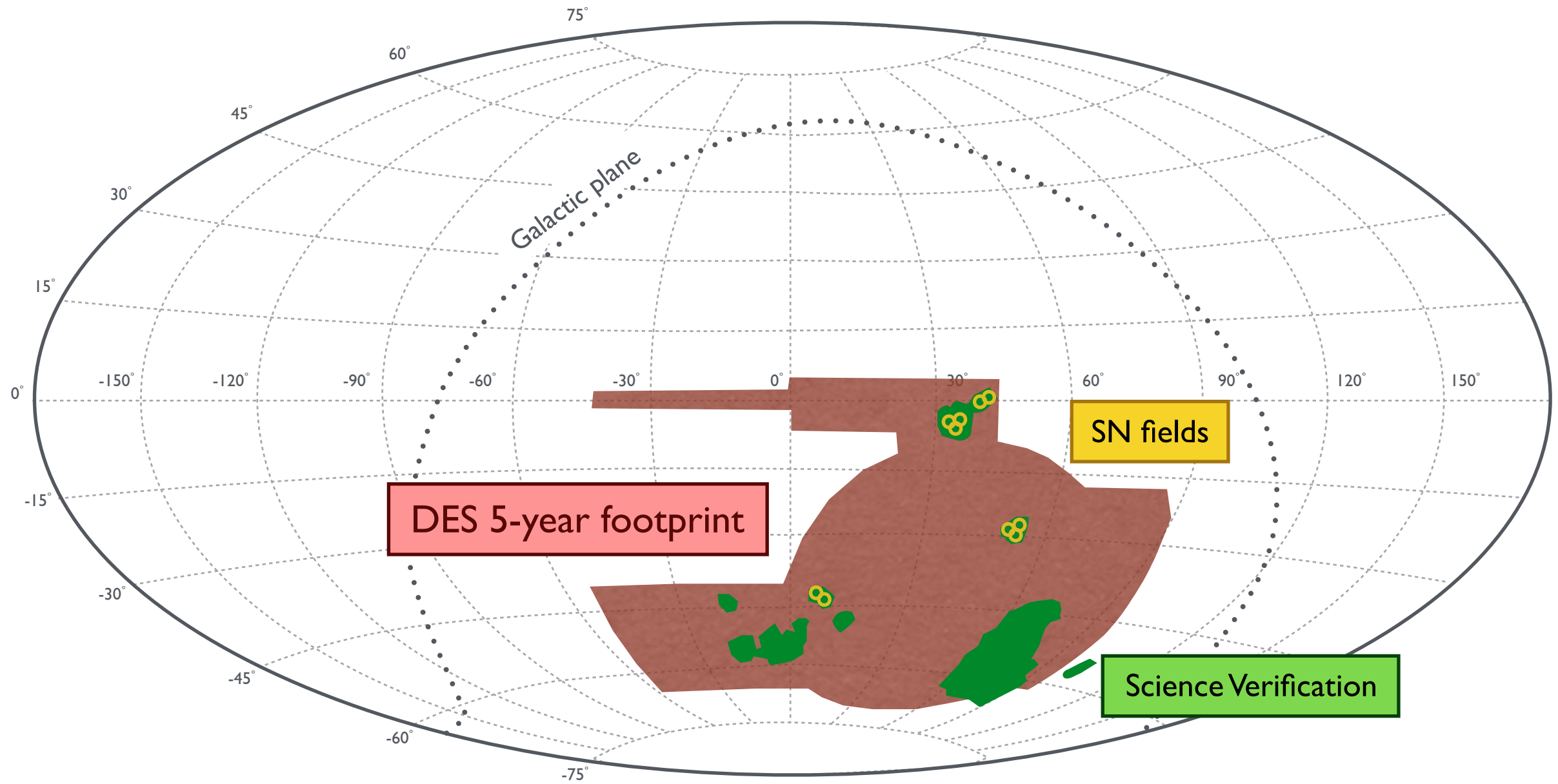
Second Season (Y2)

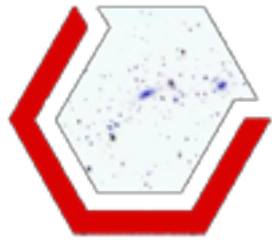
2015-2018

Third-Fifth Seasons

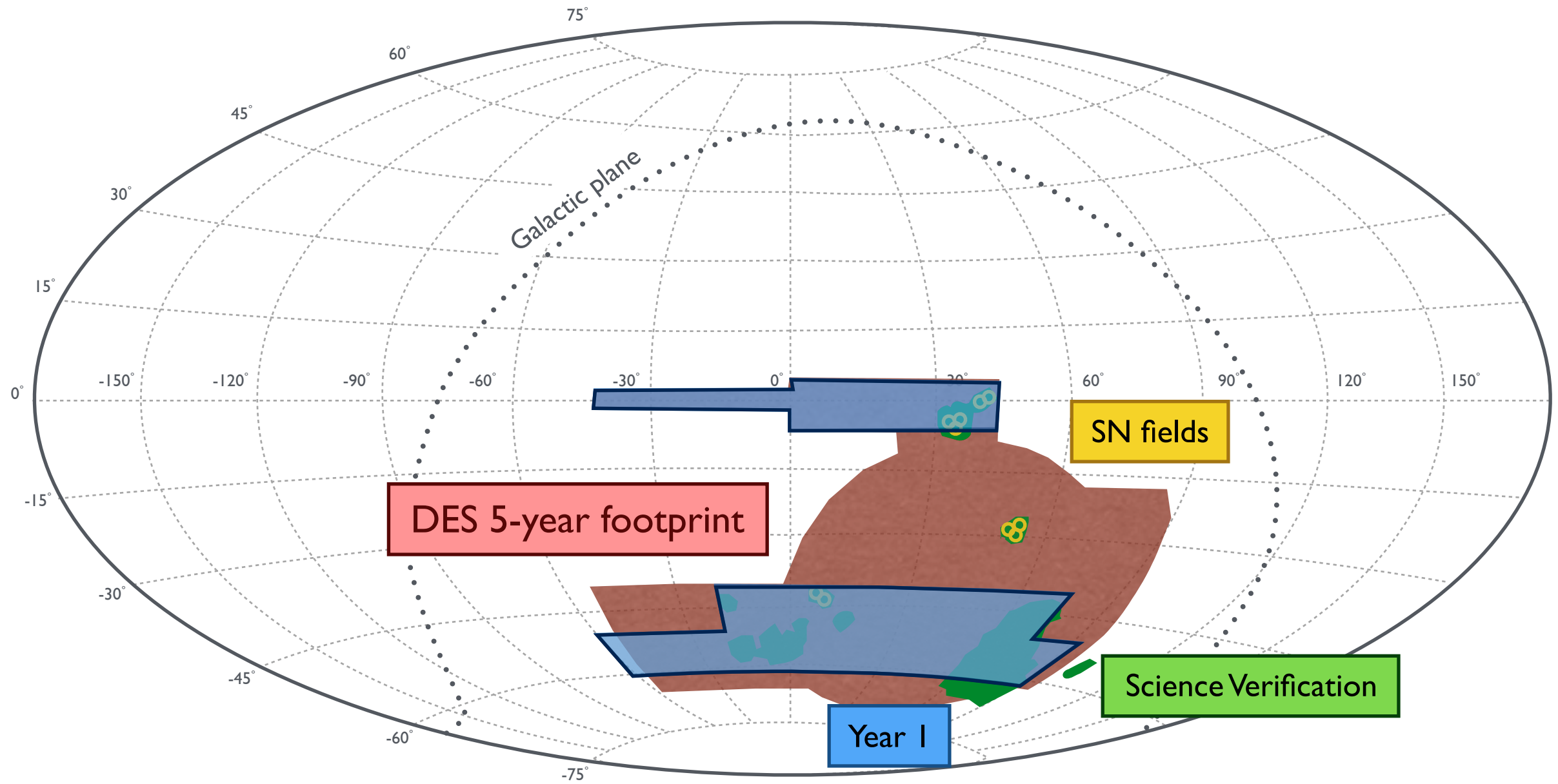


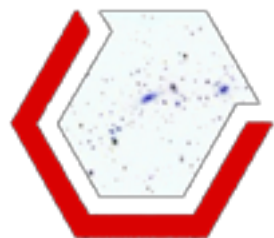
Observing strategy



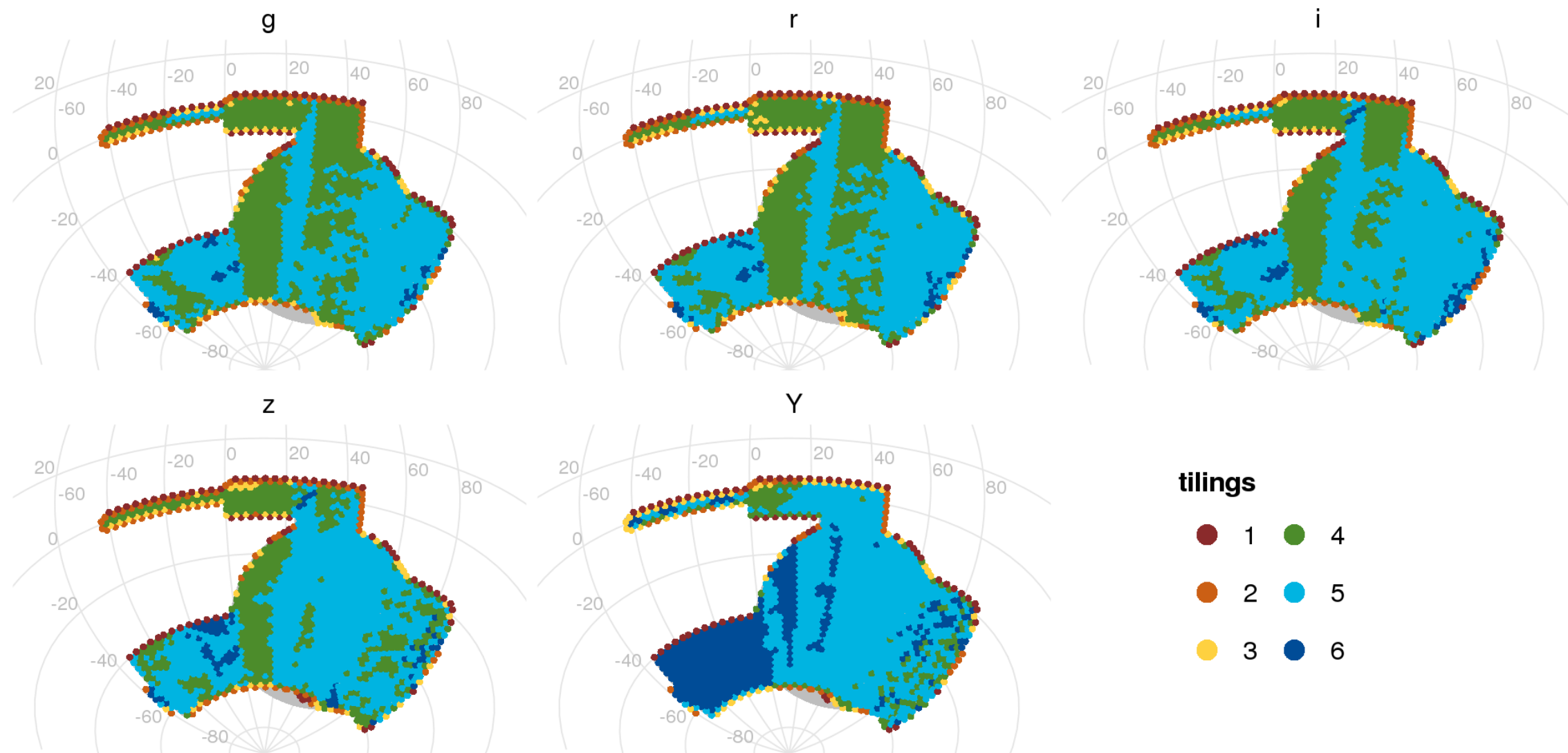


Observing strategy

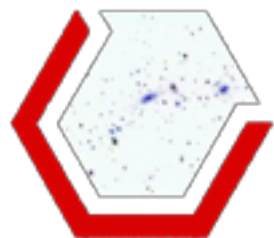




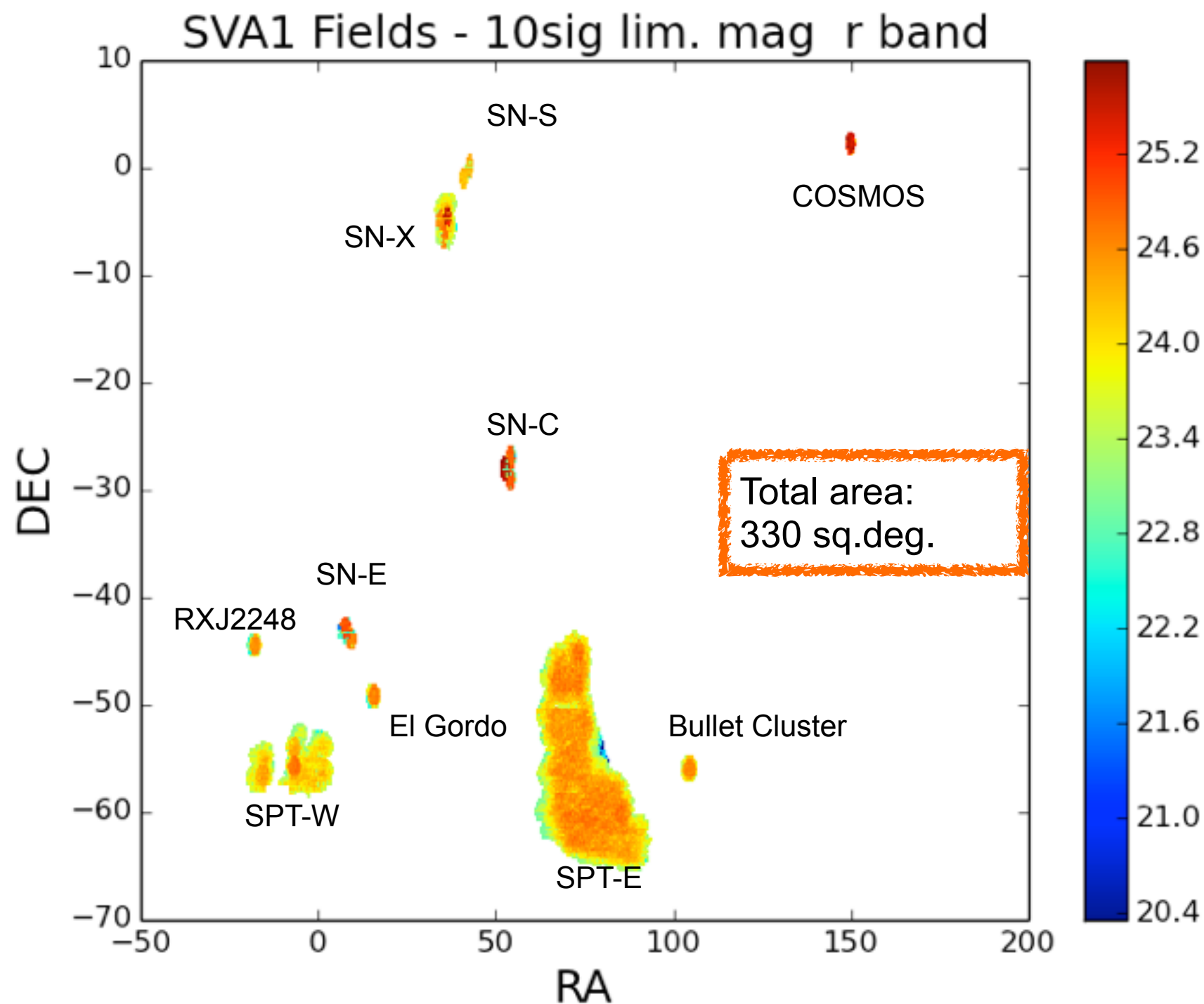
Observing strategy



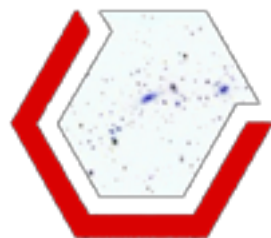
At end of Year 3 (Feb. 2016), following major El Nino
(Y4 was MUCH better)



Nov. 2012 - Feb. 2013: Science Verification campaign



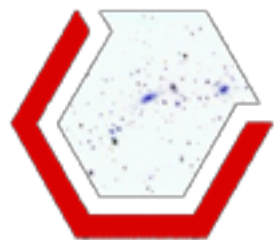
All the results presented in this talk are based on these pre-survey data



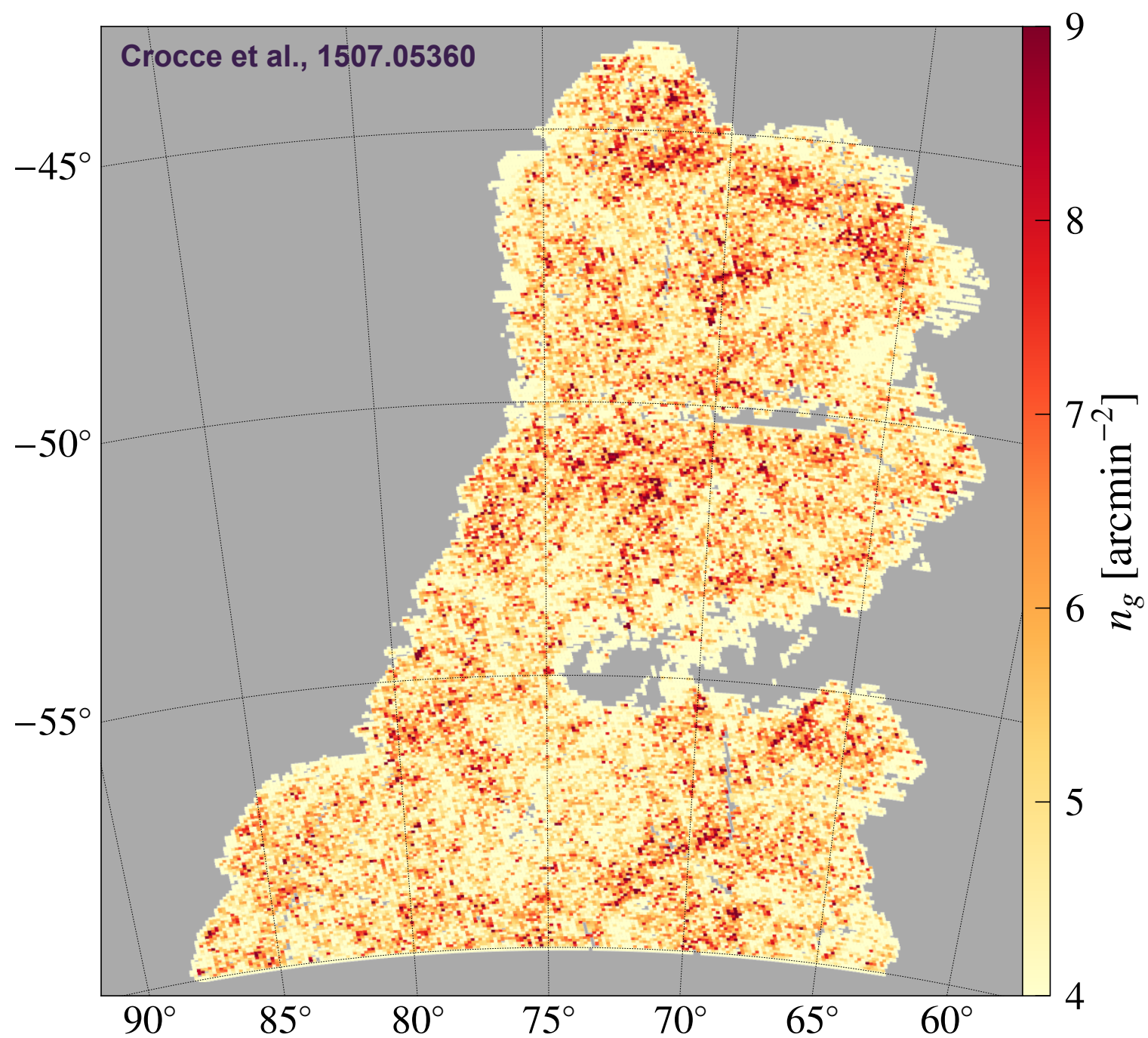
DES Early Results

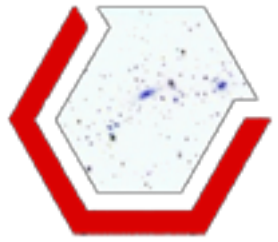
- 96 publications submitted since May 2014
- Majority of results using Science Verification data
- Various fields of astronomy represented

| | | | | |
|-----------------------------|---------------------|--|-----------------------|---------------------------|
| NGC 1398, single DECam tile | Gerdes et al. | Observation of Two New L4 Neptune Trojans in the Dark Energy Survey Supernova Fields | arXiv:1507.05177 | Solar system |
| | Park et al. | Joint Analysis of Galaxy-Galaxy Lensing and Galaxy Clustering: Methodology and Forecasts for DES | arXiv:1507.05353 | |
| | Rozo et al. | redMaGiC: Selecting Luminous Red Galaxies from the DES Science Verification Data | arXiv:1507.05460 | |
| | Giannantonio et al. | CMB lensing tomography with the DES Science Verification galaxies | arXiv:1507.05551 | |
| | Crocce et al. | Galaxy Clustering, Photometric Redshifts and Diagnosis of Systematics in the Dark Energy Survey Science Verification data | arXiv:1507.05360 | Cosmology |
| | Jarvis et al. | The Dark Energy Survey Science Verification Shear Catalog | arXiv:1507.05603 | |
| | Bonnett et al. | Photometric redshifts for weak lensing in the DES Science Verification data | arXiv:1507.05909 | photo-z |
| | Becker et al. | Cosmic Shear 2 point Measurements with DES Science Verification Data | arXiv:1507.05598 | |
| | Leistedt et al. | Mapping and simulating systematics due to spatially-varying observing conditions in DES Science Verification data | arXiv:1507.05647 | Cluster |
| | Gruen et al. | Weak lensing by galaxy troughs in DES Science Verification data | arXiv:1507.05090 | |
| | Abbott et al. | Cosmology from Cosmic Shear with DES Science Verification Data | arXiv:1507.05552 | SN Ia |
| | Kessler et al. | The Difference Imaging Pipeline for the Transient Search in the Dark Energy Survey | arXiv:1507.05137 | |
| | Saro et al. | Constraints on the Richness-Mass Relation and the Optical-SZE Positional Offset Distribution for SZE-Selected Clusters | arXiv:1506.07814 | QSO & High-z |
| | Chang et al. | Wide-Field Lensing Mass Maps from DES Science Verification Data | arXiv:1505.01871 | |
| | Reed et al. | DES J0454-4448: Discovery of the First Luminous $z \geq 6$ Quasar from the Dark Energy Survey | arXiv:1504.03264 | Milky Way |
| | Yuan et al. | OzDES multi-fibre spectroscopy for the Dark Energy Survey: first-year operation and results | arXiv:1504.03039 | |
| | Vikram et al. | Wide-Field Lensing Mass Maps from DES Science Verification Data: Methodology and Detailed Analysis | arXiv:1504.03002 | SV papers (as of July 15) |
| | Zhang et al. | Galaxies in X-ray Selected Clusters and Groups in Dark Energy Survey Data: Stellar Mass Growth of Bright Central Galaxies Since $z \sim 1.2$ | arXiv:1504.02983 | |
| | Poci et al. | DESIAlert: Enabling Real-Time Transient Follow-Up with Dark Energy Survey Data | arXiv:1504.02996 | |
| | Goldstein et al. | Automated Transient Identification in the Dark Energy Survey | arXiv:1504.02936 | |
| | Flaugher et al. | The Dark Energy Camera | arXiv:1504.02900 | |
| | Simon et al. | Stellar Kinematics and Metallicities in the Ultra-Faint Dwarf Galaxy Reticulum II | arXiv:1504.02889 | |
| | Bruderer et al. | Calibrated Ultra Fast Image Simulations for the Dark Energy Survey | arXiv:1504.02778 | |
| | Fermi LAT + DES | Search for Gamma-Ray Emission from DES Dwarf Spheroidal Galaxy Candidates with Fermi-LAT Data | arXiv:1503.02632 | |
| | Bechtörl et al. | Eight New Milky Way Companions Discovered in First-Year Dark Energy Survey Data | arXiv:1503.02584 | |
| | Balbinot et al. | The LMC geometry and outer stellar populations from early DES data | MNRAS 449 (2015) 1129 | |
| | Papadopoulos et al. | DES J1352+0000: The First Superluminous Supernova from the Dark Energy Survey | MNRAS 449 (2015) 1215 | |
| | Banerji et al. | Combining Dark Energy Survey Science Verification Data with Near Infrared Data from the ESO VISTA Hemisphere Survey | MNRAS 446 (2015) 2523 | |
| | Sanchez et al. | Photometric redshift analysis in the Dark Energy Survey Science Verification data | MNRAS 445 (2014) 1482 | |
| | Melchior et al. | Mass and galaxy distributions of four massive galaxy clusters from Dark Energy Survey Science Verification data | MNRAS 449 (2015) 2219 | |

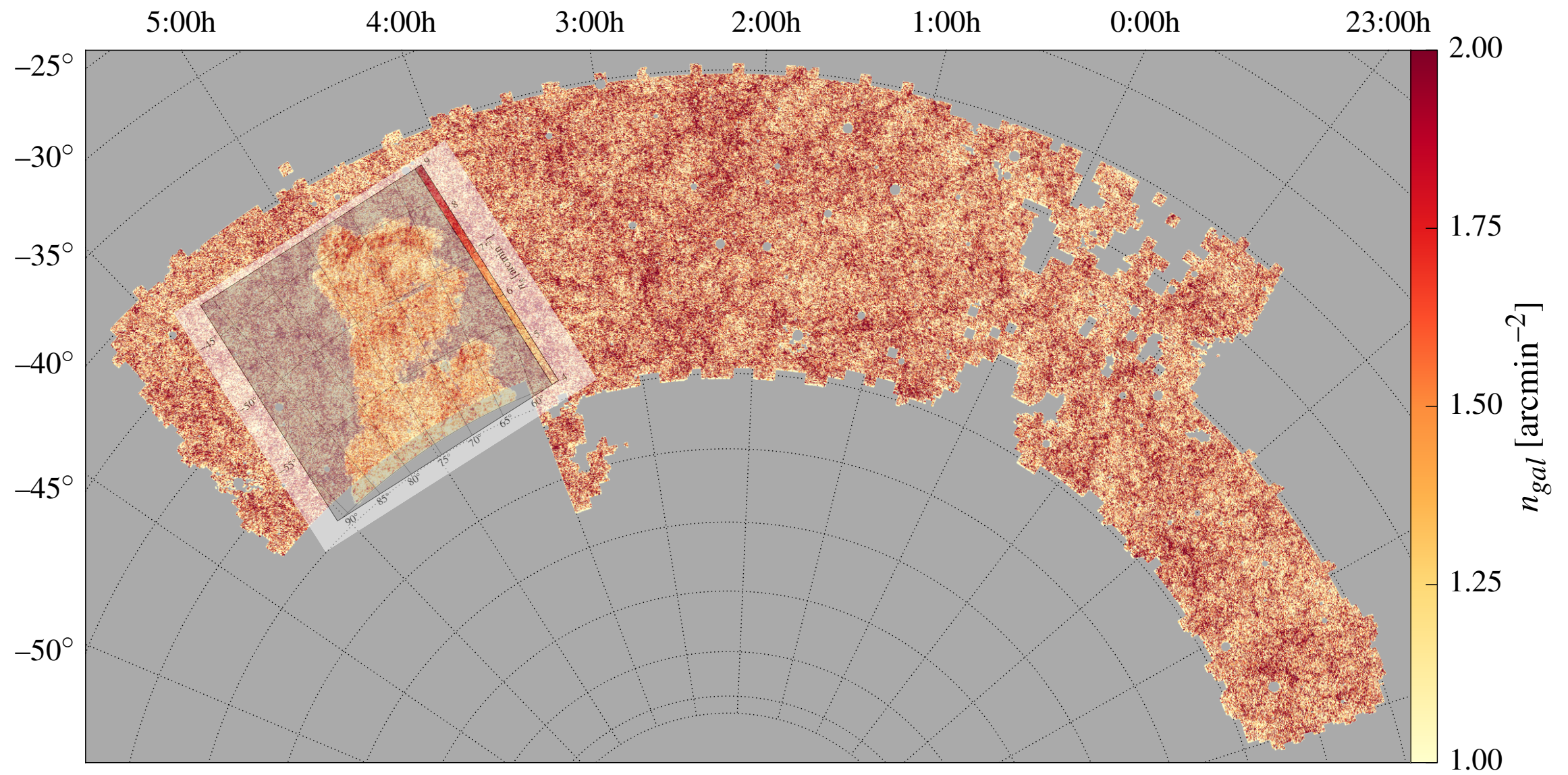


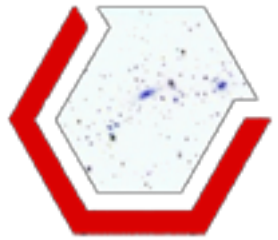
The DES SV galaxy catalog





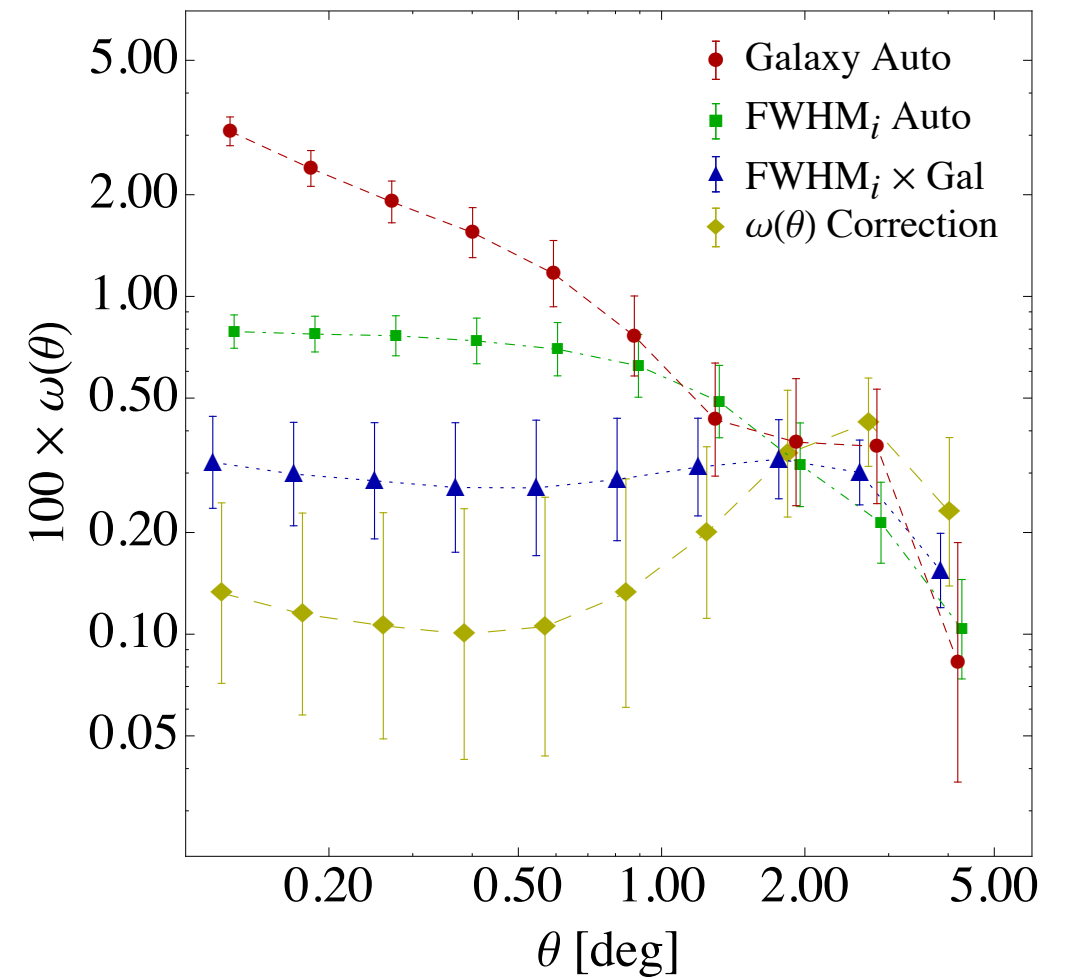
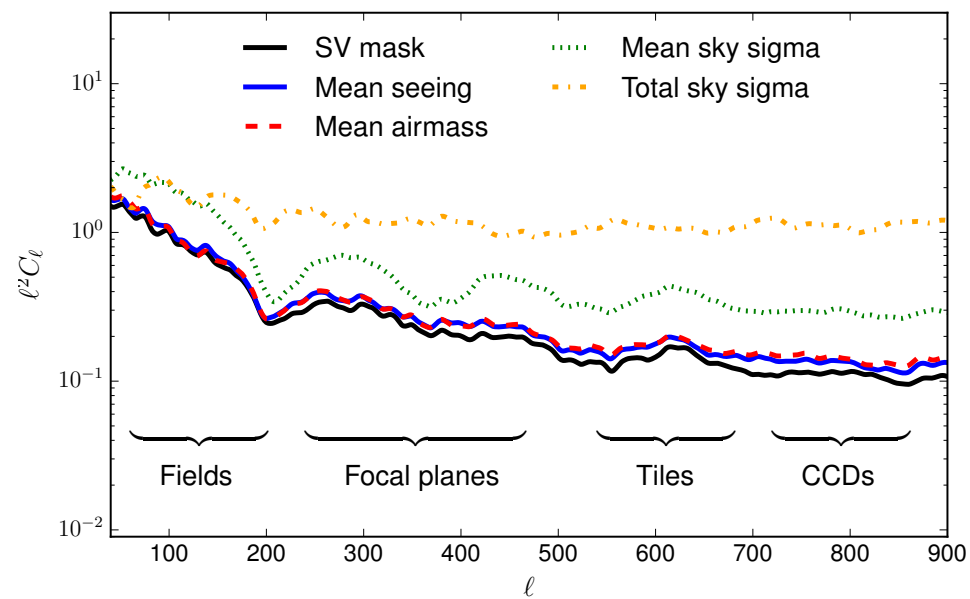
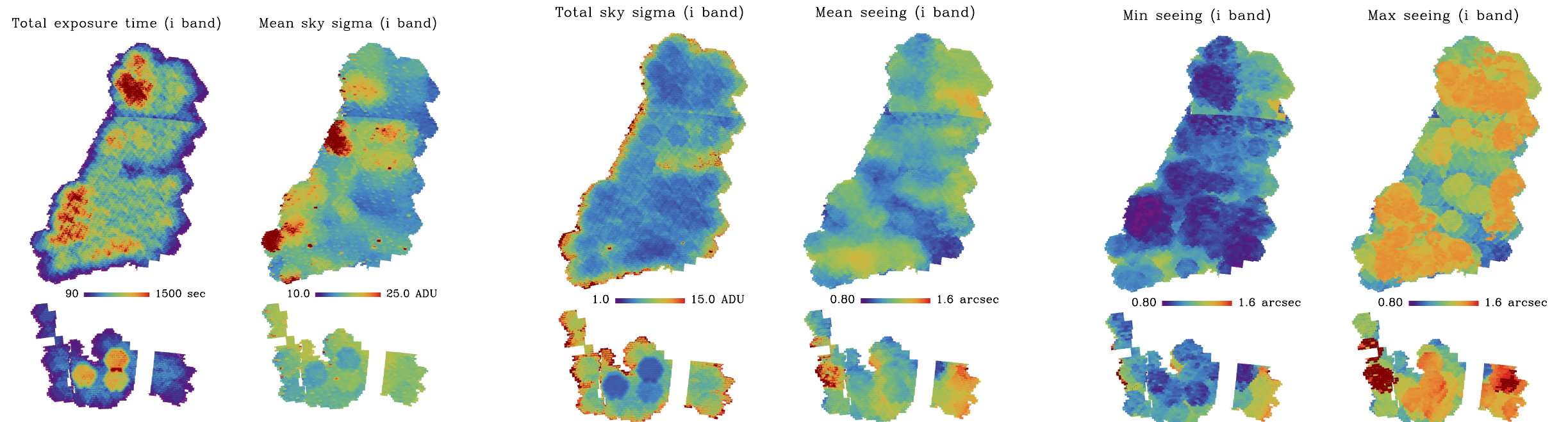
The DES Y1 galaxy catalog

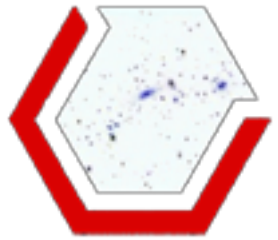




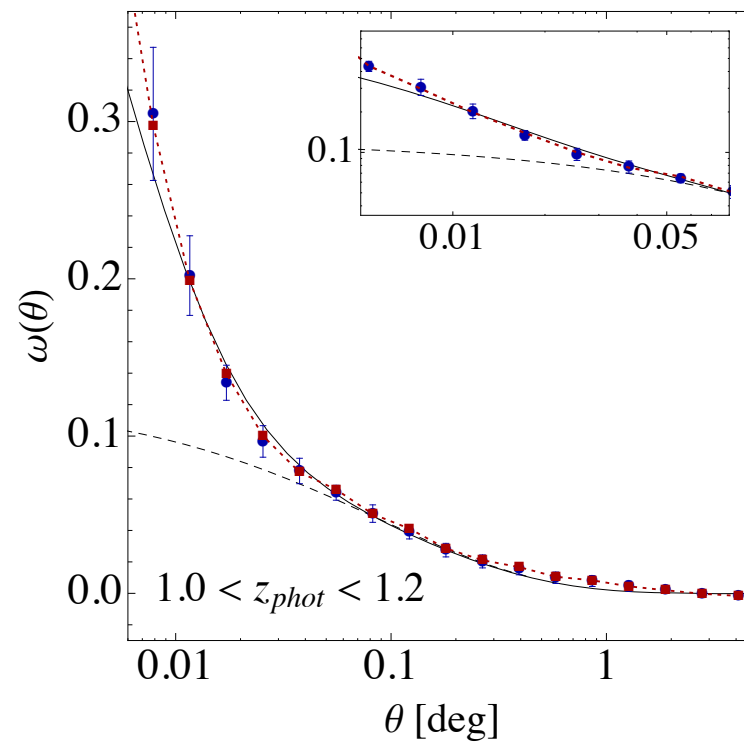
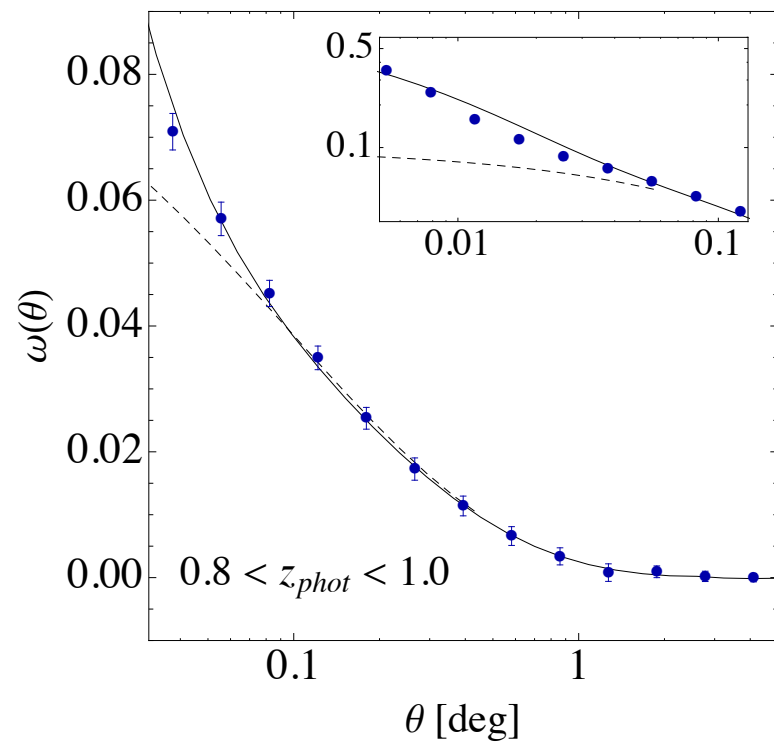
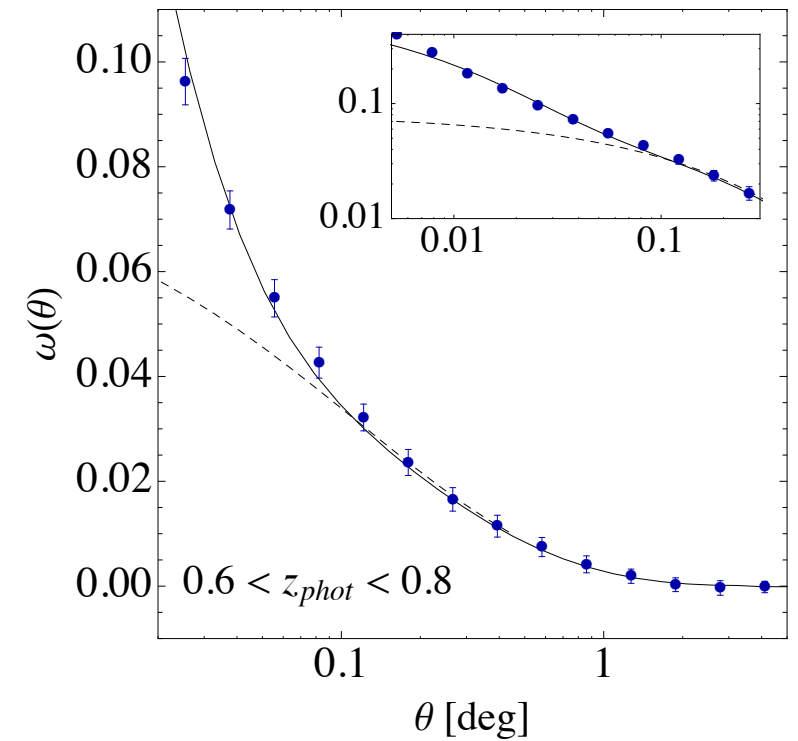
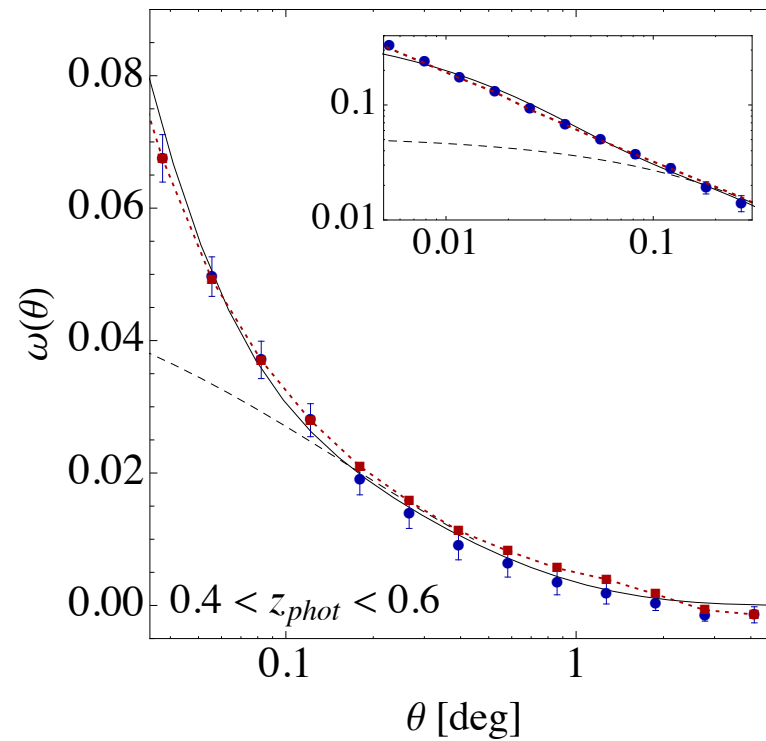
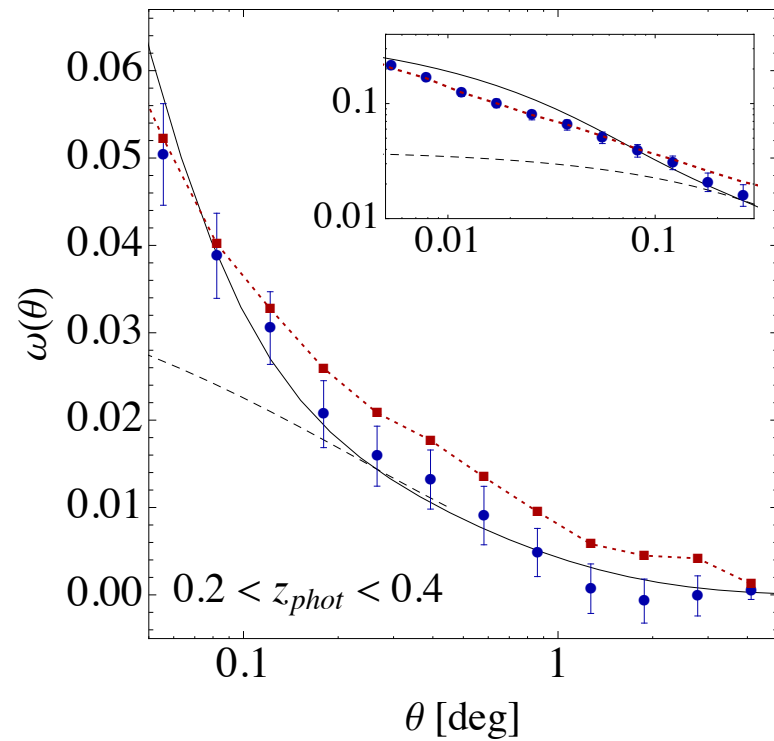
Systematics maps

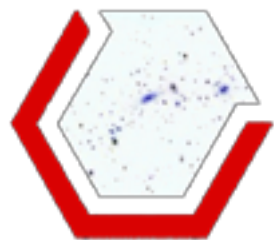
Leistedt, Peiris, Elsner, Benoit-Lévy, et al., 1507.05360





Galaxy clustering, photometric redshifts and diagnosis of systematics in the DES Science Verification data

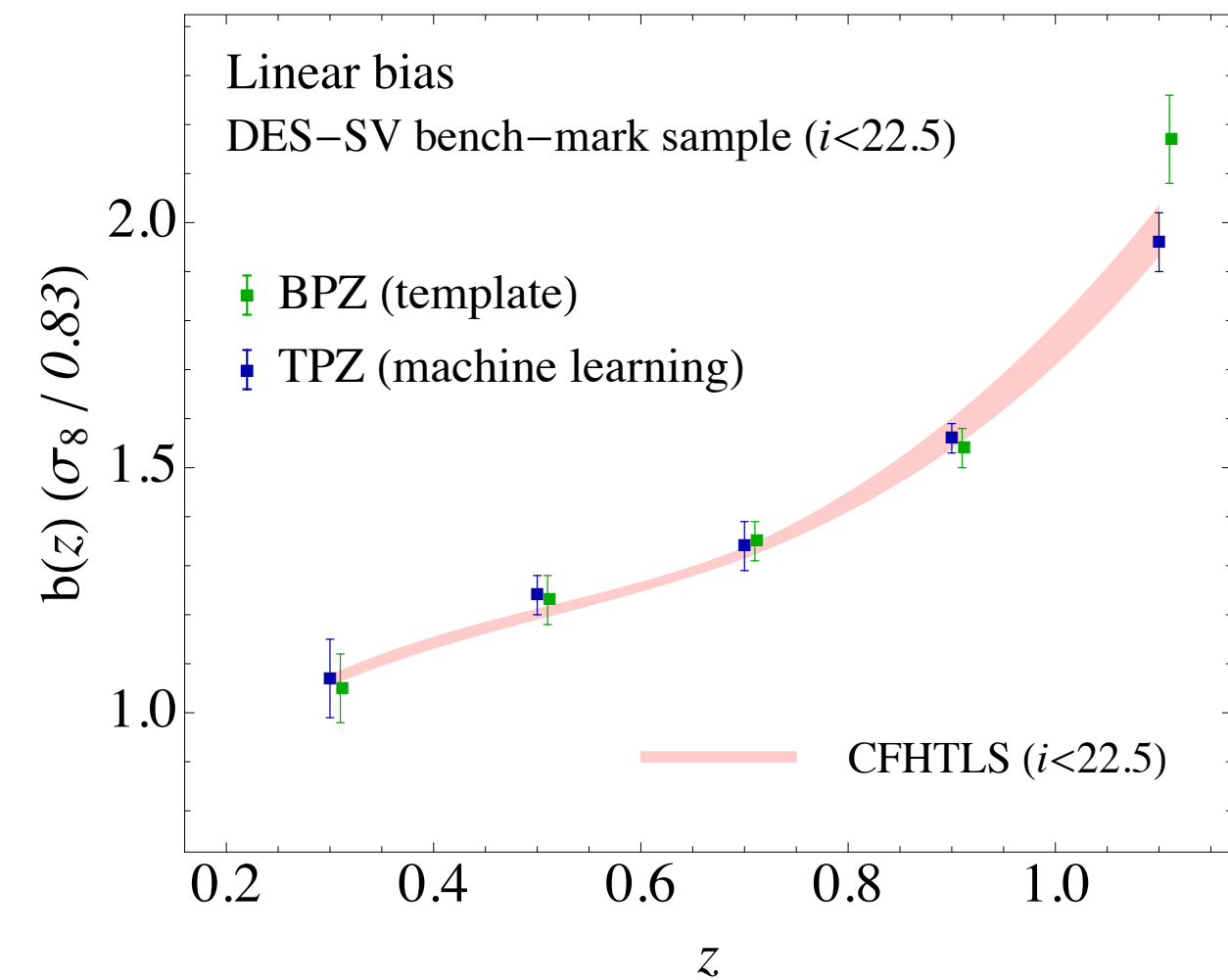




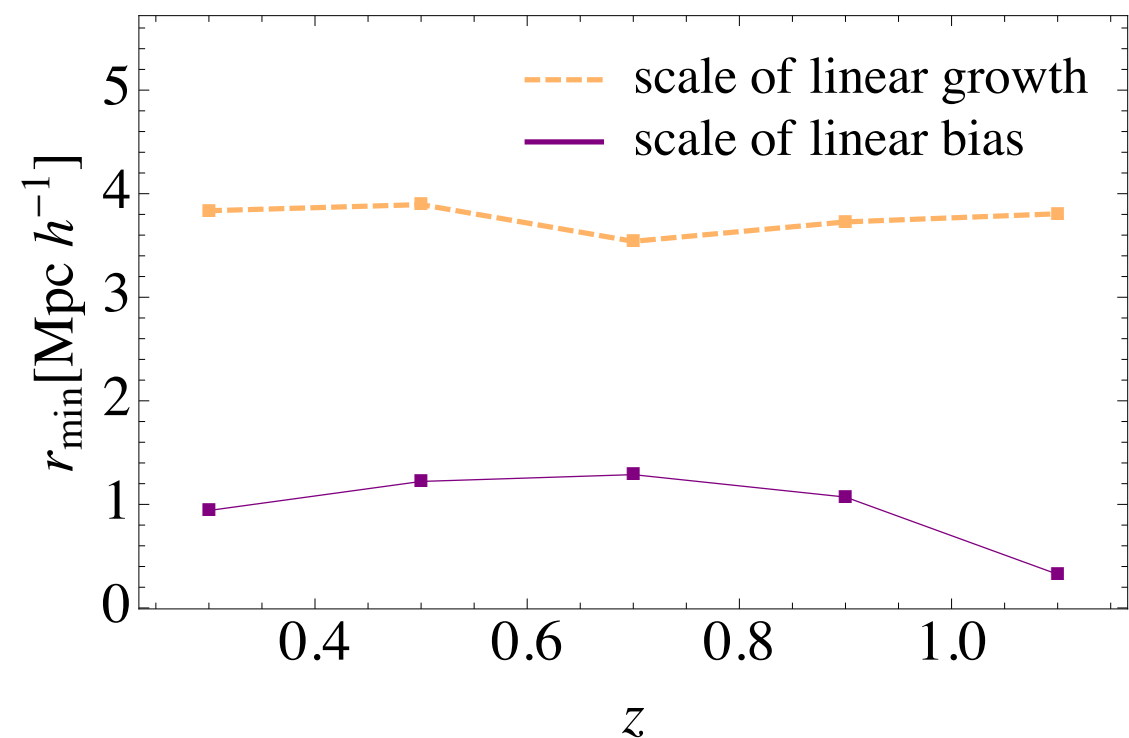
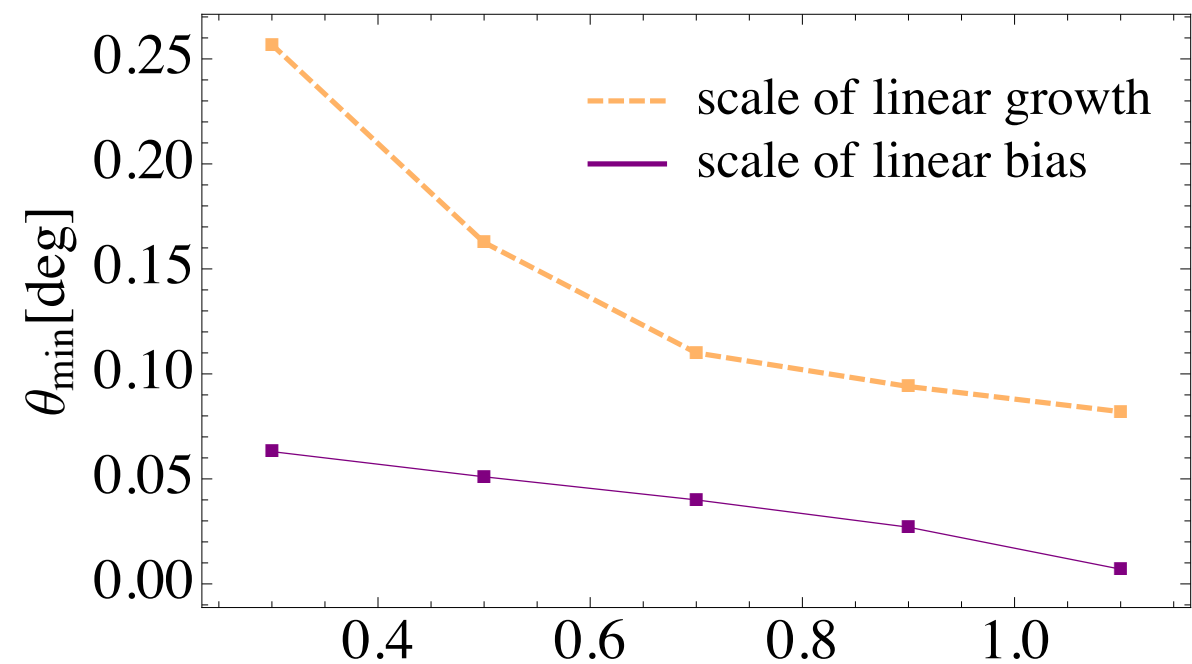
Galaxy clustering, photometric redshifts and diagnosis of systematics in the DES Science Verification data

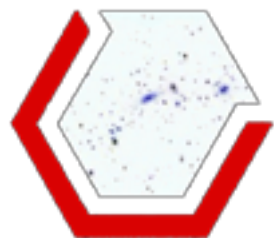
Comparison with CFHTLS

(Coupon *et al.* 2012)



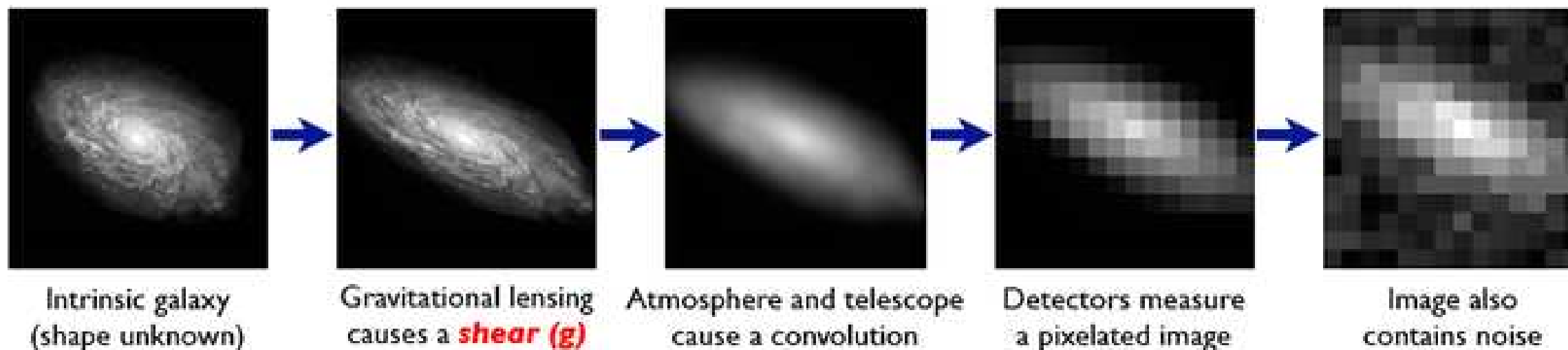
Linear scale “breakings”



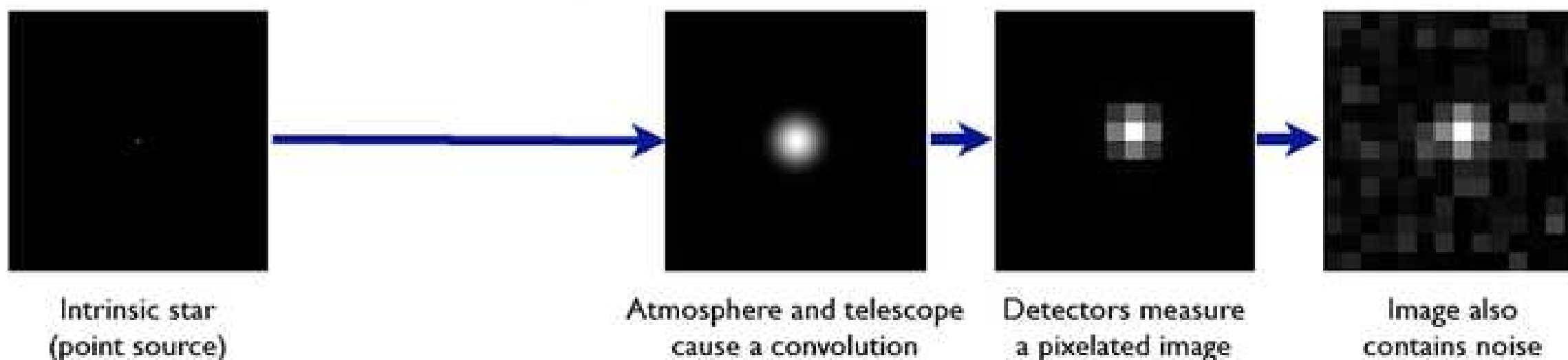


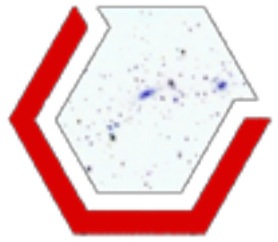
The Forward Process.

Galaxies: Intrinsic galaxy shapes to measured image:

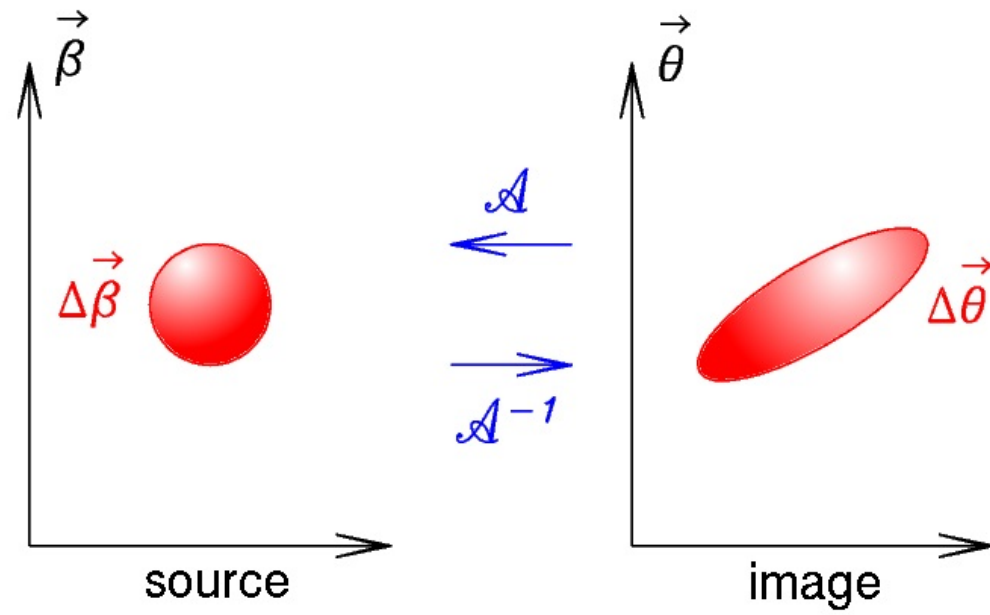


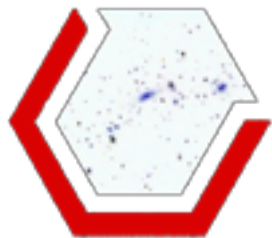
Stars: Point sources to star images:



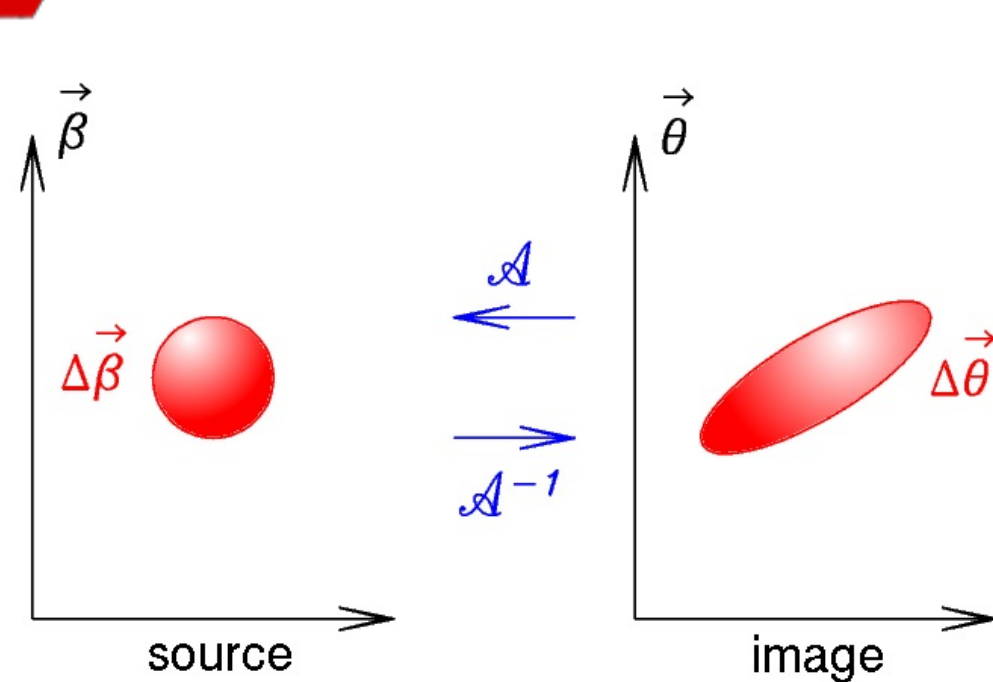




From measurements to mass maps



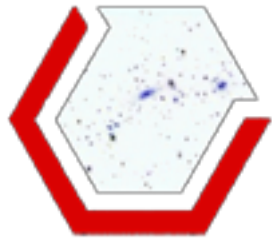


From measurements to mass maps

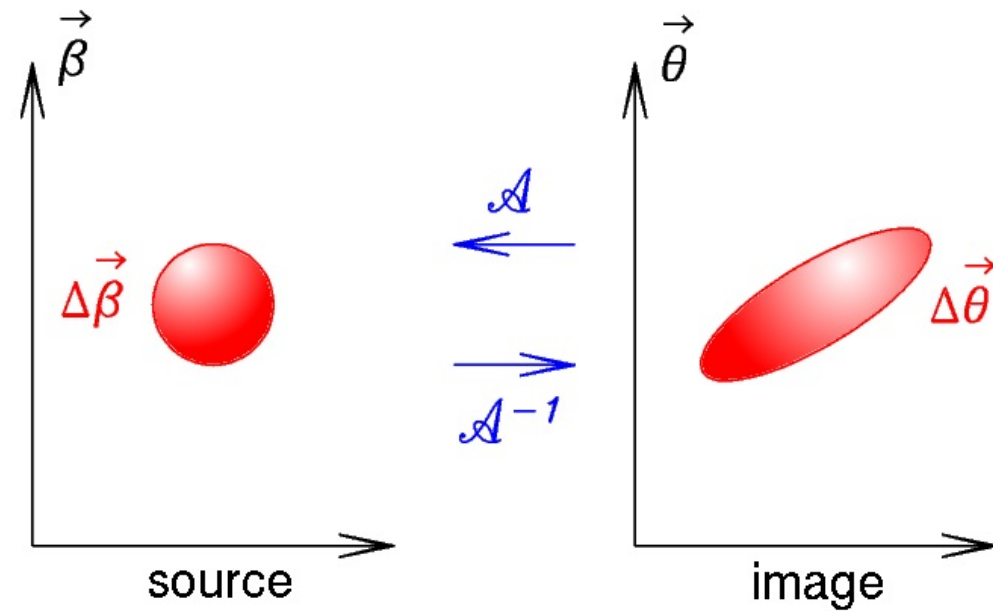


 convergence
 shear

$$\mathcal{A}(\theta) = \begin{pmatrix} 1 - \text{convergence} - \text{shear}_1 & -\text{shear}_2 \\ -\text{shear}_2 & 1 - \text{convergence} + \text{shear}_1 \end{pmatrix}$$



From measurements to mass maps

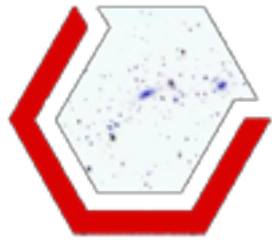


- convergence
- shear
- lensing potential

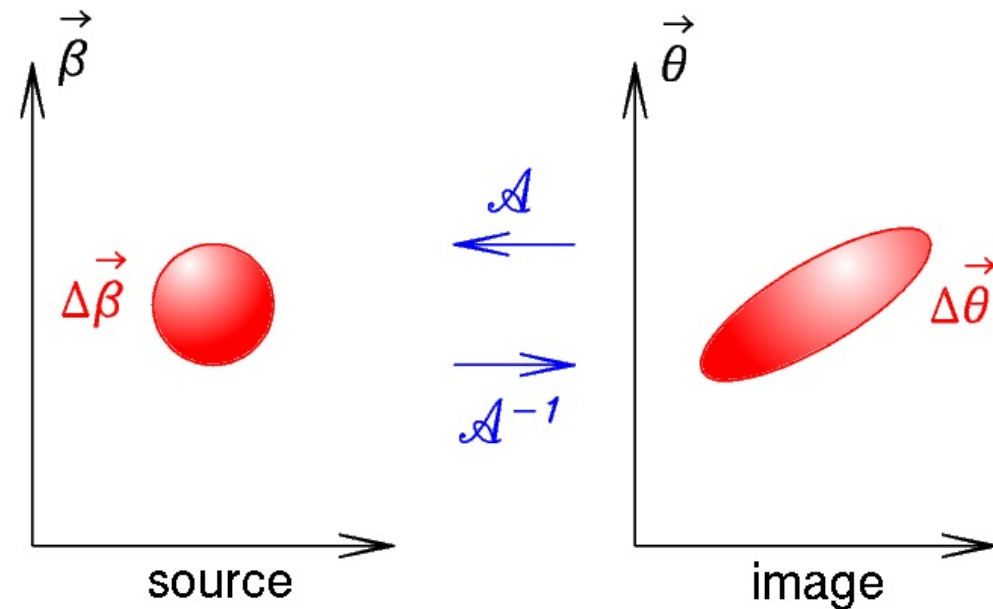
$$\mathcal{A}(\theta) = \begin{pmatrix} 1 - \kappa - \gamma_1 & -\gamma_2 \\ -\gamma_2 & 1 - \kappa + \gamma_1 \end{pmatrix}$$

$$\gamma = \gamma_1 + i\gamma_2 = \frac{1}{2} (\psi_{,11} - \psi_{,22}) + i\psi_{,12},$$

$$\kappa = \frac{1}{2} \nabla^2 \psi = \frac{1}{2} (\psi_{,11} + \psi_{,22}).$$



From measurements to mass maps



- convergence
- shear
- lensing potential

$$\mathcal{A}(\theta) = \begin{pmatrix} 1 - \textcolor{blue}{\kappa} - \textcolor{red}{\gamma}_1 & -\textcolor{red}{\gamma}_2 \\ -\textcolor{red}{\gamma}_2 & 1 - \textcolor{blue}{\kappa} + \textcolor{red}{\gamma}_1 \end{pmatrix}$$

$$\textcolor{red}{\gamma} = \textcolor{red}{\gamma}_1 + i\textcolor{red}{\gamma}_2 = \frac{1}{2} (\textcolor{green}{\psi}_{,11} - \textcolor{green}{\psi}_{,22}) + i\textcolor{green}{\psi}_{,12},$$

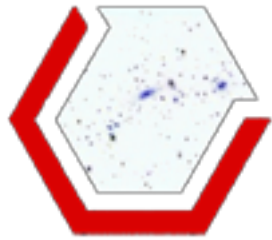
$$\textcolor{blue}{\kappa} = \frac{1}{2} \nabla^2 \textcolor{green}{\psi} = \frac{1}{2} (\textcolor{green}{\psi}_{,11} + \textcolor{green}{\psi}_{,22}).$$

$$\textcolor{green}{\psi}(\theta, r) = -2 \int_0^r dr' \frac{r - r'}{rr'} \Phi(\theta, r').$$

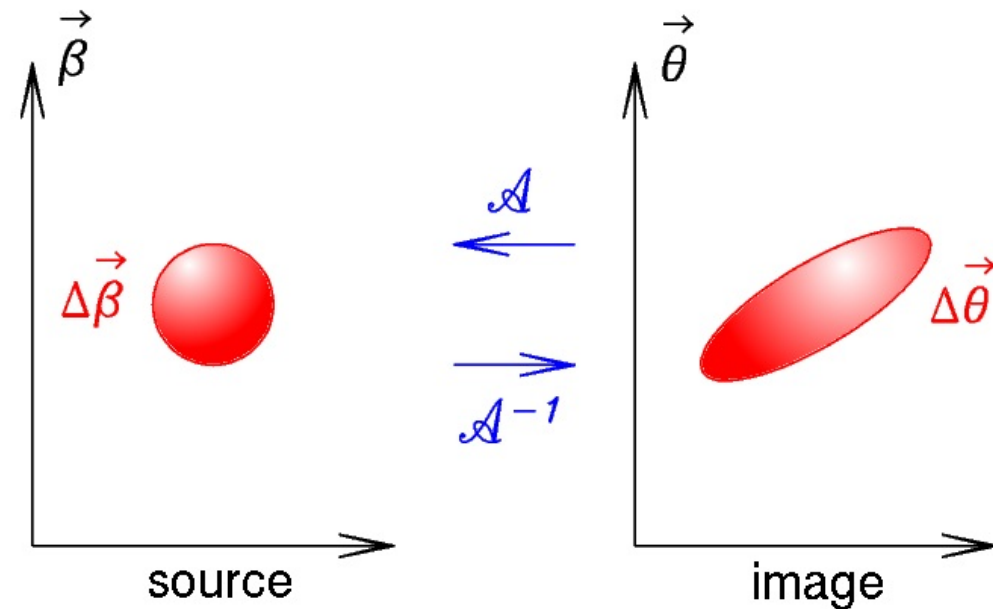
↘
 Gravitational potential
 of LSS

$$\textcolor{blue}{\kappa}(\theta, r) = \frac{3H_0^2 \Omega_m}{2c^2} \int_0^r dr' \frac{(r - r')r'}{r} \frac{\delta(\theta, r')}{a(r')}.$$

↘
 Matter density contrast



From measurements to mass maps



- convergence
- shear
- lensing potential

$$\mathcal{A}(\theta) = \begin{pmatrix} 1 - \textcolor{blue}{\kappa} - \textcolor{red}{\gamma}_1 & -\textcolor{red}{\gamma}_2 \\ -\textcolor{red}{\gamma}_2 & 1 - \textcolor{blue}{\kappa} + \textcolor{red}{\gamma}_1 \end{pmatrix}$$

$$\textcolor{red}{\gamma} = \textcolor{red}{\gamma}_1 + i\textcolor{red}{\gamma}_2 = \frac{1}{2} (\textcolor{green}{\psi}_{,11} - \textcolor{green}{\psi}_{,22}) + i\textcolor{green}{\psi}_{,12},$$

$$\textcolor{blue}{\kappa} = \frac{1}{2} \nabla^2 \textcolor{green}{\psi} = \frac{1}{2} (\textcolor{green}{\psi}_{,11} + \textcolor{green}{\psi}_{,22}).$$

$$\textcolor{green}{\psi}(\theta, r) = -2 \int_0^r dr' \frac{r - r'}{rr'} \Phi(\theta, r').$$

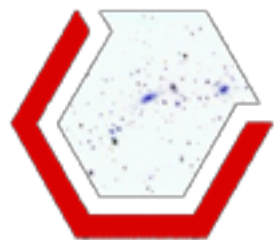
Gravitational potential
of LSS

$$\textcolor{blue}{\kappa}(\theta, r) = \frac{3H_0^2 \Omega_m}{2c^2} \int_0^r dr' \frac{(r - r')r'}{r} \frac{\delta(\theta, r')}{a(r')}.$$

Matter density contrast

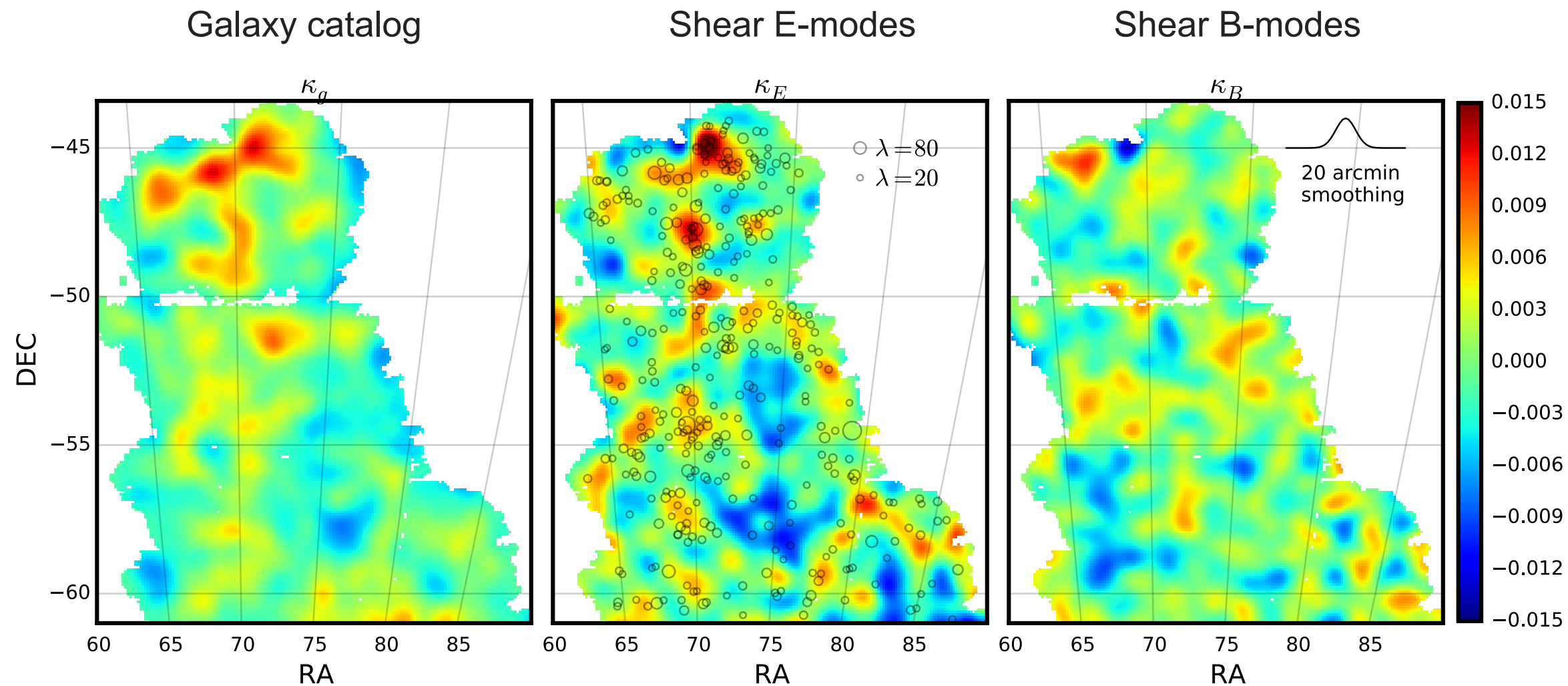
It gets simpler in Fourier space:

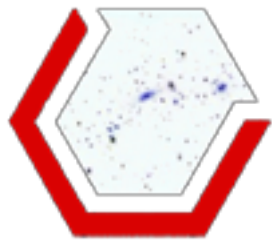
$$\textcolor{blue}{\hat{\kappa}}_l = D_l^* \textcolor{red}{\hat{\gamma}}_l, \quad \text{Kaiser \& Squires, 93}$$



Wide-Field Lensing Mass Maps from DES Science Verification Data

Convergence maps reconstructed from





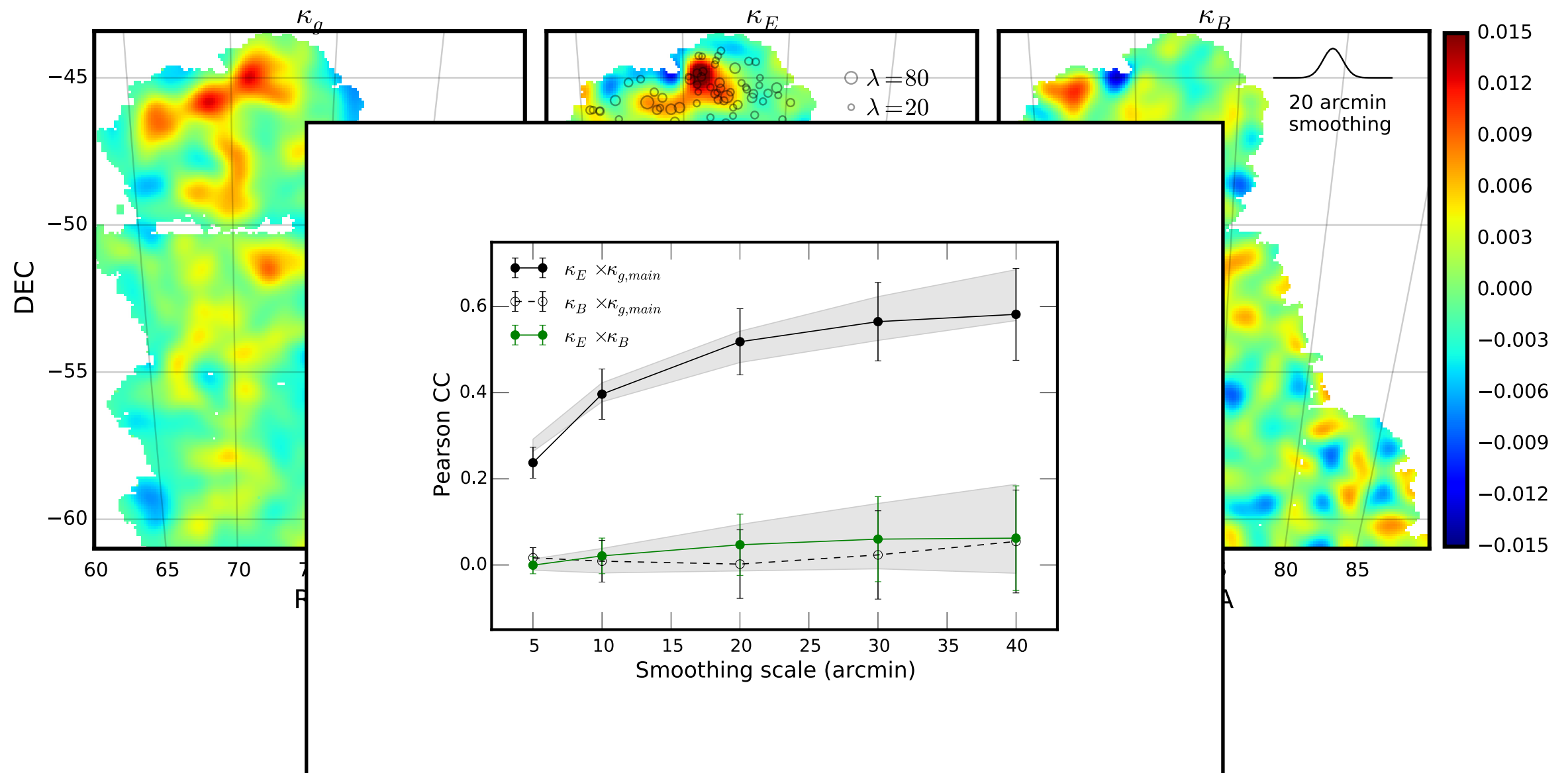
Wide-Field Lensing Mass Maps from DES Science Verification Data

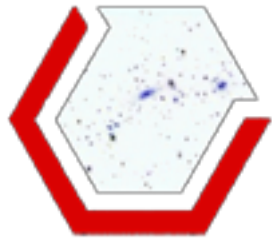
Convergence maps reconstructed from

Galaxy catalog

Shear E-modes

Shear B-modes



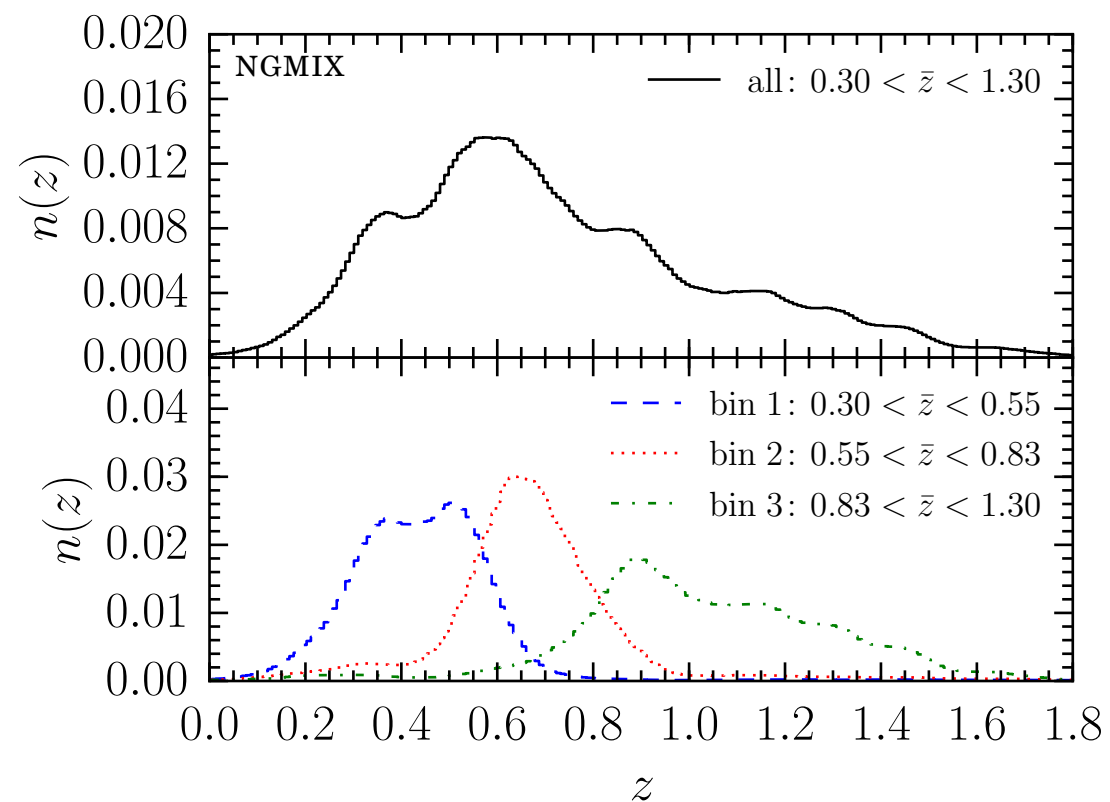


The DES weak lensing catalog

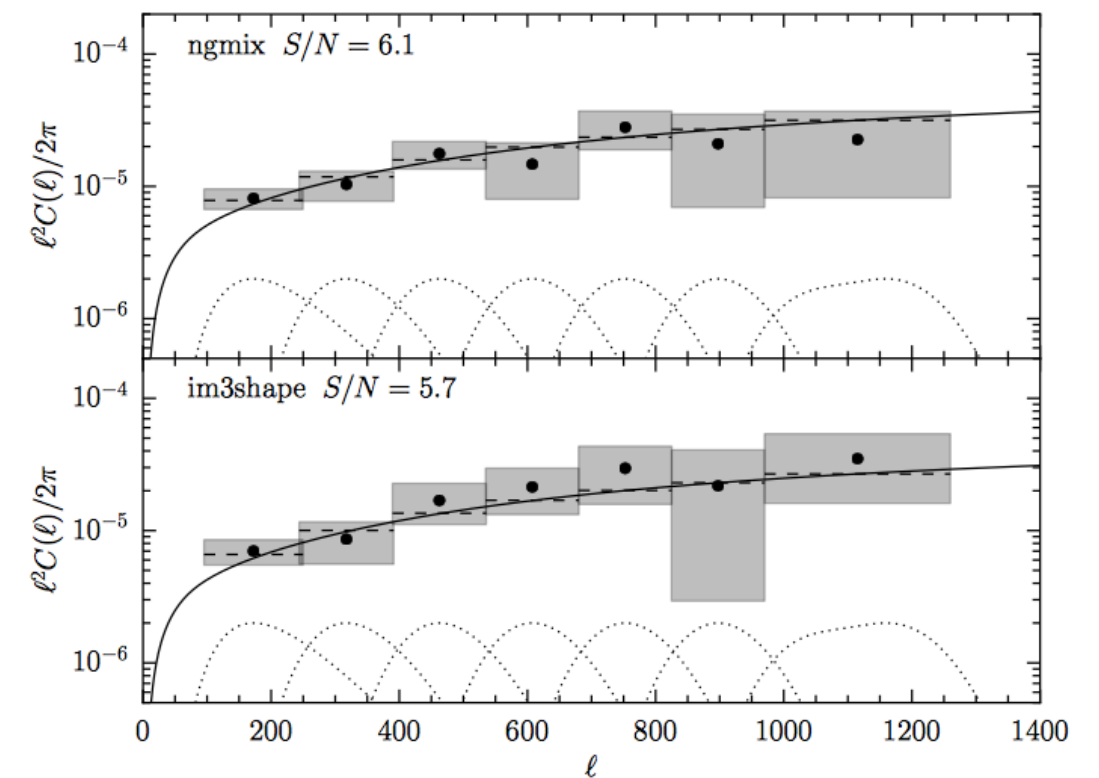
Shape measurements from single-epoch images

Two pipelines: ngmix (3.44m) and im3shape (2.12m) over ~ 140 sq.deg.

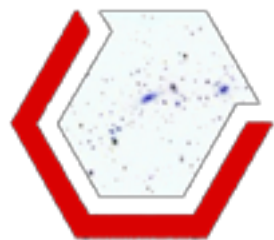
Redshift distributions



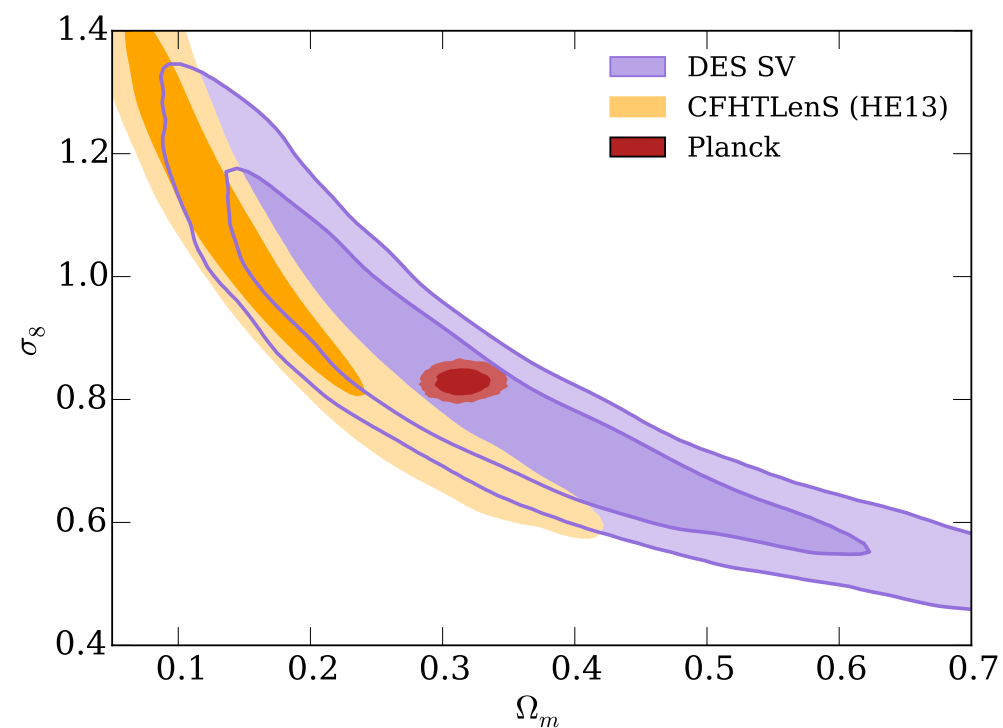
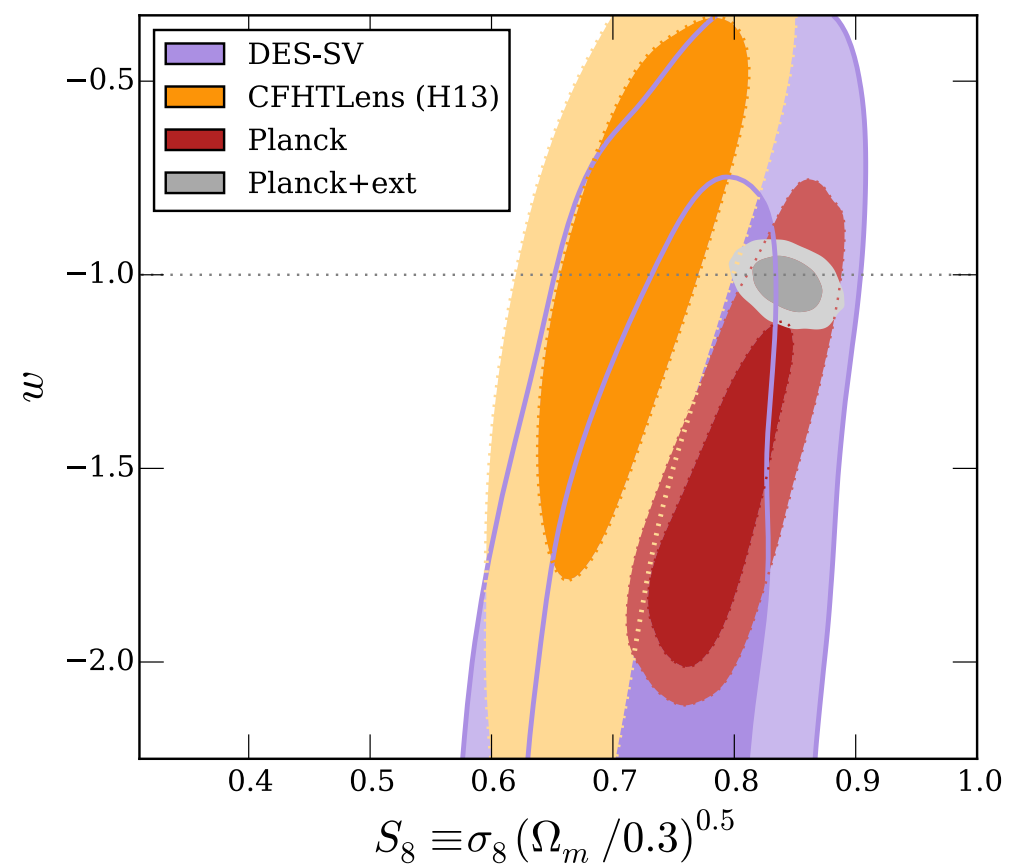
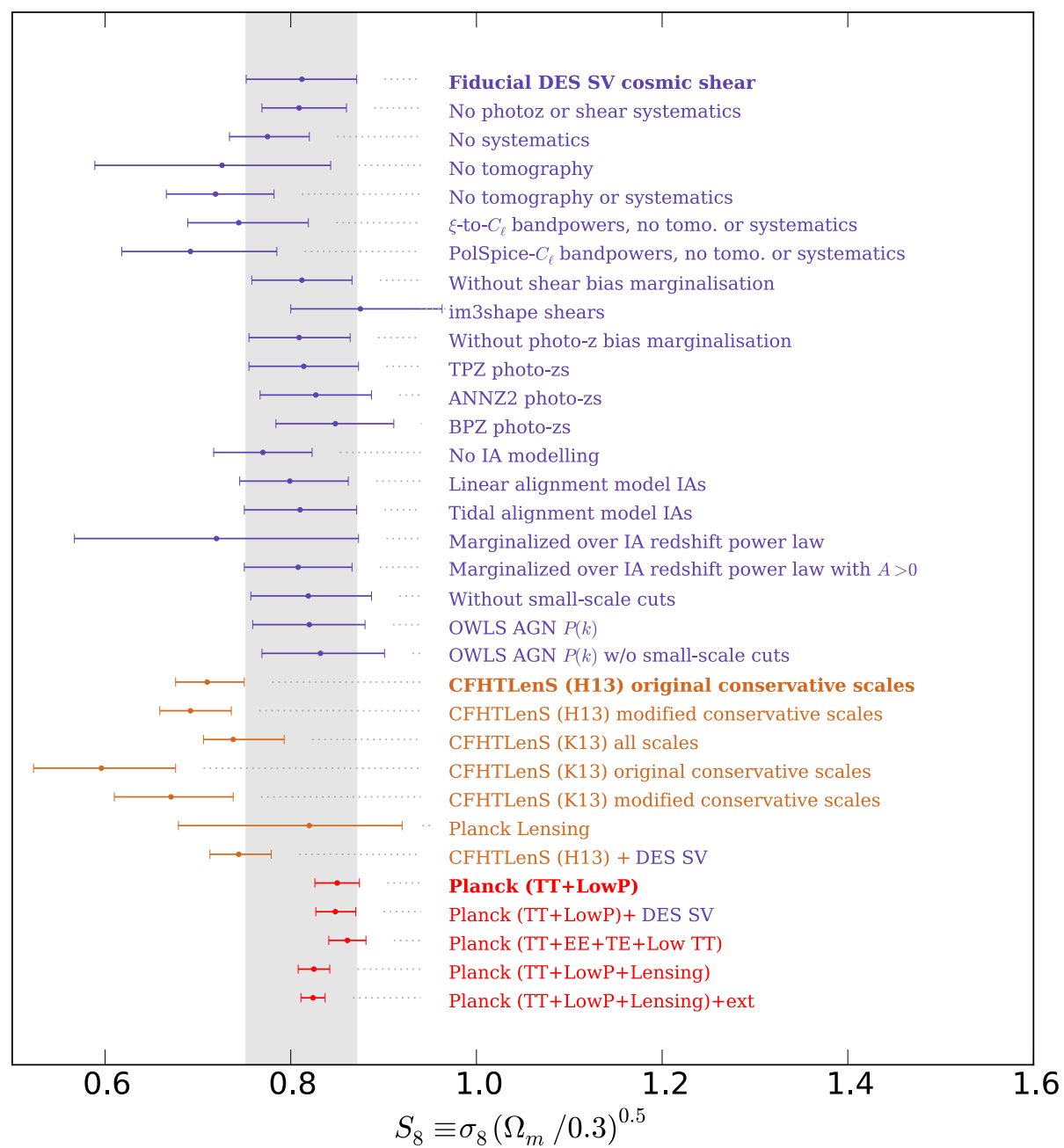
Shear-Shear power spectrum

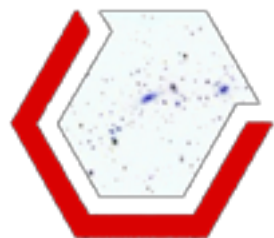


Jarvis et al., 1507.05603
 Becker et al, 1507.05598
 Bonnet et al, 1507.05909
 DES collaboration, 1507.05552



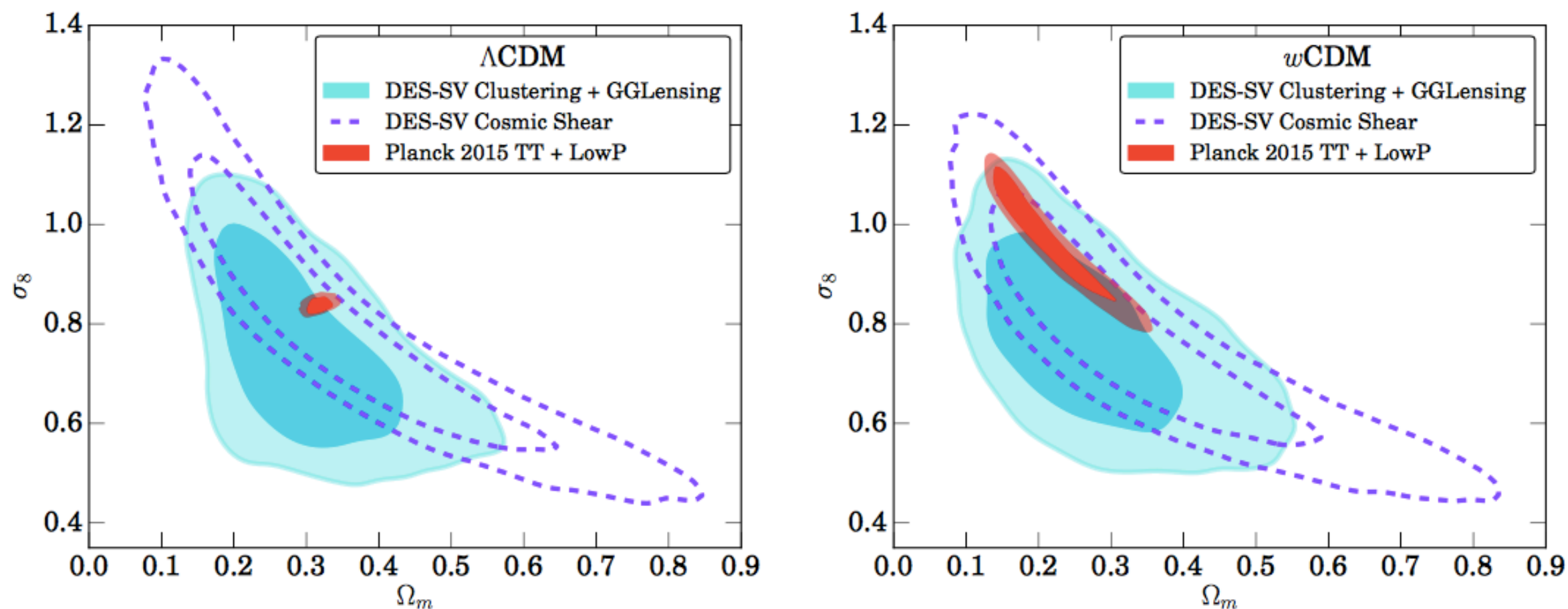
Weak lensing: cosmology results





Combining probes

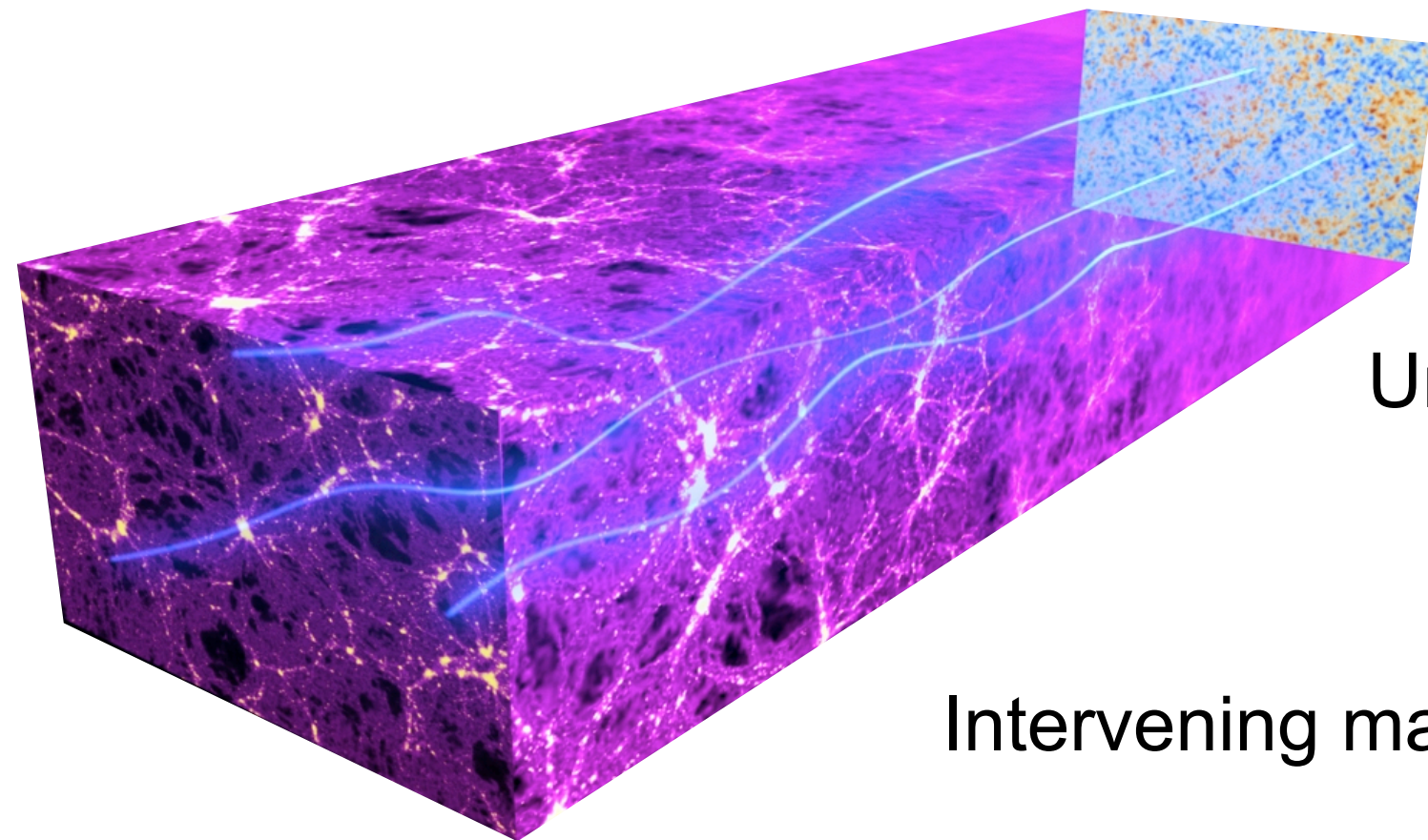
Using galaxy clustering + galaxy-galaxy lensing



Next Y1 analysis will consider galaxy clustering +
galaxy-galaxy lensing + galaxy lensing



Photons from last scattering surface deflected by gravitational potential of large-scale structure



Unlensed CMB

Observed CMB
is lensed

Intervening matter



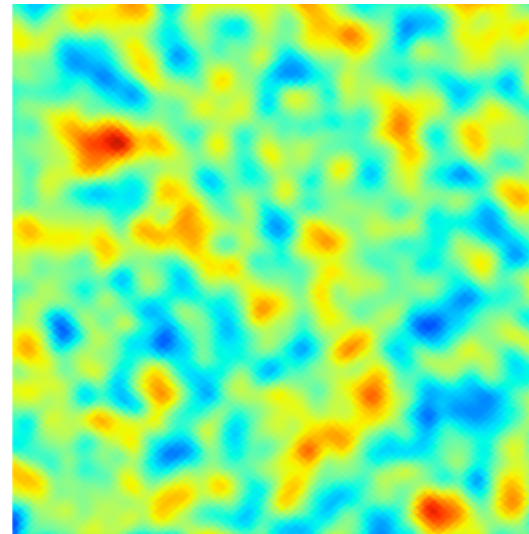
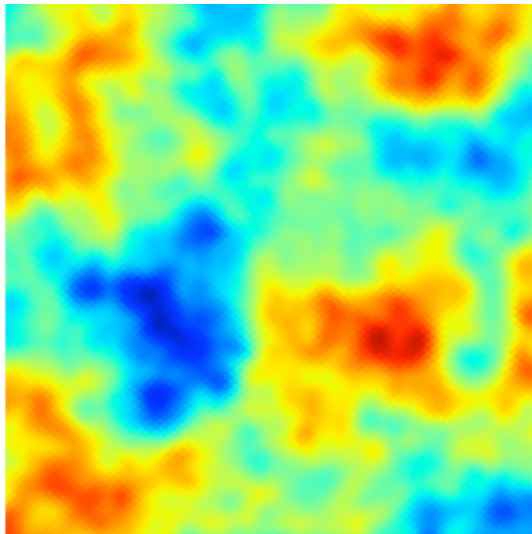
$$\Theta[\hat{n}] = \tilde{\Theta}[\hat{n} + \nabla\phi(\hat{n})]$$

Temperature

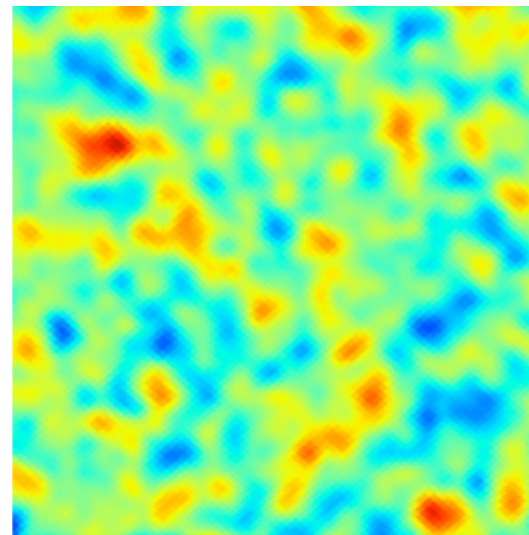
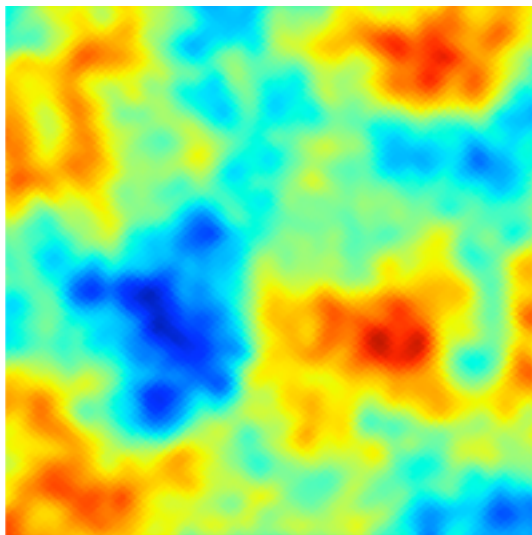
E-modes

B-modes

Unlensed



Unlensed



← 2.5° →

CMB lensing



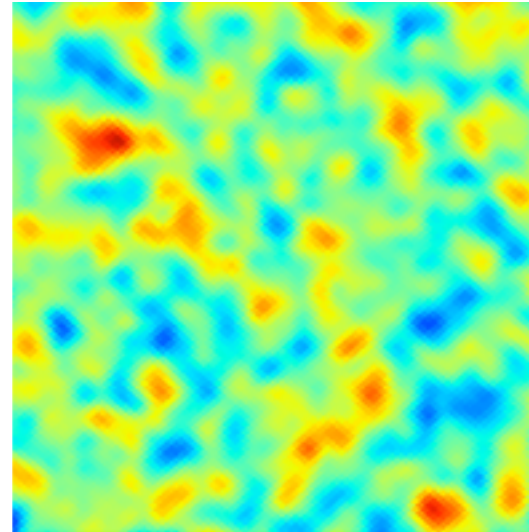
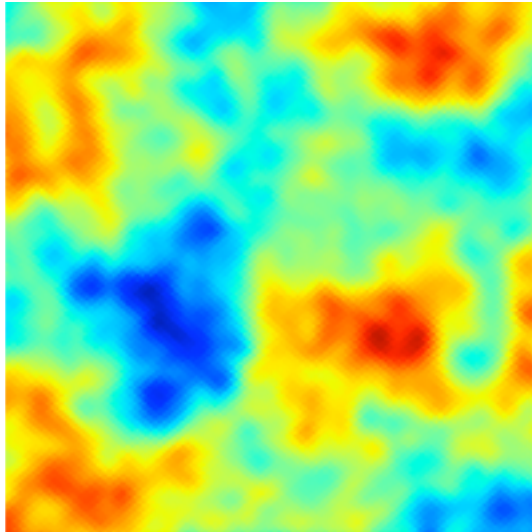
$$\Theta[\hat{\mathbf{n}}] = \tilde{\Theta}[\hat{\mathbf{n}} + \nabla\phi(\hat{\mathbf{n}})]$$

Temperature

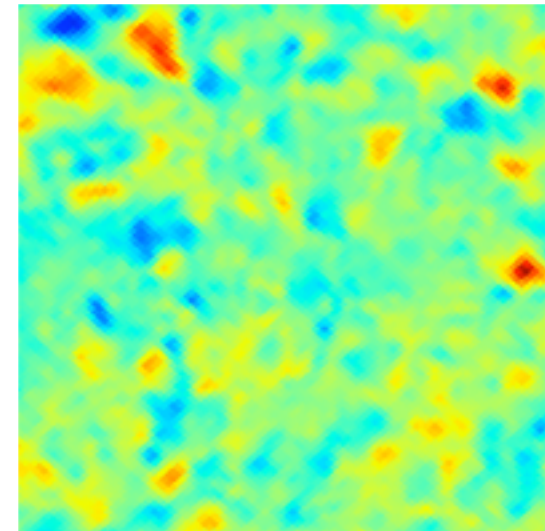
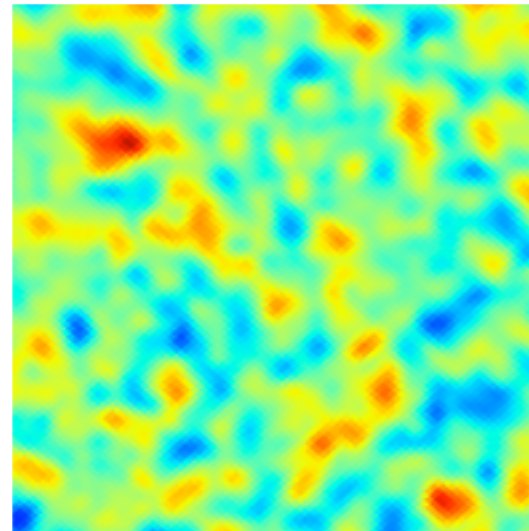
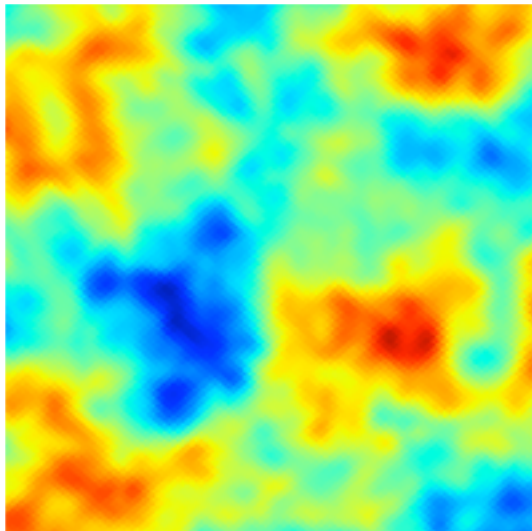
E-modes

B-modes

Unlensed



Lensed



← 2.5° →



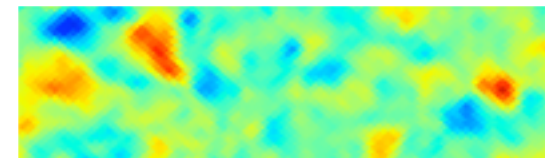
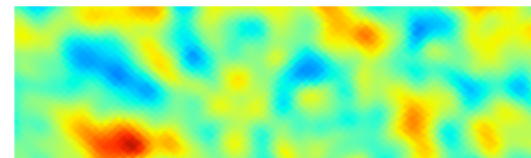
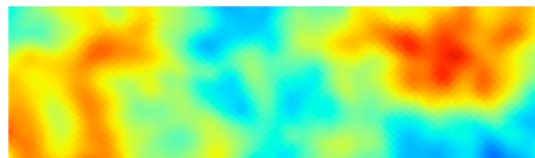
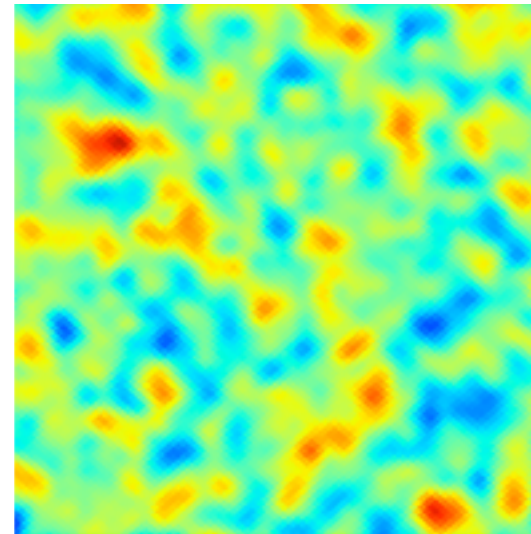
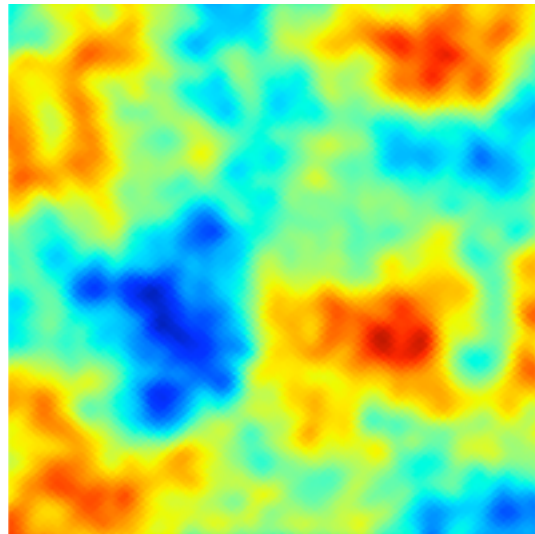
$$\Theta[\hat{\mathbf{n}}] = \tilde{\Theta}[\hat{\mathbf{n}} + \nabla\phi(\hat{\mathbf{n}})]$$

Temperature

E-modes

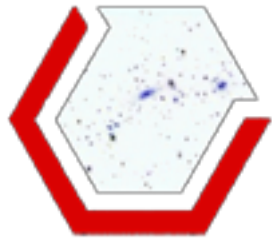
B-modes

Unlensed



- Typical deflections: ~ 2.5 arcmin
- Coherent on the degree scale
- CMB lensing induces temperature-gradient correlations

$$\Theta[\hat{\mathbf{n}}] = \tilde{\Theta}[\hat{\mathbf{n}} + \nabla\phi(\hat{\mathbf{n}})] \approx \tilde{\Theta}[\hat{\mathbf{n}}] + \nabla\phi[\hat{\mathbf{n}}] \nabla\tilde{\Theta}[\hat{\mathbf{n}}] + \dots$$

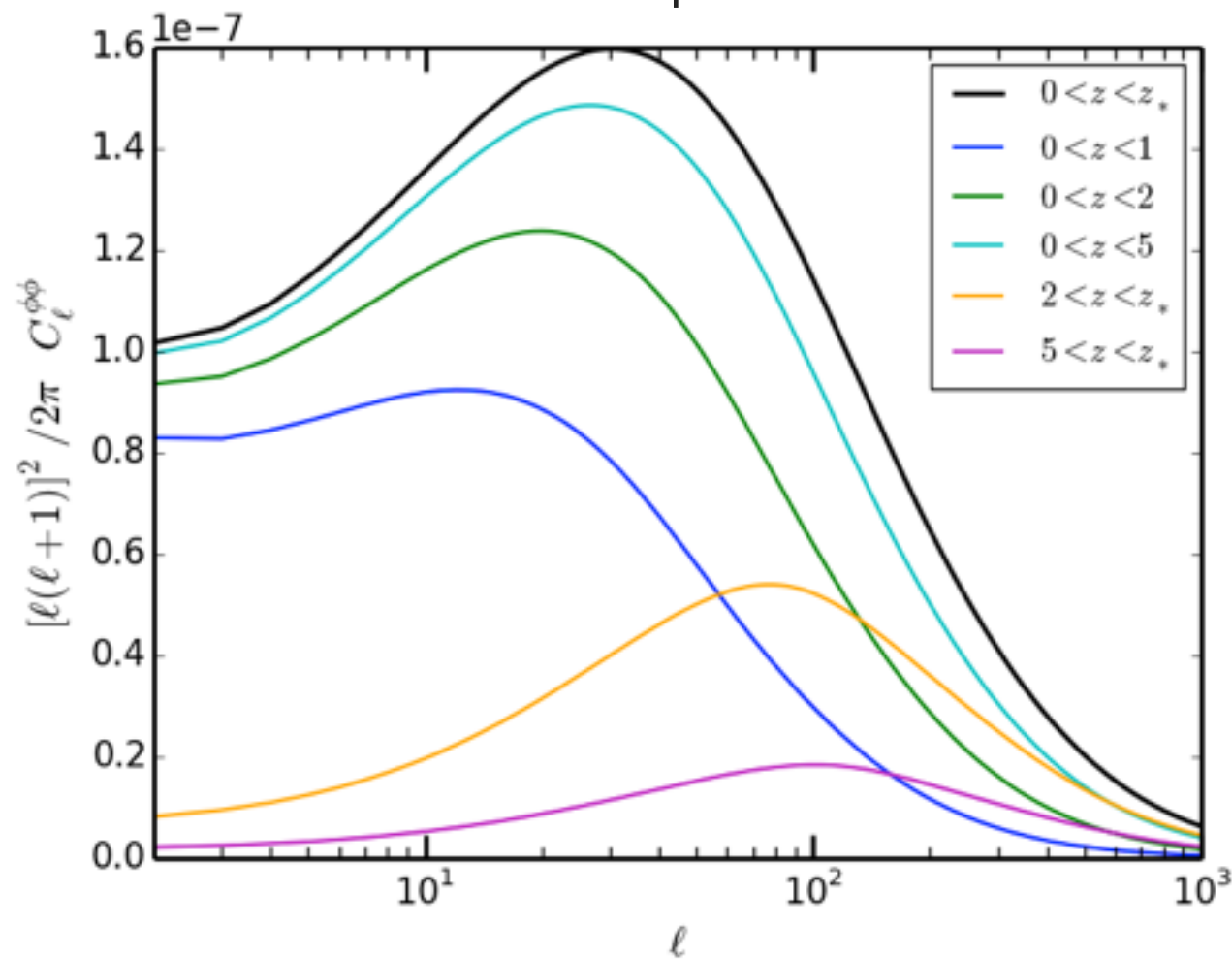


CMB lensing potential

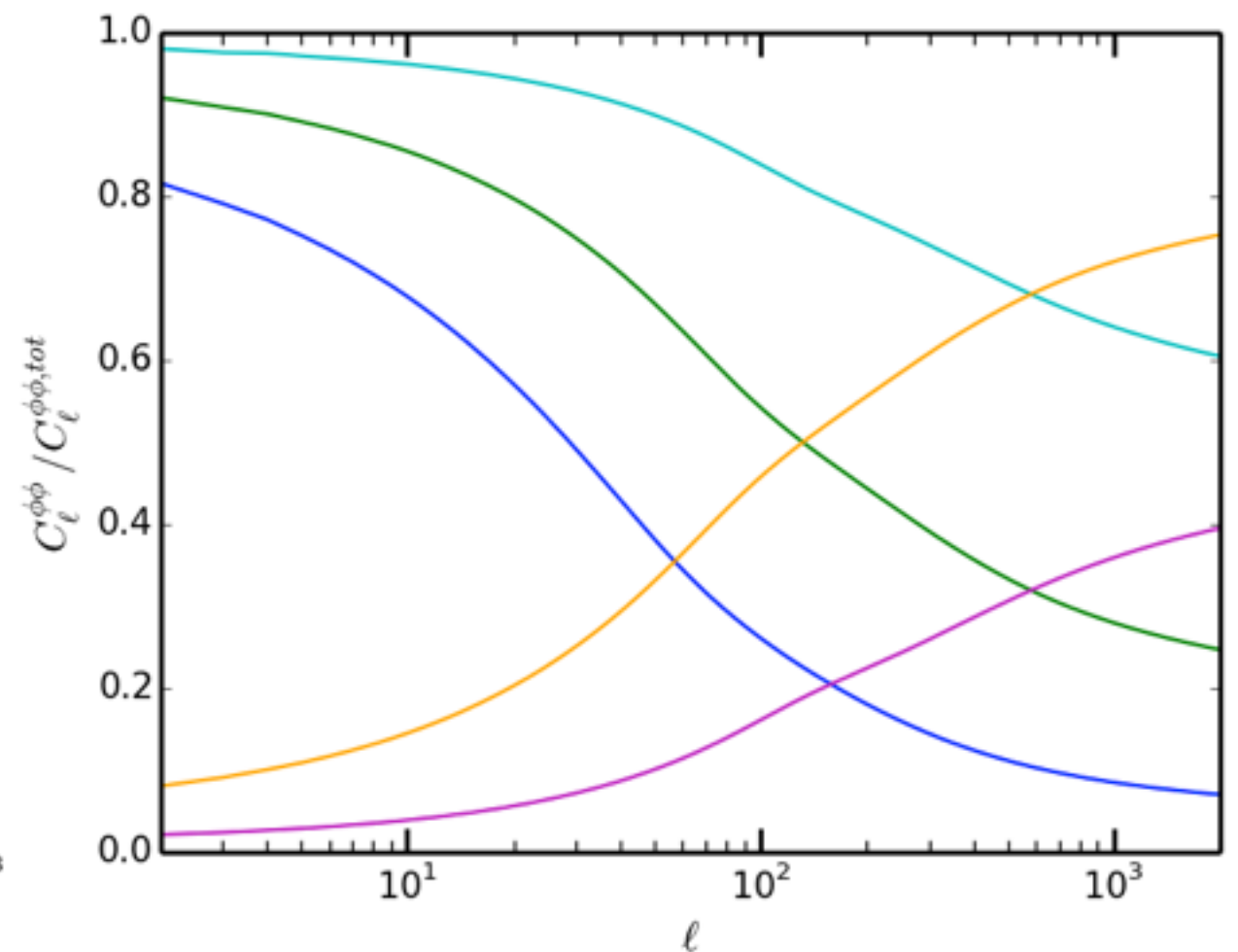
CMB lensing potential is an unbiased tracer of all the matter distribution up to $z \sim 1100$

$$\phi(\hat{n}) = -2 \int_0^{\chi_*} d\chi \frac{f_K(\chi_* - \chi)}{f_K(\chi_*) f_K(\chi)} \Psi(\chi \hat{n}; \eta_0 - \chi).$$

Absolute spectrum

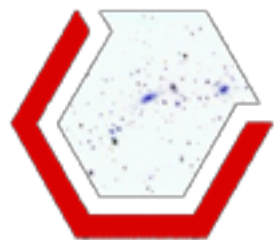


Ratio



CMB Lensing kernel is wide and peaks at $z \sim 2$

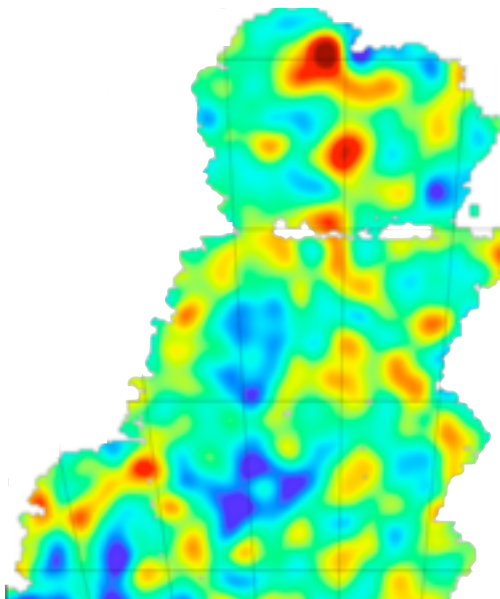
DES will enable CMB lensing tomography



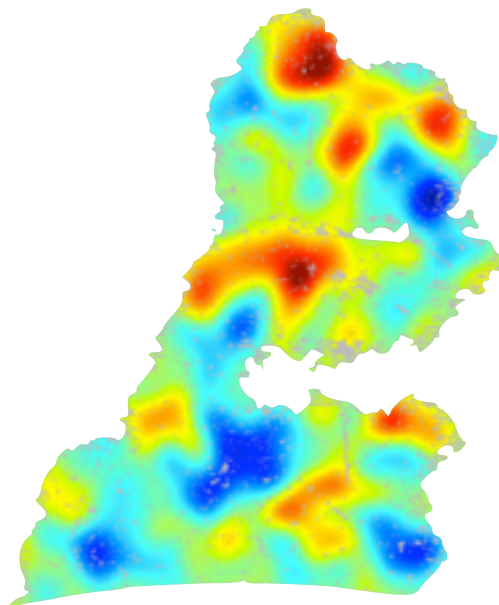
CMB lensing from South Pole Telescope and Planck

Same structure seen by different techniques

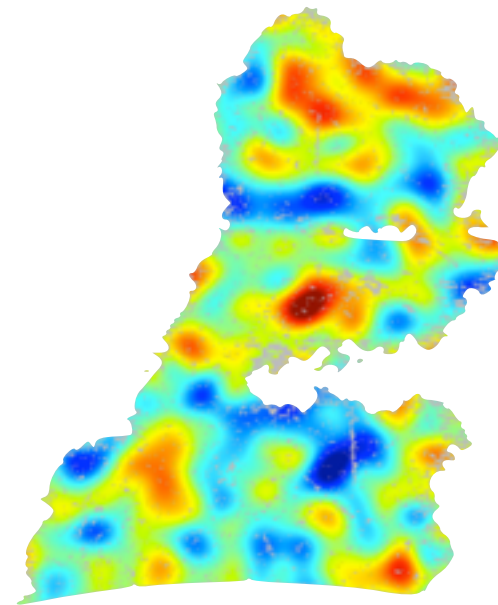
Cosmic shear
(données DES-SV)

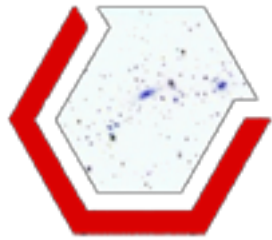


DES-galaxies



CMB lensing
(SPT data)

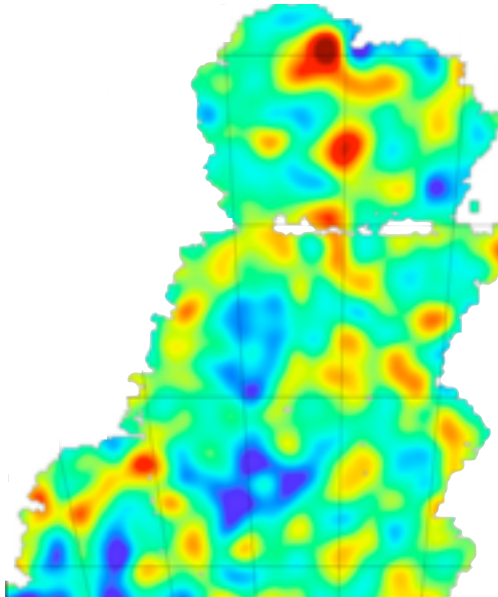




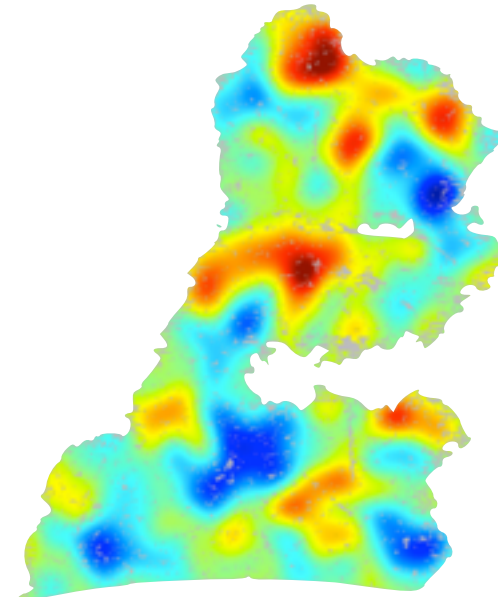
CMB lensing from South Pole Telescope and Planck

Same structure seen by different techniques

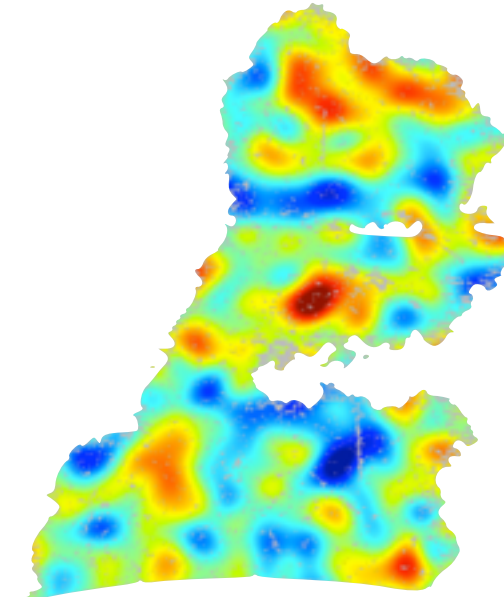
Cosmic shear
(données DES-SV)



DES-galaxies



CMB lensing
(SPT data)

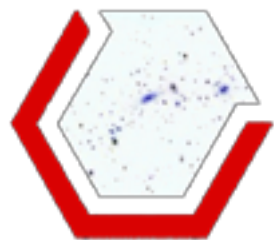


$$\int_0^{\chi_*} d\chi \chi \int_{\chi}^{\chi_*} d\chi' \frac{dn}{d\chi'} \frac{\chi' - \chi}{\chi'} \left(\frac{\delta(\chi \hat{\mathbf{n}}, \chi)}{a} \right)$$

$$\int_0^{\infty} dz b(z) \frac{dn}{dz}(z) \left(\delta(\chi \hat{\mathbf{n}}, \chi) \right)$$

$$\int_0^{\chi_*} d\chi \chi^2 \frac{\chi_* - \chi}{\chi_* \chi} \left(\frac{\delta(\chi \hat{\mathbf{n}}, \chi)}{a} \right)$$

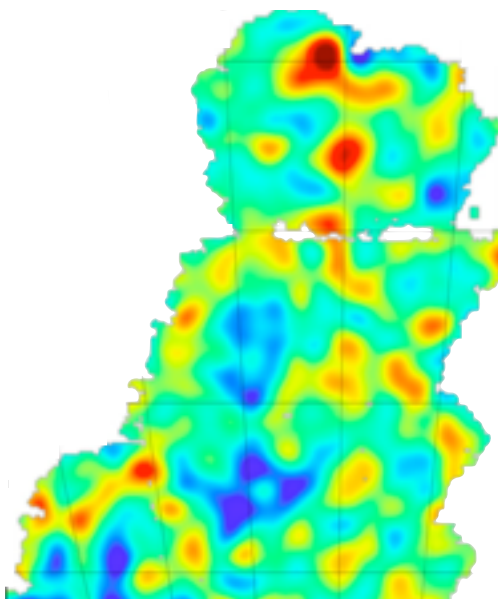
matter density contrast



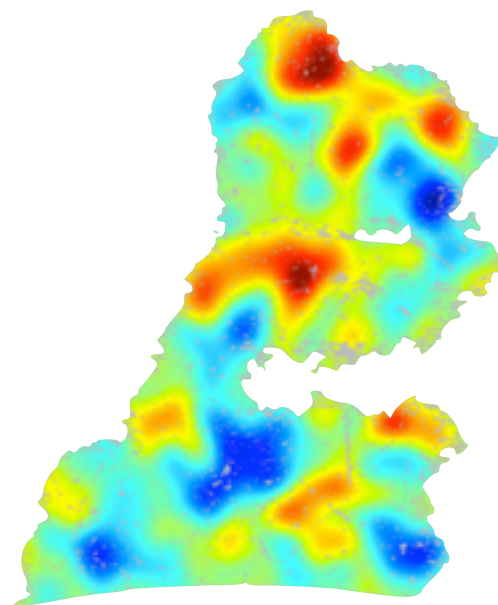
CMB lensing from South Pole Telescope and Planck

Same structure seen by different techniques

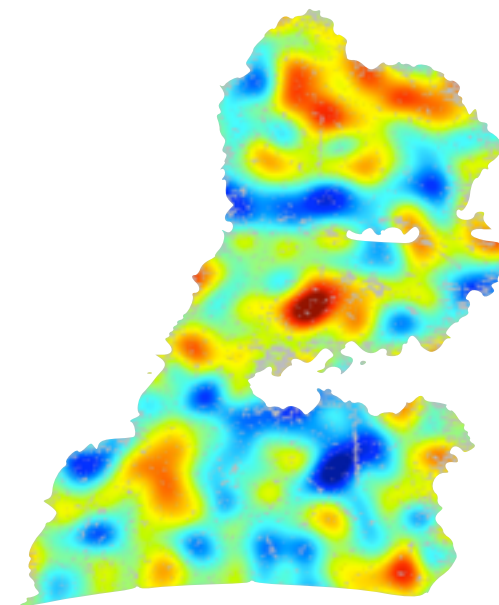
Cosmic shear
(données DES-SV)



DES-galaxies



CMB lensing
(SPT data)



Source redshift distribution

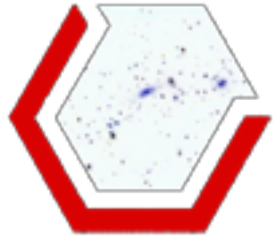
$$\int_0^{\chi_*} d\chi \chi \int_{\chi}^{\chi_*} d\chi' \frac{dn}{d\chi'} \frac{\chi' - \chi}{\chi'} \frac{\delta(\chi \hat{\mathbf{n}}, \chi)}{a}$$

$$\int_0^{\infty} dz b(z) \frac{dn}{dz}(z) \frac{\delta(\chi \hat{\mathbf{n}}, \chi)}{a}$$

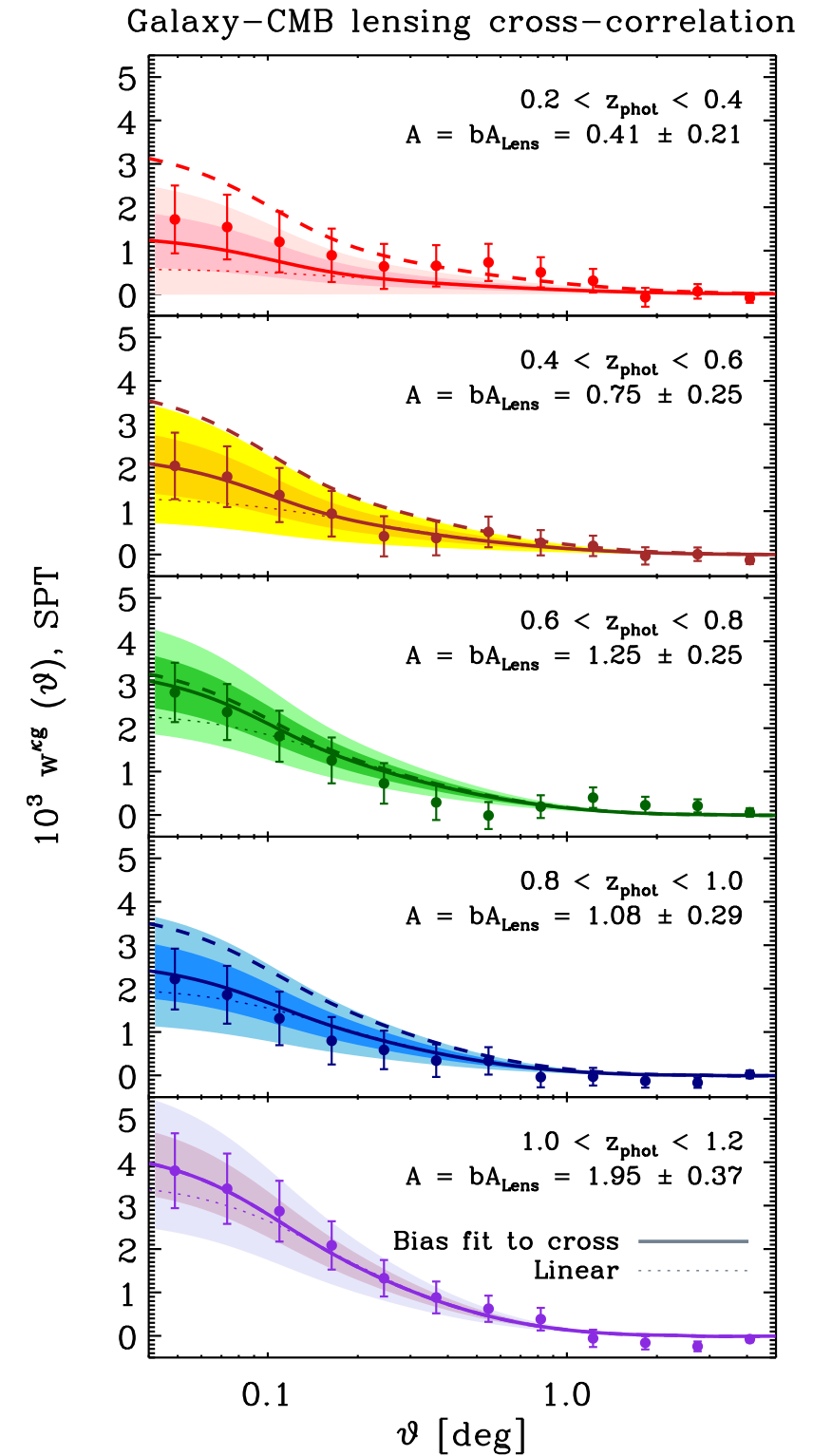
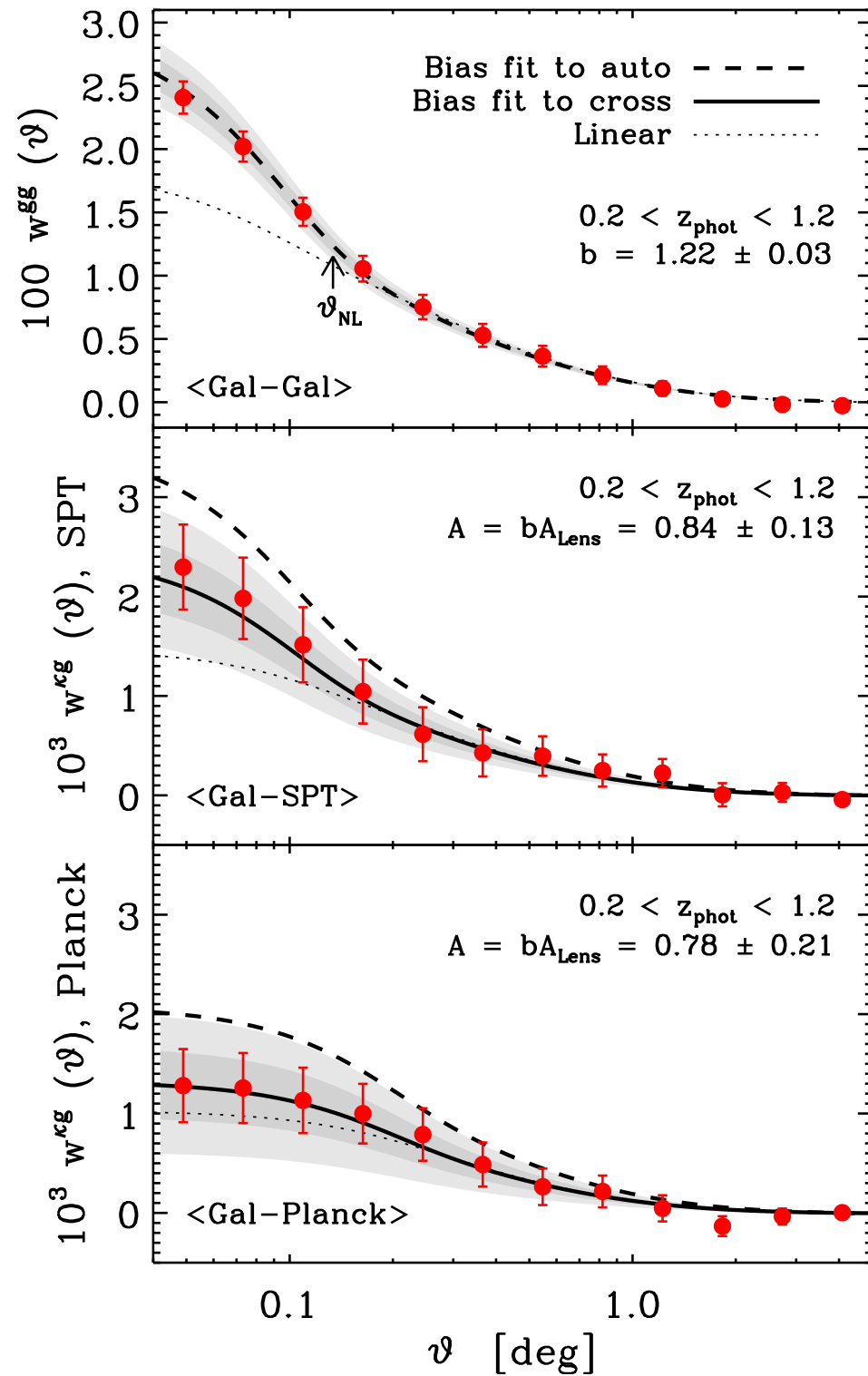
bias

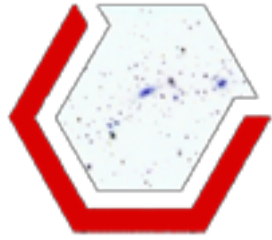
matter density contrast

$$\int_0^{\chi_*} d\chi \chi^2 \frac{\chi_* - \chi}{\chi_* \chi} \frac{\delta(\chi \hat{\mathbf{n}}, \chi)}{a}$$



CMB lensing tomography



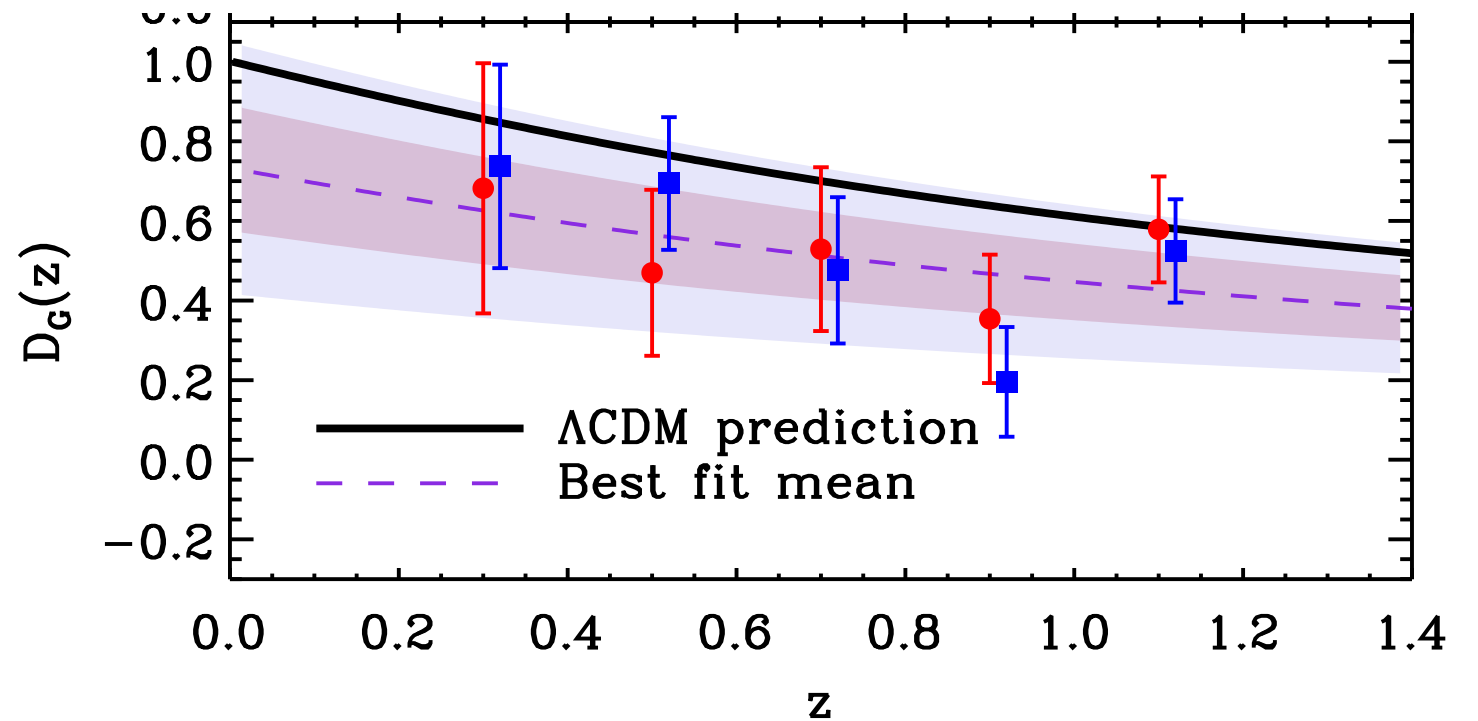


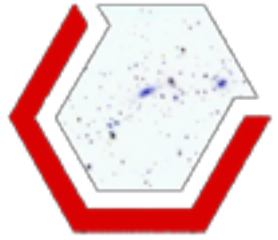
CMB lensing tomography

Measuring the linear growth function with photometric surveys

$$C_{\ell}^{gg}(z) \propto b^2(z) D^2(z), \quad C_{\ell}^{kg}(z) \propto b(z) D^2(z),$$

$$(\hat{D}_G)_i \equiv \left\langle \frac{(C_{\ell}^{kg})_{\text{obs}}^i}{(\mathcal{C}_{\ell}^{kg})_{\text{the}}^i} \sqrt{\frac{(\mathcal{C}_{\ell}^{gg})_{\text{the}}^i}{(C_{\ell}^{gg})_{\text{obs}}^i}} \right\rangle_{\ell}.$$



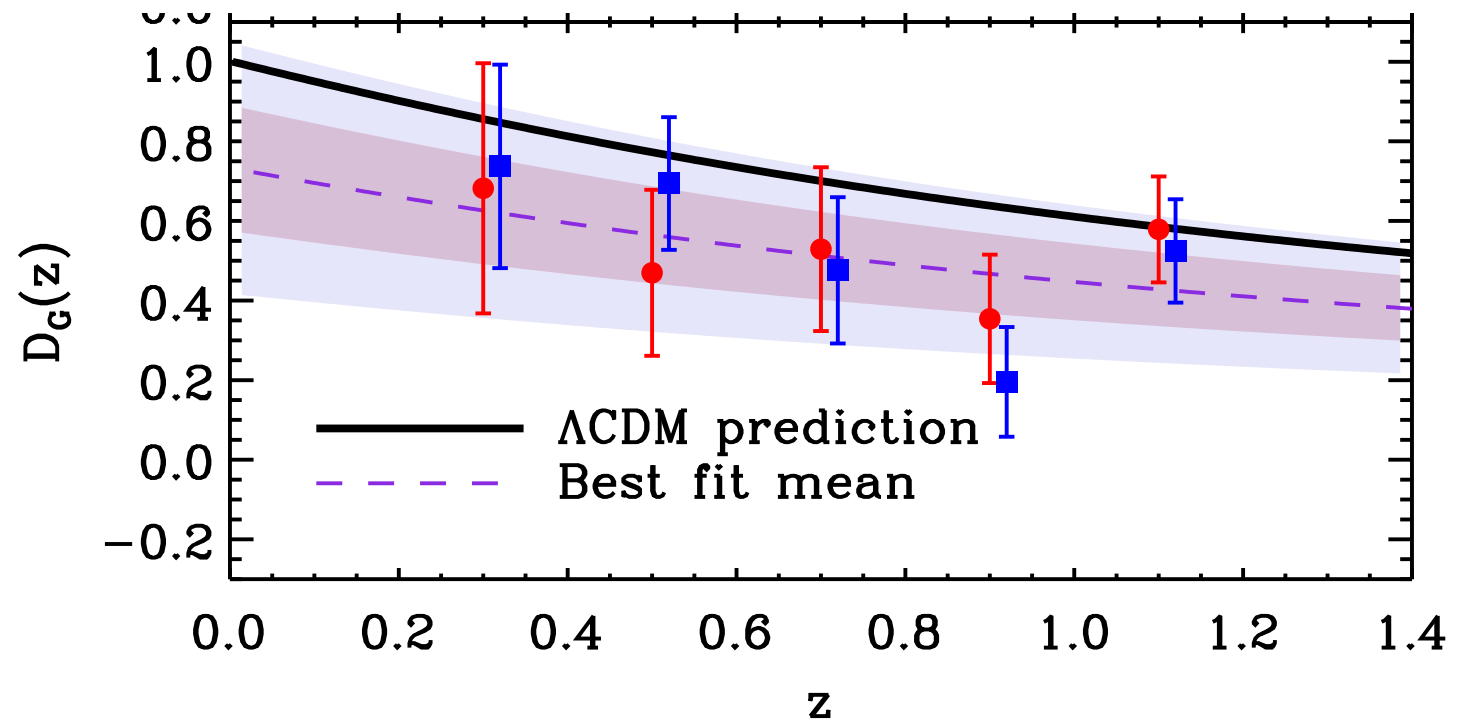


CMB lensing tomography

Measuring the linear growth function with photometric surveys

$$C_{\ell}^{gg}(z) \propto b^2(z) D^2(z), \quad C_{\ell}^{kg}(z) \propto b(z) D^2(z),$$

$$(\hat{D}_G)_i \equiv \left\langle \frac{(C_{\ell}^{kg})_{\text{obs}}^i}{(\mathcal{C}_{\ell}^{kg})_{\text{the}}^i} \sqrt{\frac{(\mathcal{C}_{\ell}^{gg})_{\text{the}}^i}{(C_{\ell}^{gg})_{\text{obs}}^i}} \right\rangle_{\ell}.$$

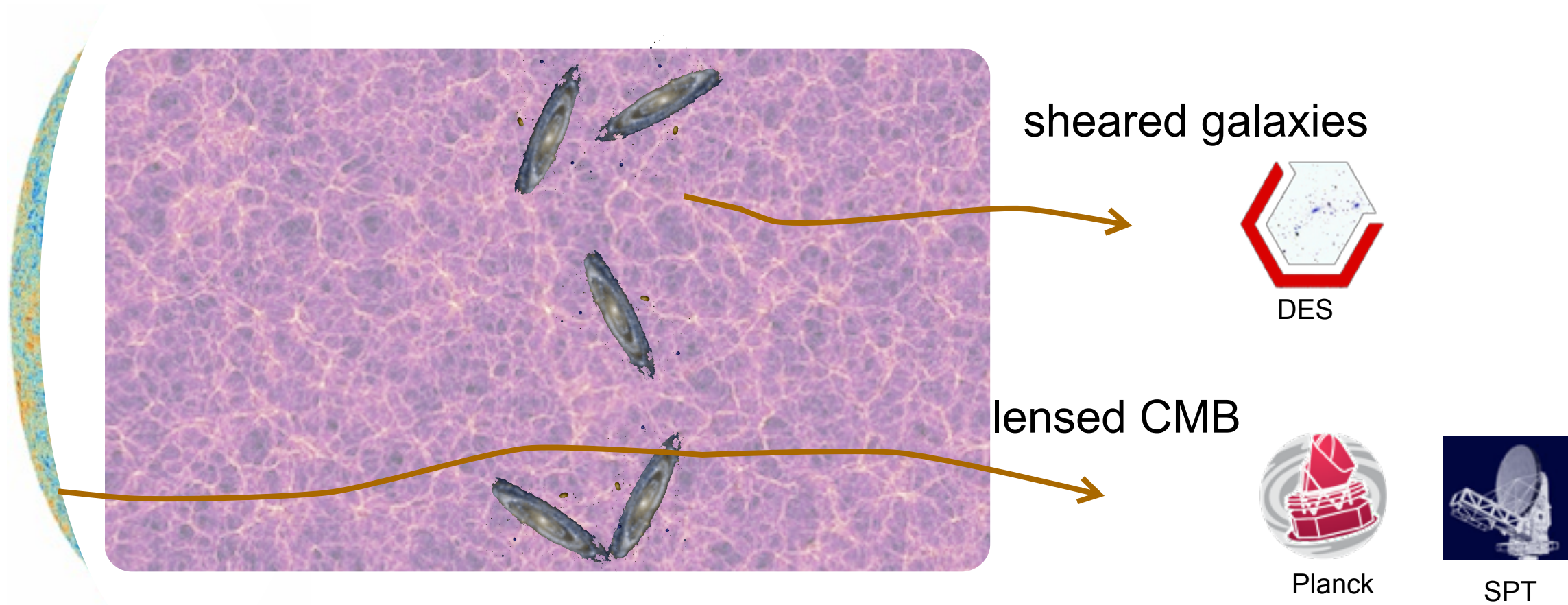


$$C_{\ell}^{gg} = \frac{2}{\pi} \int_0^{\infty} dk k^2 P(k) W_{\ell}^g(k) W_{\ell}^g(k)$$

$$C_{\ell}^{kg} = \frac{2}{\pi} \int_0^{\infty} dk k^2 P(k) W_{\ell}^k(k) W_{\ell}^g(k),$$

$$W_{\ell}^g(k) = \int_0^{\infty} dz b(z) \frac{dn}{dz}(z) D(z) j_{\ell}[k\chi(z)]$$

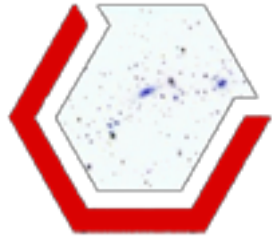
$$W_{\ell}^k(k) = \frac{3\Omega_m H_0^2}{2} \int_0^{\infty} dz \frac{\chi_* - \chi}{\chi_* \chi}(z) D(z) j_{\ell}[k\chi(z)],$$



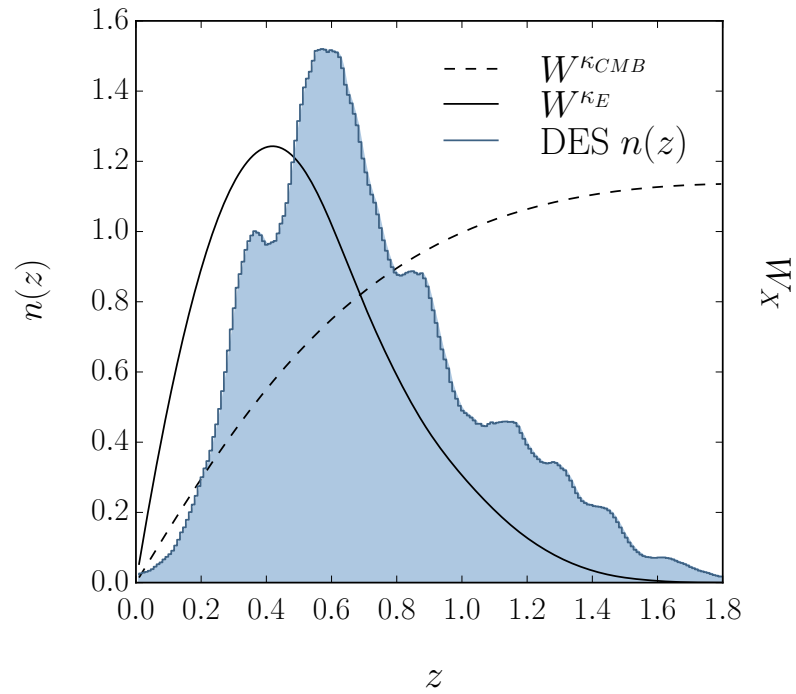
$$C_{\text{GWL,CMBWL}}(\ell) = \int_0^{\chi_{\text{hor}}} \frac{d\chi}{\chi(z)^2} W_{\text{GWL}}[\chi(z)] W_{\text{CMBWL}}[\chi(z)] P_{\delta\delta} \left(\frac{\ell}{\chi(z)}, z \right),$$

$$W_{\text{GWL}}[\chi(z)] = \frac{3H_0^2\Omega_m}{2c^2} \frac{\chi}{a(\chi)} \int_{\chi}^{\chi_{\text{hor}}} d\chi' n(\chi') \frac{\chi' - \chi}{\chi'},$$

$$W_{\text{CMBWL}}[\chi(z)] = \frac{3H_0^2\Omega_m}{2c^2} \frac{\chi}{a(\chi)} \frac{\chi_* - \chi}{\chi_*},$$

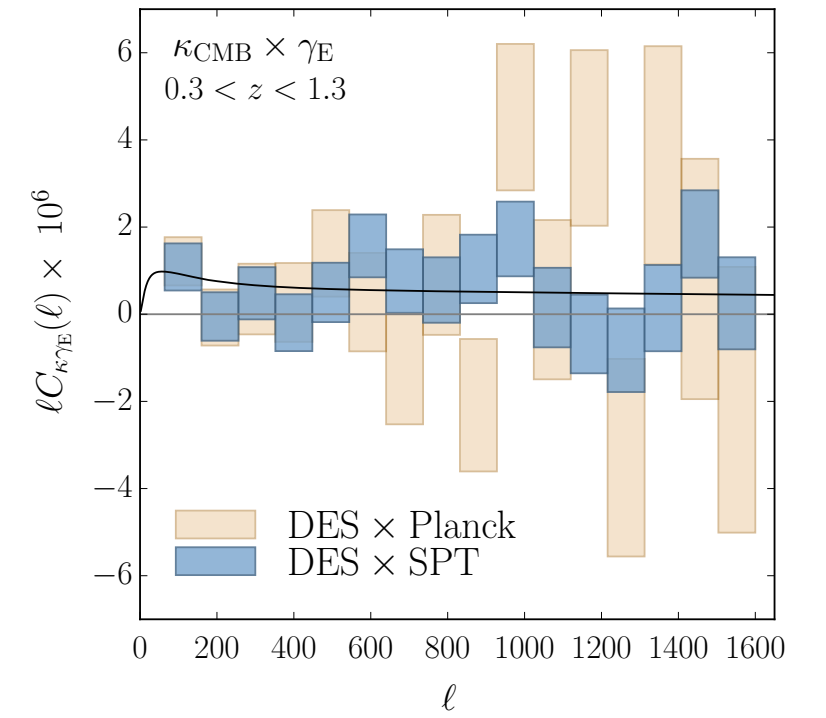


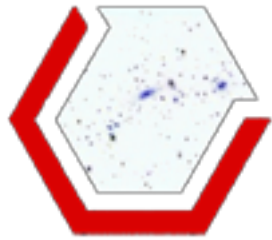
CMB lensing x DES shear



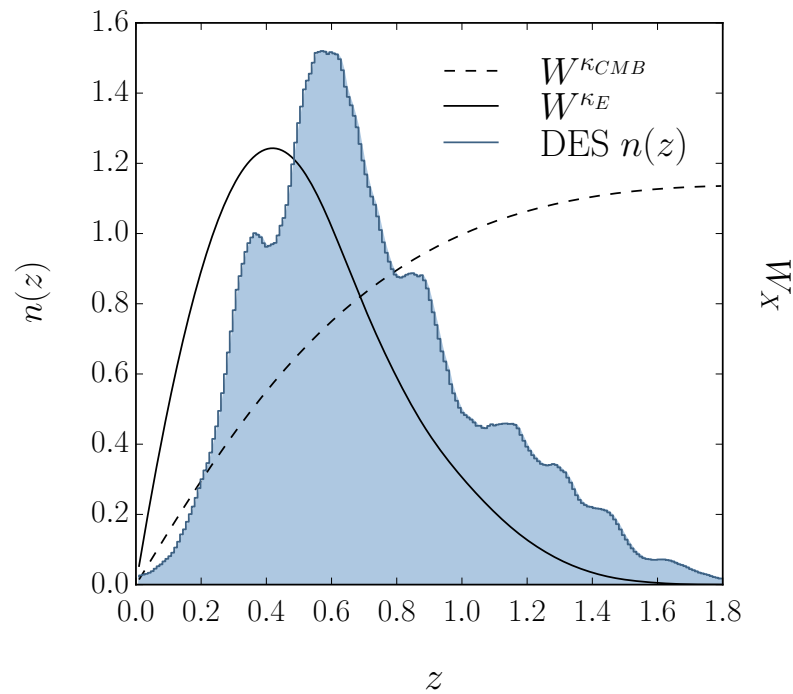
Considered galaxy ellipticities
(γ_1, γ_2) as spin-2 field, and use CMB
tools (POLSPICE)

| Redshift Range | $0.3 < z < 1.3$ | |
|-------------------------|------------------------|------------------------|
| $\kappa_{CMB} \gamma_E$ | A | $\chi^2/\text{d.o.f.}$ |
| ngmix \times SPT | $0.88^{+0.30}_{-0.30}$ | 0.93 |
| ngmix \times Planck | $0.86^{+0.39}_{-0.39}$ | 1.52 |



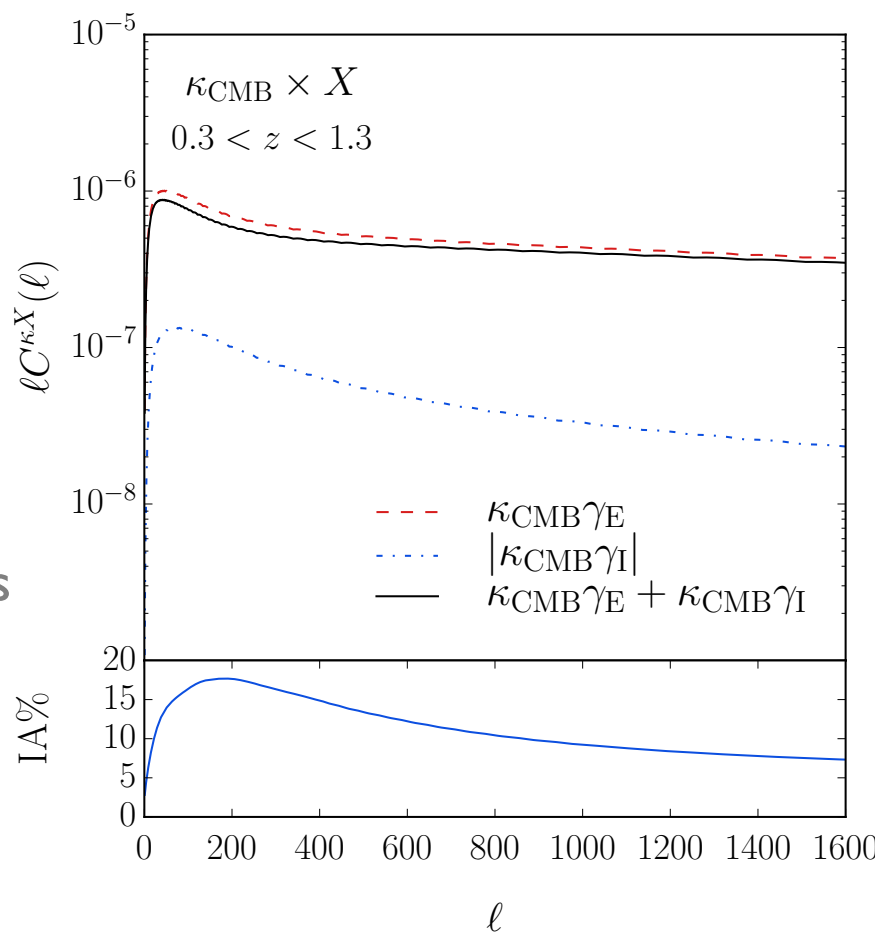
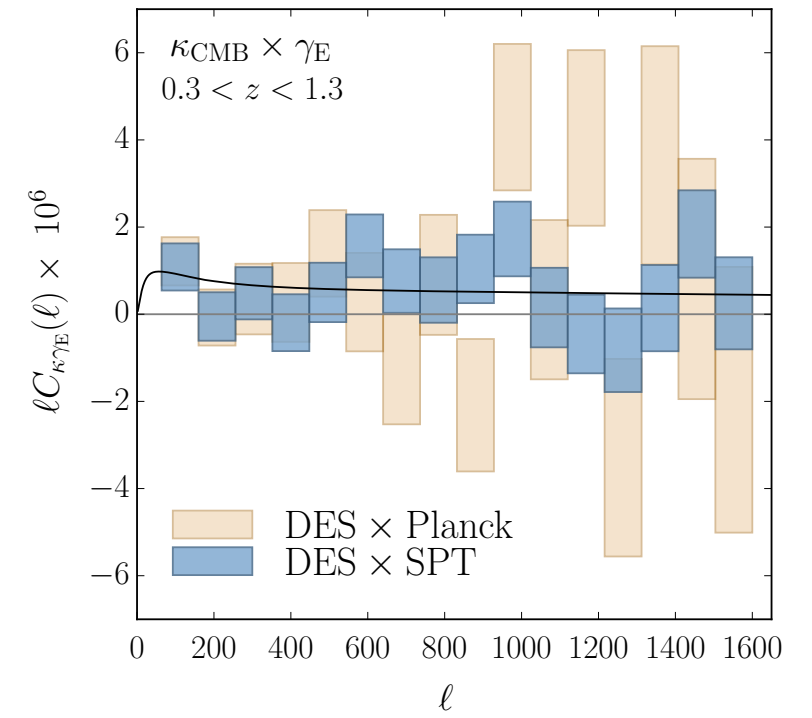


CMB lensing x DES shear



Considered galaxy ellipticities (γ_1, γ_2) as spin-2 field, and use CMB tools (PoLSPICE)

| Redshift Range | $0.3 < z < 1.3$ | |
|-------------------------------|------------------------|------------------------|
| $\kappa_{\text{CMB}}\gamma_E$ | A | $\chi^2/\text{d.o.f.}$ |
| ngmix \times SPT | $0.88^{+0.30}_{-0.30}$ | 0.93 |
| ngmix \times Planck | $0.86^{+0.39}_{-0.39}$ | 1.52 |



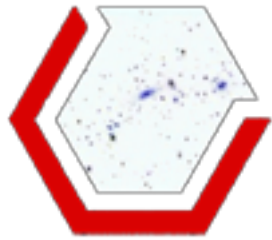
Intrinsic alignments are a major contaminant for cosmic shear

unsheared ellipticities are correlated with gravitational potential

Assume no IAs: $A=0.88\pm0.30$

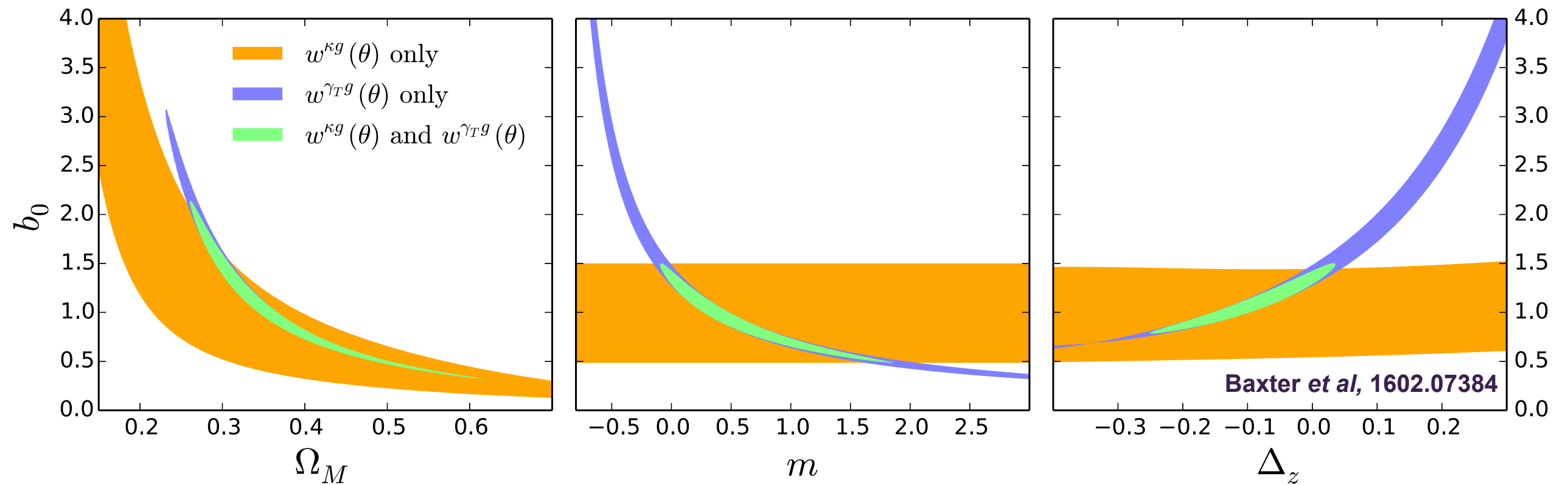
Assume NLA model: $A=1.08\pm0.36$

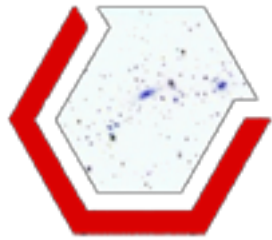
CMB lensing will provide an additional handle to probe/constrain/alleviate IAs.



Combining probes

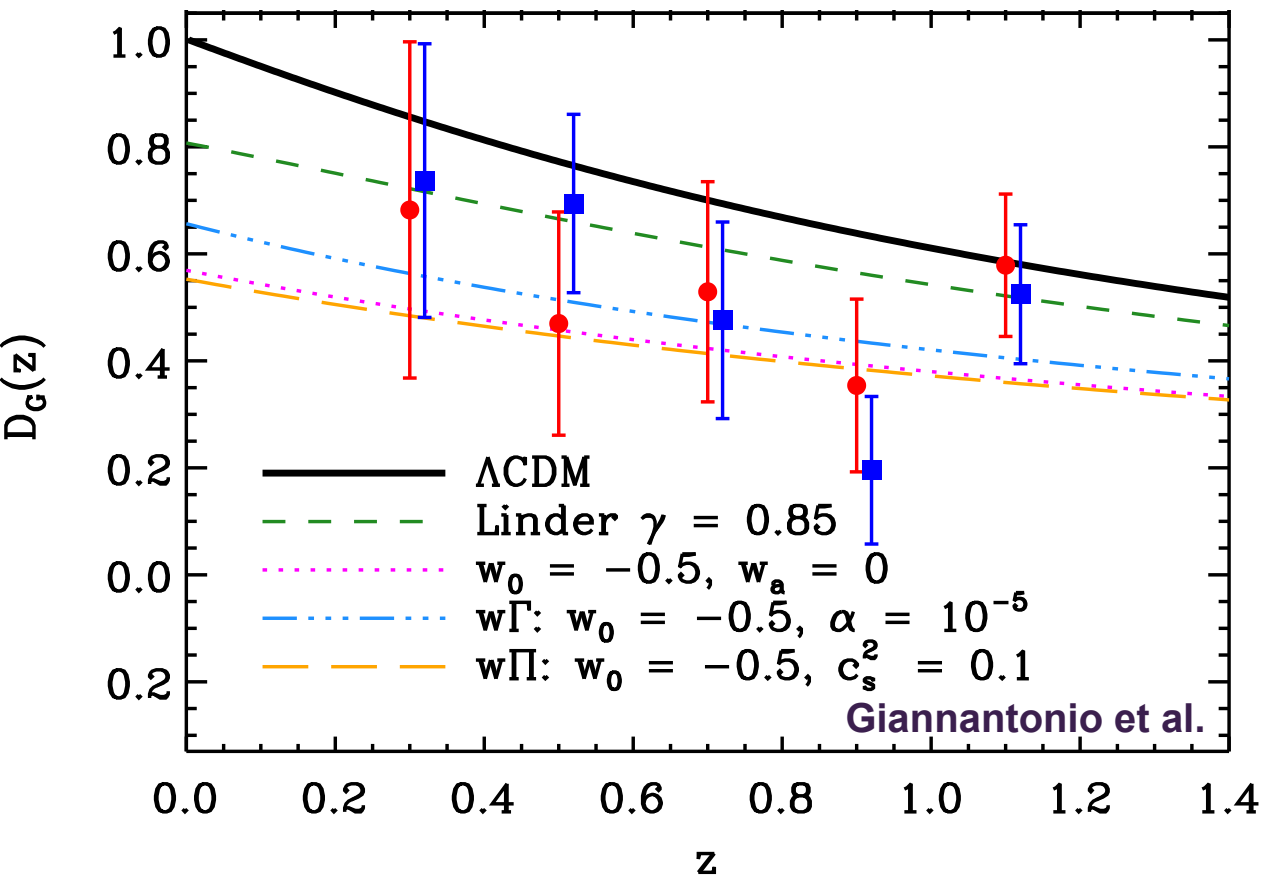
Using galaxy clustering + galaxy-galaxy lensing
and galaxy clustering + CMB lensing



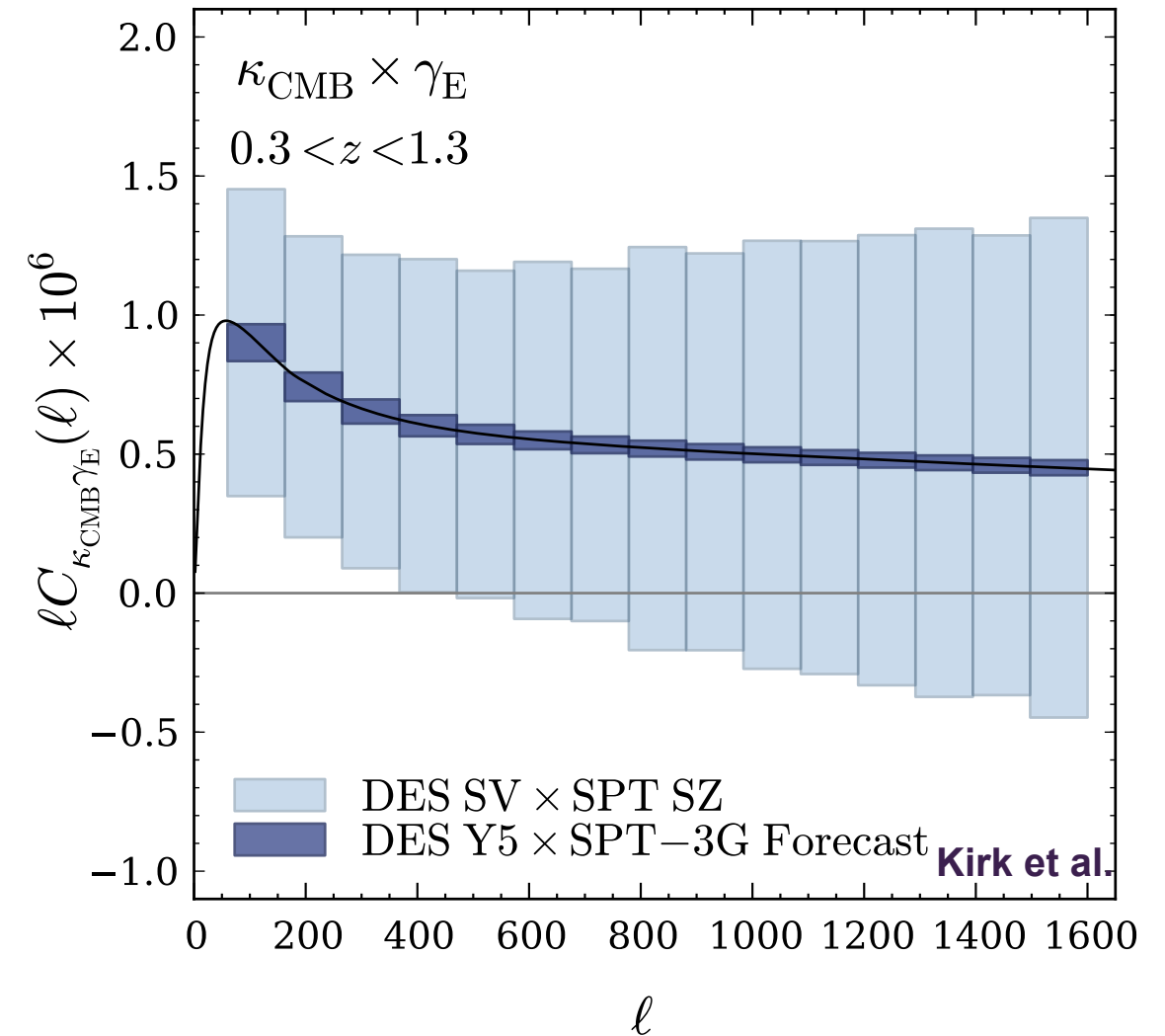


CMB lensing x DES: prospects

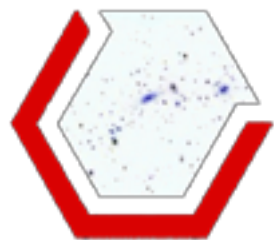
galaxy - CMB lensing



galaxy lensing - CMB lensing



Complementarity between surveys (LSST, Euclid)
and CMB (S4, COrE) must be exploited



Conclusion

SV analysis is finished, now public:

<http://des.ncsa.illinois.edu/releases/sva1>

Y1 reduced images are now public:

<http://data.darkenergysurvey.org/aux/releasenotes/DESDMrelease.html>

First results from Y1. More in the coming months

Collaboration is working on Y1 and Y1-3 data (>1500 sq.deg.)

10sig. limiting magnitude in a 2" diameter aperture (made with Mangle)

